

Zeta Function Zeros, Dirichlet Products, Möbius Inversion, and the Probit Function

Darrell Cox

April 15, 2018

Abstract

Forward and inverse transformations involving the non-trivial Riemann zeta function zeros are investigated. These transformations give a simple method to find and accurately approximate new zeros given a baseline of accurate zeros to extrapolate from. The relevance of the probit function, log-normal distributions, Ramanujan sums, and Dirichlet inverses to the zeros is also investigated. The generalized probit function is used to model the distribution of the zeros and the differences between them.

1 Introduction

Let $\theta_1, \theta_2, \theta_3, \dots$ denote the imaginary parts of the nontrivial zeros of the Riemann zeta function (Odlyzko's [1] tables will be used). Dirichlet products have the form $\sum_{d|n} f(d)g(n/d)$. Initially, f is set to a constant function having values of 1. The equation $f(n) = \sum_{d|n} (g/d)$ implies $g(n) = \sum_{d|n} f(d)\mu(n/d)$ where μ is the Möbius function. This is known as Möbius inversion. This is the motivation for starting with trivial Dirichlet products. The cumulative distribution function is denoted by $\Phi(p)$ where p are probabilities between 0 and 1. The probit function is the inverse cumulative distribution function for the standard normal distribution. The probit function can be computed using an ordinary differential equation. The more general function $F^{-1}(p) = \mu + \sigma\Phi^{-1}(p)$ where μ and σ are the mean and standard deviation of the distribution will be used here. The distribution of the zeta function zeros appears to be log-normal. The logarithm of the logarithm of the zeros etc., also appear to be log-normal. An upper bound of the zeros is determined (empirically) by taking repeated logarithms of the zeros. Generalized Ramanujan sums have the form $\sum_{d|(n,k)} f(d)g(k/d)$ where (n, k) denotes the greatest common divisor function. These sums have a finite Fourier expansion. Fourier analysis of the zeta function zeros can then be done.

2 Dirichlet Products Involving θ

Hutchinson [2] computed the first 138 non-trivial zeros of the Riemann zeta function. See Figure (1) for a plot of $\sum_{i|x} \log(\theta_{x/i})$ for $x = 1, 2, 3, \dots, 135$. The plot consists of 12 different slowly increasing "curves" with gaps in them. Curve #0 (numbering from the bottom) consists of a single element at $x = 1$ and having a value of $\log(\theta_1)$. Curve #1 consists of elements at $x = 2, 3, 5, \dots$ (the primes) and having values of $\log(\theta_1) + \log(\theta_x)$. Curve #2 consists of elements at $x = 2^2, 3^2, 5^2, \dots$. Curve #3 consists of elements at $x = 2^3, 3^3, 5^3, \dots$ and x values that are the product of two distinct primes. Curve #4 consists of elements at $x = 2^4, 3^4, 5^4, \dots$. Curve #5 consists of elements at $x = 2^5, 3^5, 5^5, \dots$ and x values that are the product of the square of a prime and a different prime. Curve #6 consists of elements at $x = 2^6, 3^6, 5^6, \dots$. Curve #7 consists of elements at $x = 2^7, 3^7, 5^7, \dots$, x values that are the product of the cube of a prime and a different prime, and x values that are the product of three distinct primes. Curve #8 (not shown) consists of elements at $x = 2^8, 3^8, 5^8, \dots$. Curve #9 consists of elements at $x = 2^9, 3^9, 5^9, \dots$, x values that are the product of the fourth power of a prime and a different prime, and x values that are the product of the square of a prime and the square of a different prime (a secondary curve). The values of the secondary curve are somewhat less than those of the primary curve. Curve #10 (not shown) consists of elements at $x = 2^{10}, 3^{10}, 5^{10}, \dots$. Curve #11 consists of elements at $x = 2^{11}, 3^{11}, 5^{11}, \dots$, x values that are the product of the fifth power of a prime and a different prime, x values that are the product of the cube of a prime and the square of a different prime, and x values that are the product of the square of a prime and two other distinct primes. Curve #12 (not shown) consists of elements at $x = 2^{12}, 3^{12}, 5^{12}, \dots$. Curve #13 consists of elements at $x = 2^{13}, 3^{13}, 5^{13}, \dots$, x values that are the product of the sixth power of a prime and a different prime (a secondary curve), x values that are the product of the fourth power of a prime and the square of a different prime (another secondary curve), x values that are the product of the cube of a prime and the cube of a different prime, x values that are the product of the cube of a prime and two other distinct primes, and x values that are the product of four distinct primes. The x values other than those in the secondary curves constitute the primary curve. The first secondary curve has smaller values than those of the second secondary curve. Curve #14 (not shown) consists of elements at $x = 2^{14}, 3^{14}, 5^{14}, \dots$. Curve #15 (not shown) consists of elements at $x = 2^{15}, 3^{15}, 5^{15}, \dots$, x values that are the product of the seventh power of a prime and a different prime (a secondary curve), x values that are the product of the fifth power of a prime and the square of a different prime, x values that are the product of the fourth power of a prime and the cube of a different prime (the primary curve), x values that are the product of the fourth power of a prime and two other distinct primes, and x values that are the product of the square of a prime, the square of a different prime, and another distinct prime. The x values other than those in the first secondary curve and the primary curve constitute the second secondary curve. The first secondary curve has smaller values than those of the second secondary curve. The first

secondary curve coincides with the primary curve in Curve #13. Curve #16 (not shown) consists of elements at $x = 2^{16}, 3^{16}, 5^{16}, \dots$. Curve #17 (not shown) consists of elements at $x = 2^{17}, 3^{17}, 5^{17}, \dots$, x values that are the product of the eighth power of a prime and another prime (a secondary curve), x values that are the sixth power of a prime and the square of another prime (another secondary curve), x values that are the product of the fifth power of a prime and the cube of another prime, x values that are the product of the cube of a prime, the square of another prime, and another distinct prime, and x values that are the product of the square of a prime and three other distinct primes. The x values other than those in the secondary curves constitute the primary curve. The first secondary curve has smaller values than those of the second secondary curve. The first secondary curve coincides with the primary curve in Curve #15. In general, Curve # k consists of at least elements at $x = 2^k, 3^k, 5^k, \dots$. The logarithm of the θ values was used to help identify the curves. See Figure (2) for a plot of $\sum_{i|x} \theta_{x/i}$ for $x = 1, 2, 3, \dots, 135$. Möbius inversion can be used to regenerate the θ values from these curves.

3 A Technique for Finding Zeros Given Other Zeros

See Figure (3) for a plot of the 148933 θ_x values at $x = 2, 3, 5, \dots, 1,999,993$ (the primes less than 2,000,000). For a linear least squares fit of the curve, $p_1 = 7.587$ with a 95% confidence interval of (7.587, 7.587), $p_2 = 3578$ with a 95% confidence interval of (3568, 3587), $SSE=1.323 \cdot 10^{11}$, R-square=1, and RMSE=942.6. See Figure (4) for a plot of the 223 $\sum_{i|x} \theta_{x/i} - \theta_1$ values at $x = 2^2, 3^2, 5^2, \dots, 1409^2$ (x values at the squares of primes less than 2,000,000). For a quadratic least squares fit of the curve, $p_1 = 24.55$ with a 95% confidence interval of (24.31, 24.78), $p_2 = -626.4$ with a 95% confidence interval of (-681.9, -571), $p_3 = 9172$ with a 95% confidence interval of (6480, 11860), $SSE=9.989 \cdot 10^9$, R-square=0.9996, and RMSE=6738. See Figure (5) for a plot of the 30 $\sum_{i|x} \theta_{x/i} - \theta_1$ values at $x = 2^3, 3^3, 5^3, \dots, 117^3$ (x values at the cubes of primes less than 2,000,000). For a cubic least-squares fit of the curve, R-square=0.9947. In general, the $\sum_{i|x} \theta_{x/i} - \theta_1$ values can be predicted fairly accurately for x values that are powers of primes.

Let $\kappa_1(1), \kappa_1(2), \kappa_1(3), \dots$, denote $\theta_1, \theta_2, \theta_3, \dots$ and let $\kappa_n(x)$, $n = 2, 3, 4, \dots$, denote these values and $n - 1$ values that have been linearly interpolated between successive values. In 1903, Gram [3] published a list of the first 15 zeros. Let $y_1, y_2, y_3, \dots, y_{43}$ equal the values of $\sum_{i|x} \kappa_1(x/i) - \theta_1$ at x values that are the cube of a prime and x values that are the product of two distinct primes for x less than or equal to 135. Let $z_1, z_2, z_3, \dots, z_{43}$ equal the values of $\sum_{i|x} \kappa_9(x/i) - \theta_1$ at x values that are the cube of a prime and x values that are the product of two distinct primes for x less than or equal to 135. (Note that only the zeros computed by Gram were used.) See Figure (6) for a plot of y

and z . To compare the curves, they would have to be first normalized (reduced in value by subtracting the first element of the array from all the elements) and then the normalized z values could be scaled up by multiplying by the ratio of the last elements of the normalized arrays. These are the parameters needed to predict the y values using the z values. See Figure (7) for a plot of the normalized and scaled y and z values. See Figure (8) for a plot of the differences between the normalized and scaled y and z values divided by the normalized y values (where the first element of the resulting array is not shown). The relative error is usually less than 5%. Let $y_1, y_2, y_3, \dots, y_{19}$ equal the values of $\sum_{i|x} \kappa_1(x/i) - \theta_1$ at x values that are the fifth power of a prime and x values that are the product of the square of a prime and another prime for x less than or equal to 135. Let $z_1, z_2, z_3, \dots, z_{19}$ equal the values of $\sum_{i|x} \kappa_9(x/i) - \theta_1$ at x values that are the fifth power of a prime and x values that are the product of the square of a prime and another prime for x less than or equal to 135. See Figure (9) for a plot of y and z . See Figure (10) for a plot of the normalized and scaled y and z values. See Figure (11) for a plot of the differences between the normalized and scaled y and z values divided by the normalized y values (where the first element of the resulting array is not shown). The relative error is less than 9%.

Let $y_1, y_2, y_3, \dots, y_{2600}$ equal the values of $\sum_{i|x} \kappa_1(x/i) - \theta_1$ at x values that are the product of two distinct primes for x less than 10,000. See Figure (12) for a plot of the y values. In the following, the corresponding 2850 y values for x less than 11,000 will be approximated. Then Möbius inversion will be used to compare the new 250 zero values to the predicted values. Let $y_1, y_2, y_3, \dots, y_{145}$ equal the values of $\sum_{i|x} \kappa_1(x/i) - \theta_1$ at x values that are the product of two distinct primes for x less than 500. Let $z_1, z_2, z_3, \dots, z_{145}$ equal the values of $\sum_{i|x} \kappa_2(x/i) - \theta_1$ at x values that are the product of two distinct primes for x less than 500. The minimum y value is 83.619076 and the minimum z value is 66.318290. The maximum y value is 1266.394397 and the maximum z value is 747.781093. The scaling factor is then $(1266.394397 - 83.619076) / (747.781093 - 66.318290)$ of about 1.73564. See Figure (13) for a plot of the corresponding scaling factors for x values less than 500, 1,000, 1,500, ..., 10,000. The corresponding numbers of x values that are the product of two distinct primes are 145, 288, 424, 563, 694, 825, 962, 1087, 1216, 1346, 1477, 1601, 1724, 1844, 1986, 2105, 2241, 2357, 2472, and 2600 respectively. The sample sizes of multiples of 500 are large enough that the curve is relatively smooth. The curve is locally quadratic. The last four scaling factors are 1.806791, 1.808142, 1.809158, and 1.810204. See Figure (14) for a plot of these values. For a quadratic least-squares fit of the values, $p_1 = -0.00007625$ with a 95% confidence interval of $(-0.0005948, 0.0004423)$, $p_2 = 0.001507$ with a 95% confidence interval of $(-0.001127, 0.00414)$, $p_3 = 1.805$ with a 95% confidence interval of $(1.802, 1.808)$, $\text{SSE} = 6.661 \cdot 10^{-9}$, $\text{R-square} = 0.999$, and $\text{RMSE} = 8.162 \cdot 10^{-5}$. Using this formula gives two more extrapolated scaling factors of 1.810629 and 1.811297. Let w_x equal $\sum_{i|x} \kappa_2(x/i) - \theta_1$ for $x = 1, 2, 3, \dots, 11,000$. Let

$w'_x = (w_x + 66.318290) * 1.811297$, $x = 1, 2, 3, \dots, 11,000$. Möbius inversion is then done on w' and the 2850 estimated zeros at x values that are the product of two distinct primes are isolated. See Figure (15) for a plot of these estimated zeros and the actual zeros (similarly isolated). See Figure (16) for a plot of the differences (estimated zeros minus actual zeros) of the two curves. See Figure (17) for a plot of the relative errors of the approximations (differences divided by actual zeros). See Figure (18) for a plot of the sorted relative errors of the new 250 estimated zeros. The relative errors of the new estimated zeros are between 0.08% and 0.21%.

Trivial Dirichlet products of the standard uniform distribution can be used as a reference point for locating zeros. In the following, the standard uniform distribution (of 2000 values) is scaled up by a factor of 5600.0. See Figure (19) for a plot of these values for $x = 1, 2, 3, \dots, 138$ (corresponding to the zeros that Hutchinson computed). See Figure (20) for a plot of these values at x values that are the product of two distinct primes and Dirichlet products of θ at x values that are the product of two distinct primes.

4 The Generalized Probit Function, Zeta Function Zeros, and the Möbius Function

For convenience, let $w(p)$ denote the probit function. The differential equation that can be used to compute w is $\frac{dw}{dp} = \frac{1}{f(w)}$ where $f(w)$ is the probability density function of w . In the case of the Gaussian distribution, $\frac{d^2w}{dp^2} = w(\frac{dw}{dp})^2$ with initial conditions of $w(\frac{1}{2}) = 0$ and $w'(\frac{1}{2}) = \sqrt{2\pi}$. Steinbrecher and Shaw's [4] method is used to solve this ODE.

Let y_x denote $\sum_{i|x} \theta_i \mu(i)$. For a normal probability distribution fit of y_x for x less than or equal to 9,999, the mean is -21.5933 with a 95% confidence interval of $(-86.9019, 43.7153)$ and the standard deviation is 3331.6 with a 95% confidence interval of $(3286.0, 3378.4)$. See Figure (21) for a plot of the sorted y_x values and $F^{-1}(p) = \mu + \sigma\Phi^{-1}(p)$ (where $\mu = -21.5933$ and $\sigma = 3331.6$) for $p = 0.0001, 0.0002, 0.0003, \dots, 0.9999$. The minimum and maximum y_x values are -9840.91 and 9411.65 and the minimum and maximum F^{-1} values are -10653 and 10610 . For larger samples of zeros, the y_x values are similarly bounded by the generalized probit function. The minimum y_x values are about 92% larger than the minimum F^{-1} values and the maximum y_x values are about 90% smaller than the maximum F^{-1} values. See Figure (22) for a plot of the means of y_x for $x = 999, 1,999, 2,999, \dots, 99,999$. There doesn't appear to be any way to predict what the means of the distributions will be, but they are small and relatively insignificant. See Figure (23) for a plot of the standard deviations of y_x for $x = 999, 1,999, 2,999, \dots, 99,999$. For a cubic least-squares fit of these values, $p_1 = 0.00364$ with a 95% confidence interval of $(0.003284,$

0.003995), $p_2 = -0.8748$ with a 95% confidence interval of $(-0.9294, -0.8201)$, $p_3 = 301.5$ with a 95% confidence interval of $(299.1, 303.9)$, $p_4 = 349.6$ with a 95% confidence interval of $(321.7, 377.5)$, $SSE=1.099 \cdot 10^5$, $R\text{-square}=1$, and $RMSE=33.83$. The curve of standard deviations is almost quadratic. See Figure (24) for a plot of the maximum y_x and F^{-1} values for $x = 999, 1,999, 2,999, \dots, 19,999$. See Figure (25) for the minimum y_x and F^{-1} values for $x = 999, 1,999, 2,999, \dots, 19,999$.

Let θ'_i denote $\theta_i / \log(\theta_i)$. Let z_x denote $\sum_{i|x} \theta'_i \mu(i)$. For a normal probability distribution fit of z_x for x less than or equal to 9,999, the mean is -3.4582 with a 95% confidence interval of $(-10.4901, 3.5736)$ and the standard deviation is 358.7124 with a 95% confidence interval of $(353.8090, 363.7546)$. See Figure (26) for a plot of the sorted z_x values and $F^{-1}(p) = \mu + \sigma \Phi^{-1}(p)$ (where $\mu = -3.4582$ and $\sigma = 358.7124$) for $p = 0.0001, 0.0002, 0.0003, \dots, 0.9999$. The minimum and maximum z_x values are -1066.36 and 992.0359 and the minimum and maximum F^{-1} values are -1148.1 and 1141.1 . For larger samples of zeros, the z_x values are similarly bounded by the generalized probit function. The minimum z_x values are about 92% larger than the minimum F^{-1} values and the maximum z_x values are about 89% smaller than the maximum F^{-1} values. See Figure (27) for a plot of the means of z_x for $x = 999, 1,999, 2,999, \dots, 19,999$. See Figure (28) for a plot of the standard deviations of z_x for $x = 999, 1,999, 2,999, \dots, 19,999$. For a quadratic least-squares fit of the standard deviations, $p_1 = -0.3416$ with a 95% confidence interval of $(-0.393, -0.2902)$, $p_2 = 35.63$ with a 95% confidence interval of $(34.52, 36.74)$, $p_3 = 36.85$ with a 95% confidence interval of $(31.78, 41.92)$, $SSE=177.3$, $R\text{-square}=0.9997$, and $RMSE=3.23$. See Figure (29) for a plot of the maximum z_x and F^{-1} values for $x = 999, 1,999, 2,999, \dots, 19,999$. See Figure (30) for the minimum z_x and F^{-1} values for $x = 999, 1,999, 2,999, \dots, 19,999$.

Let y_x denote $\sum_{i|x} (\theta_{i+1} - \theta_i) \mu(i)$. For a normal probability fit of y_x for x less than or equal to 9999, the mean is 2.6505 with a 95% confidence interval of $(2.6095, 2.6914)$ and the standard deviation is 2.0868 with a 95% confidence interval of $(2.0583, 2.1161)$. See Figure (31) for a plot of the sorted y_x values and $F^{-1}(p) = \mu + \sigma \Phi^{-1}(p)$ (where $\mu = 2.6505$ and $\sigma = 2.0868$) for $p = 0.0001, 0.0002, 0.0003, \dots, 0.9999$. The curve of sorted y_x values has a characteristic "bump" near the end of the curve. Other than this and values at the beginning of the curve, the generalized probit function approximates the sorted y_x values fairly well. The minimum and maximum y_x values are -5.171634 and 7.786355 and the minimum and maximum F^{-1} values are -4.0085 and 9.3095 . See Figure (32) for a plot of the means of y_x for $x = 999, 1,999, 2,999, \dots, 99,999$. The means are approximately equal to 2.65 . See Figure (33) for a plot of the standard deviations of y_x for $x = 999, 1,999, 2,999, \dots, 99,999$. The standard deviations slowly increase from 2.0057 to 2.1224 . See Figure (34) for a plot of the standard deviations and $\log(x) \cdot 0.014 + 2.0057$ for $x = 1, 2, 3, \dots, 100$. The standard deviations approximately increase at a rate that is pro-

portional to the logarithm. See Figure (35) for a plot of the minima of the y_x and F^{-1} values for $x = 999, 1,999, 2,999, \dots, 39,999$. The minima of y_x are not bounded by the generalized probit function. See Figure (36) for a plot of the maxima of the y_x and F^{-1} values for $x = 999, 1,999, 2,999, \dots, 39,999$. y_x increases in value at $x = 364,182$. For a normal probability fit of y_x for x less than or equal to 364,182, the mean is 2.6538 with a 95% confidence interval of (2.6468, 2.6607) and the standard deviation is 2.1363 with a 95% confidence interval of (2.1314, 2.1412). See Figure (37) for a plot of the sorted y_x values and $F^{-1}(p) = \mu + \sigma\Phi^{-1}(p)$ (where $\mu = 2.6538$ and $\sigma = 2.1363$) for $p = 0.00000275, 0.00000549, 0.00000824, \dots, 0.99999725$. The minimum and maximum y_x values are -8.711062 and 10.520115 and the minimum and maximum F^{-1} values are -4.2141 and 9.5217. The maxima of y_x are then not bounded by the generalized probit function either.

Let l_x denote the minimum of the y_x distribution. See Figure (38) for a plot of l_x for x less than or equal to 2000. l_x is a slowly decreasing step function with an initial value of $\theta_2 - \theta_1$. See Figure (39) for a plot of $-l_x$ and the moduli of $\log(\log(\log(x))) + 3$ for $x = 1,000, 2,000, 3,000, \dots, 500,000$. $-l_x$ appears to increase at the same rate as $\log(\log(\log(x)))$ when the latter is real-valued. For x less than 500,000, l_x decreases in value at $x = 2, 3, 6, 15, 195, 435, 615, 1590, 4305, 4,935, 7,995, 17,355, 32,595, 72,615, 228,165, \text{ and } 261,555$. The prime factorizations of these values are 2, 3, 2·3, 3·5, 3·5·13, 3·5·29, 3·5·41, 2·3·5·53, 3·5·7·41, 3·5·7·47, 3·5·13·41, 3·5·13·89, 3·5·41·53, 3·5·47·103, 3·5·7·41·53, and 3·5·7·47·53 respectively. The number of prime factors is non-decreasing. The corresponding l_x values are 2.898497, 1.473297, 0.817020, -1.210552, -2.2385884, -2.584503, -3.612455, -3.717184, -3.834182, -4.450978, -5.171634, -5.675754, -6.993299, -7.754984, -8.439405, and -8.711062. The values of x that are the products of 2, 2·3, 2·3·5, 2·3·5·7, 2·3·5·7·11, ... are 2, 6, 30, 210, 2,310, 30,030, The above value of 195 is between 30 and 210, the above values of 435, 615, 1,590 are between 210 and 2,310, the above values of 4,305, 4,935, 7,995, and 17,355 are between 2,310, and 30,030, etc. This is useful in determining how frequently l_x will decrease in value. The values of y_x at $x = 2, 6, 30, 210, 2,310, 30,030, \text{ and } 510,510$ are 2.898497, 0.817020, -1.078027, 0.307918, -2.025837, -1.763924, and -4.512349 respectively.

Let g_x denote the maximum of the y_x distribution. See Figure (40) for a plot of g_x for x less than or equal to 1000. g_x is a slowly increasing step function with an initial value of $\theta_2 - \theta_1$. See Figure (41) for a plot of g_x and the moduli of $\log(\log(\log(x))) + 6$ for $x = 1,000, 2,000, 3,000, \dots, 500,000$. g_x appears to increase at the same rate as $\log(\log(\log(x)))$ when the latter is real-valued. For x less than 500,000, g_x increases in value at $x = 2, 1,806, 6,118, 17,822, 25,802, 34,314, 70,518, 131,838, 186,018, 204,078, 213,486, \text{ and } 364,182$. The prime factorizations of these values are 2, 2·3·7·43, 2·7·19·23, 2·7·19·67, 2·7·19·97, 2·3·7·19·43, 2·3·7·23·73, 2·3·7·43·73, 2·3·7·43·107, 2·3·7·13·17·23, and 2·3·7·13·23·29. The number of prime factors is non-decreasing. The

corresponding g_x values are 6.887315, 6.938951, 7.786355, 7.926703, 8.147173, 8.684880, 8.930729, 8.999220, 9.061730, 9.071198, 10.498812, and 10.520155.

5 Differences Between Zeros and the Probit Function

Let s_x denote $\theta_{x+1} - \theta_x$. For a normal probability fit of s_x where x is less than or equal to 10,000, the mean is 0.9865 with a 95% confidence interval of (0.9779, 0.9950) and the standard deviation is 0.4377 with a 95% confidence interval of (0.4317, 0.4439). See Figure (42) for a plot of the sorted s_x values and $F^{-1}(p) = \mu + \sigma\Phi^{-1}(p)$ (where $\mu = 0.9865$ and $\sigma = 0.4377$) for $p = 0.0001, 0.0002, 0.0003, \dots, 0.9999$. The minimum and maximum s_x values are 0.037699 and 6.887315 and the minimum and maximum F^{-1} values are -0.4102 and 2.3832 . See Figure (43) for a plot of the means of the normal probability fits of the s_x values for $x = 1, 000, 2,000, 3,000, \dots, 100,000$. The means approximately decrease at a rate that is proportional to the reciprocal of the logarithm. See Figure (44) for a plot of the reciprocals of the means and $\log(x) \cdot 0.1415 + 1.0/1.4067$ for $x = 1, 2, 3, \dots, 100$. See Figure (45) for a plot of the standard deviations of the normal probability fits of the s_x values for $x = 1, 000, 2,000, 3,000, \dots, 100,000$. The standard deviations approximately decrease at a rate that is proportional to the reciprocal of the logarithm. See Figure (46) for a plot of reciprocals of the standard deviations and $\log(x) \cdot 0.361 + 1.0/0.6569$ for $x = 1, 2, 3, \dots, 100$. See Figure (47) for a plot of the minimum F^{-1} values for $x = 1, 000, 2,000, 3,000, \dots, 100,000$. The minimum F^{-1} values approximately increase at a rate that is proportional to the logarithm. See Figure (48) for a plot of the maximum F^{-1} values for $x = 1, 000, 2,000, 3,000, \dots, 100,000$. The maximum F^{-1} values approximately decrease at a rate that is proportional to the reciprocal of the logarithm. See Figure (49) for a plot of the minimum s_x values for $x = 1, 000, 2,000, 3,000, \dots, 100,000$. The maximum s_x value is 6.887315. For a normal probability fit of s_x where x is less than or equal to 2,000,000, the mean is 0.5660 with a 95% confidence interval of (0.5656, 0.5663) and the standard deviation is 0.2389 with a 95% confidence interval of (0.2387, 0.2391). See Figure (50) for a plot of the sorted s_x values and $F^{-1}(p) = \mu + \sigma\Phi^{-1}(p)$ (where $\mu = 0.5660$ and $\sigma = 0.2389$) for $p = 0.0000005, 0.0000010, 0.0000015, \dots, 0.9999995$. The minimum and maximum s_x values are 0.002959 and 6.887315 and the minimum and maximum F^{-1} values are -0.2022 and 1.3342 . For a normal probability fit of s_x where x is less than or equal to 2,000,000 and s_x values greater than 2.0 are excluded, the mean is 0.5657 with a 95% confidence interval of (0.5654, 0.5661) and the standard deviation is 0.2380 with a 95% confidence interval of (0.2377, 0.2382). See Figure (51) for a plot of the sorted s_x values and $F^{-1}(p) = \mu + \sigma\Phi^{-1}(p)$ (where $\mu = 0.5657$ and $\sigma = 0.2380$) for $p = 0.00000050006, 0.00000100012, 0.00000150018, \dots, 0.999999990$. The minimum and maximum s_x values are 0.002959 and 1.997197 and the minimum and maximum F^{-1} values are -0.1996 and 1.3310 . There appear to be only 242 s_x

values greater than 2.0.

Let t_x denote $\theta'_{x+1} - \theta'_x$. For a normal probability fit of t_x where x is less than or equal to 10,000, the mean is 0.1069 with a 95% confidence interval of (0.1057, 0.1080) and the standard deviation is 0.0603 with a 95% confidence interval of (0.0595, 0.0611). See Figure (52) for a plot of the sorted t_x values and $F^{-1}(p) = \mu + \sigma\Phi^{-1}(p)$ (where $\mu = 0.1069$ and $\sigma = 0.0603$) for $p = 0.0001, 0.0002, 0.0003, \dots, 0.9999$. The minimum and maximum t_x values are 0.003777 and 1.565886 and the minimum and maximum F^{-1} values are -0.0855 and 0.2993 . See Figure (53) for a plot of the means of the normal probability fits of the t_x values for $x = 1, 000, 2,000, 3,000, \dots, 100,000$. The means approximately decrease at a rate that is proportional to the reciprocal of the logarithm squared. See Figure (54) for a plot of the reciprocals of the means and $\log(x) \cdot \log(x) \cdot 0.31 + 1.0/0.1904$ for $x = 1, 2, 3, \dots, 100$. See Figure (55) for a plot of the standard deviations of the normal probability fits of the t_x values for $x = 1, 000, 2,000, 3,000, \dots, 100,000$. The standard deviations approximately decrease at a rate that is proportional to the reciprocal of the logarithm squared. See Figure (56) for a plot of reciprocals of the standard deviations and $\log(x) \cdot \log(x) \cdot 0.74 + 1.0/0.1164$ for $x = 1, 2, 3, \dots, 100$. See Figure (57) for a plot of the minimum F^{-1} values for $x = 1, 000, 2,000, 3,000, \dots, 100,000$. See Figure (58) for a plot of the maximum F^{-1} values for $x = 1, 000, 2,000, 3,000, \dots, 100,000$. See Figure (59) for a plot of the minimum t_x values for $x = 1, 000, 2,000, 3,000, \dots, 100,000$. The maximum t_x value is 1.565886. For a normal probability fit of t_x where x is less than or equal to 2,000,000, the mean is 0.0406 with a 95% confidence interval of (0.0406, 0.0406) and the standard deviation is 0.0189 with a 95% confidence interval of (0.0189, 0.0189). See Figure (60) for a plot of the sorted t_x values and $F^{-1}(p) = \mu + \sigma\Phi^{-1}(p)$ (where $\mu = 0.0406$ and $\sigma = 0.0189$) for $p = 0.0000005, 0.0000010, 0.0000015, \dots, 0.9999995$. The minimum and maximum t_x values are 0.000204 and 1.565886 and the minimum and maximum F^{-1} values are -0.0202 and 0.1014 . For a normal probability fit of t_x where x is less than or equal to 2,000,000 and t_x values greater than 0.4 are excluded, the mean is 0.0406 with a 95% confidence interval of (0.0406, 0.0406) and the standard deviation is 0.0187 with a 95% confidence interval of (0.0187, 0.0187). See Figure (61) for a plot of the sorted t_x values and $F^{-1}(p) = \mu + \sigma\Phi^{-1}(p)$ (where $\mu = 0.0406$ and $\sigma = 0.0187$) for $p = 0.00000050001, 0.00000100002, 0.00000150003, \dots, 0.99999990$. The minimum and maximum t_x values are 0.000204 and 0.394989 and the minimum and maximum F^{-1} values are -0.0195 and 0.1007 . There appear to be only 42 t_x values greater than 0.4.

6 Log-Normal Distributions

The log-normal distribution is a continuous distribution in which the logarithm of a variable has a normal distribution. A log-normal distribution results if the variable is the product of a large number of independent identically-distributed variables. θ, θ' and their Dirichlet products appear to be log-normal. For a nor-

mal probability fit of θ for x less than or equal to 100,000, the mean is 39,694 with a 95% confidence interval of (39563, 39824) and the standard deviation is 21076 with a 95% confidence interval of (20984, 21169). Denote $\log(\log(\log(\theta_x)))$ by t_x . The mean of the normal probability fit of t_x for x less than or equal to 100,000 is 0.8460 with a 95% confidence interval of (0.8455, 0.8463) and the standard deviation is 0.0423 with a 95% confidence interval of (0.0421, 0.0425). See Figure (62) for a plot of t_x for x less than or equal to 2,000,000. The t_x values slowly approach 1. For a normal probability fit of t_x , the mean is 0.9413 with a 95% confidence interval of (0.9413, 0.9413) and the standard deviation is 0.0306 with a 95% confidence interval of (0.0306, 0.0306).

Let y_x denote $\sum_{i|x} \theta(x/i)$ and let u_x denote $\log(\log(\log(y_x)))$. For a normal probability fit of u_x for x less than or equal to 100,000, the mean is 0.8668 with a 95% confidence interval of (0.8666, 0.8671) and the standard deviation is 0.0409 with a 95% confidence interval of (0.0407, 0.0410). See Figure (63) for a plot of the sorted u_x values. The u_x values characteristically tip up slightly near the end of the curve. For a normal probability fit of u_x for x less than or equal to 2,000,000, the mean is 0.9558 with a 95% confidence interval of (0.9557, 0.9558) and the standard deviation is 0.0309 with a 95% confidence interval (0.0303, 0.0303). See Figure (64) for a plot of the sorted u values. The last 3891 values are greater than 1.

Denote $\log(\log(\log(\theta'_x)))$ by t_x . See Figure (65) for a plot of t_x for x less than or equal to 2,000,000. For a normal probability fit of t_x , the mean is 0.8513 with a 95% confidence interval of (0.8513, 0.8514) and the standard deviation is 0.0393 with a 95% confidence interval of (0.0393, 0.0393). The arguments of $\log(t_x)$ other than the first 14 are π . See Figure (66) for a plot of the exceptions. For a cubic least-squares fit of the values, $p_1 = 0.0004801$ with a 95% confidence interval of (0.0003184, 0.0006417), $p_2 = -0.01133$ with a 95% confidence interval of (-0.01501, -0.007649), $p_3 = 0.1343$ with a 95% confidence interval of (0.1101, 0.1585), $p_4 = 1.594$ with a 95% confidence interval of (.55, 1.637), SSE=0.001842, R-square=0.9977, and RMSE=0.01357.

Let y_x denote $\sum_{i|x} \theta'(x/i)$ and let u_x denote $\log(\log(\log(y_x)))$. See Figure (67) for a plot of the sorted u_x values for x less than or equal to 2,000,000. For a normal probability fit of u_x , the mean is 0.8726 with a 95% confidence interval of (0.8726, 0.8727) and the standard deviation is 0.0384 with a 95% confidence interval of (0.0384, 0.0384). The arguments of $\log(u_x)$, are usually π , the exceptions being 1.7011, 2.2352, 2.3117, and 2.5454 at the beginning of the curve. See Figure (68) for a plot of these values. For a cubic least-squares fit of the values, $p_1 = 0.1025$, $p_2 = -0.8436$, $p_3 = 2.348$, $p_4 = 0.0946$, and R-square=1.0.

7 Generalized Ramanujan Sums Involving θ

In the following, the values of both f and g (in the expression $\sum_{d|(n,k)} f(d)g(k/d)$) are set to the θ values. Let $r(x, k)$ denote this convolution. The same curves occur as for the Dirichlet products of θ , but the number of distinct (non-overlapping) curves is determined by the number of divisors of k . See Figure (69) for a plot of $r(x, 11)$ for x less than or equal to 100,000. See Figure (70) for a plot of the sorted $r(x, 11)$ values. The tail at the end of the curve consists of $r(x, 11)$ values at x values that are a multiple of 11. For a quadratic least-squares fit of the curve (including the tail), $p_1 = 0.0007672$ with a 95% confidence interval of (0.0006829, 0.0008515), $p_2 = 680.2$ with a 95% confidence interval of (679.3, 681.1), $p_3 = 7975$ with a 95% confidence interval of (6090, 9860), SSE=1.027·10¹³, R-square=0.9997, and RMSE=3.205·10⁴. Similar curves are obtained for prime k values. See Figure (71) for a plot of $r(x, 5)$ for x less than or equal to 100. Discounting the x values that are a multiple of 5, the values increase almost linearly in groups of 4. See Figure (72) for a plot of $r(x, 6)$ for x less than or equal to 10,000. See Figure (73) for a plot of the moduli of the Fourier transform of $r(x, 6)$. See Figure (74) for a plot of the arguments of the Fourier transform of $r(x, 6)$. In general, there are k relatively large spikes in the moduli other than those at the start and end of the curve. See Figure (75) for a plot of the first 50 moduli and Figure (76) for a plot of the last 50 moduli. There is then no significant “information” in this convolution other than the k spikes.

Let $s(x, k)$ denote the above convolution when both f and g are set to the θ' values. See Figure (77) for a plot of $s(x, 13)$ for x less than or equal to 10,000. See Figure (78) for a plot of the sorted $s(x, 13)$ values. For a linear least-squares fit of the curve (including the tail), $p_1 = 72.12$ with a 95% confidence interval of (72.1, 72.14) and $p_2 = -292.33$ with a 95% confidence interval of (-388.4, -196.1), SSE=6.011·10⁸, R-square=0.999, and RMSE=2452. Curves with a better linear least-squares fit can be obtained by using larger prime k values. See Figure (79) for a plot of $s(x, 11)$ for x less than or equal to 100. See Figure (80) for a plot of $s(x, 30)$ for x less than or equal to 10,000. See Figure (81) for a plot of the moduli of the Fourier transform of $s(x, 30)$. See Figure (82) for a plot of the arguments of the Fourier transform of $s(x, 30)$.

8 Dirichlet Inverses of θ

The inverse Dirichlet product of an arithmetical function f where $f(1) \neq 0$ is given by the recursion formula $f^{-1}(1) = 1/f(1)$, $f^{-1}(n) = (-1/f(1)) \sum_{d|n, d < n} f(n/d)f^{-1}(d)$ for $n > 1$. Let y_x denote the Dirichlet inverse of θ_x . For a normal probability fit of y_x for x less than or equal to 9,999, the mean is -1.7016 with a 95% confidence interval of (-1.9293, -1.4740) and the standard deviation is 11.6133 with a 95% confidence interval of (11.4546, 11.7766). See Figure (83) for a plot

of the sorted y_x values and $F^{-1}(p) = \mu + \sigma\Phi^{-1}(p)$ (where $\mu = -1.7016$ and $\sigma = 11.6133$) for $p = 0.0001, 0.0002, 0.0003, \dots, 0.9999$. The minimum and maximum y_x values are -49.3269 and 31.6628 and the minimum and maximum F^{-1} values are -38.7599 and 35.3567 . In general, the minimum y_x value is less than the minimum F^{-1} value and the maximum y_x value is less than the maximum F^{-1} value. See Figure (84) for a plot of the means of the distributions of y_x for x less than or equal to 1,000, 2,000, 3,000, ..., 100,000. For a cubic least-squares fit of the means, $p_1 = -2.165 \cdot 10^{-6}$ with a 95% confidence interval of $(-2.433 \cdot 10^{-6}, -1.896 \cdot 10^{-6})$, $p_2 = 0.0005025$ with a 95% confidence interval of $(0.0004612, 0.0005437)$, $p_3 = -0.1513$ with a 95% confidence interval of $(-0.1531, -0.1495)$, $p_4 = -0.198$ with a 95% confidence interval of $(-0.2191, -0.1769)$, SSE=0.06266, R-square=0.9999, and RMSE=0.02555. The curve of means is almost quadratic. See Figure (85) for a plot of the standard deviations of the distributions of y_x for x less than or equal to 1,000, 2,000, 3,000, ..., 100,000. For a cubic least-squares fit of the standard deviations, $p_1 = 1.543 \cdot 10^{-5}$ with a 95% confidence interval of $(1.38 \cdot 10^{-5}, 1.706 \cdot 10^{-5})$, $p_2 = -0.003588$ with a 95% confidence interval of $(-0.003837, -0.003338)$, $p_3 = 0.9721$ with a 95% confidence interval of $(0.9612, 0.9829)$, $p_4 = 1.991$ with a 95% confidence interval of $(1.864, 2.119)$, SSE=2.299, R-square=1, and RMSE=0.1548. The curve of standard deviations is almost quadratic. The curves of minimum and maximum y_x values are also cubic.

Let y'_x denote the Dirichlet inverse of θ'_x . For a normal probability fit of y'_x for x less than or equal to 9,999, the mean is -1.9315 with a 95% confidence interval of $(-2.1039, -1.7591)$ and the standard deviation is 8.7933 with a 95% confidence interval of $(8.6731, 8.9169)$. See Figure (86) for a plot of the sorted y'_x values and $F^{-1}(p) = \mu + \sigma\Phi^{-1}(p)$ (where $\mu = -1.9315$ and $\sigma = 8.7933$) for $p = 0.0001, 0.0002, 0.0003, \dots, 0.9999$. The minimum and maximum y'_x values are -37.6306 and 19.8090 and the minimum and maximum F^{-1} values are -29.9911 and 26.1281 . In general, the minimum y'_x value is less than the minimum F^{-1} value and the maximum y'_x value is less than the maximum F^{-1} value. See Figure (87) for a plot of the means of the distributions of y'_x for x less than or equal to 1,000, 2,000, 3,000, ..., 20,000. For a quadratic least-squares fit of the means, $p_1 = 0.001844$ with a 95% confidence interval of $(0.001564, 0.002124)$, $p_2 = -0.1937$ with a 95% confidence interval of $(-0.1997, -0.1876)$, $p_3 = -0.1805$ with a 95% confidence interval of $(-0.2081, -0.1529)$, SSE=0.005255, R-square=0.9997, and RMSE=0.01758. See Figure (88) for a plot of the standard deviations of the distributions of y'_x for x less than or equal to 1,000, 2,000, 3,000, ..., 20,000. For a quadratic least-squares fit of the standard deviations, $p_1 = -0.008785$ with a 95% confidence interval of $(-0.01017, -0.007401)$, $p_2 = 0.8265$ with a 95% confidence interval of $(0.7965, 0.8564)$, $p_3 = 1.412$ with a 95% confidence interval of $(1.276, 1.548)$, SSE=0.1285, R-square=0.9995, and RMSE=0.08693.

Let z_x denote the Dirichlet inverse of $\theta_{x+2} - \theta_x$. For a normal probability fit of z_x for x less than or equal to 9,999, the mean is -0.00053505 with a 95%

confidence interval of $(-0.0010, 0)$ and the standard deviation is 0.0249 with a 95% confidence interval of $(0.0245, 0.0252)$. See Figure (89) for a plot of z_x for x less than or equal to 9,999. See Figure (90) for a plot of the sorted z_x values and $F^{-1}(p) = \mu + \sigma\Phi^{-1}(p)$ (where $\mu = -0.00053505$ and $\sigma = 0.0249$) for $p = 0.0001, 0.0002, 0.0003, \dots, 0.9999$. The minimum and maximum z_x values are -0.2699 and 0.3007 and the minimum and maximum F^{-1} values are -0.08 and 0.0789 . In general, the z_x values bound the F^{-1} values. See Figure (91) for a plot of the means of the distributions of z_x for x less than or equal to 1,000, 2,000, 3,000, ..., 60,000. Other than being small, there isn't much pattern to the means. See Figure (92) for a plot of the standard deviations of the distributions of z_x for x less than or equal to 1,000, 2,000, 3,000, ..., 60,000. The standard deviations slowly decrease. See Figure (93) for a plot of the reciprocals of the standard deviations and $\log(x) \cdot 0.3 + 1.0/0.0283$ for $x = 1, 2, 3, \dots, 60$. The two curves appear to increase at about the same rate.

For x less than or equal to 1,000,000, the maximum z_x values increase at $x = 390, 2,340, 6,930, 13,260, 30,030, 46,410, 79,560, 119,340,$ and $180,180$. The prime factorizations of these values are $2 \cdot 3 \cdot 5 \cdot 13, 2^2 \cdot 3^2 \cdot 5 \cdot 13, 2 \cdot 3^2 \cdot 5 \cdot 7 \cdot 11, 2^2 \cdot 3 \cdot 5 \cdot 13 \cdot 17, 2 \cdot 3 \cdot 5 \cdot 7 \cdot 11 \cdot 13, 2 \cdot 3 \cdot 5 \cdot 7 \cdot 13 \cdot 17, 2^3 \cdot 3^2 \cdot 5 \cdot 13 \cdot 17, 2^2 \cdot 3^3 \cdot 5 \cdot 13 \cdot 17,$ and $2^2 \cdot 3^2 \cdot 5 \cdot 7 \cdot 11 \cdot 13$. The number of prime factors (counting powers of primes) is non-decreasing and even. The corresponding maximum z_x values are $0.091944, 0.148888, 0.212224, 0.300685, 0.359688, 0.431405, 0.437987, 0.547892, 0.682205,$ and 1.091032 . See Figure (94) for a plot of the maxima of the z_x distributions for x less than or equal to 5,000.

For x less than or equal to 1,000,000, the minimum z_x values decrease at $x = 2, 78, 630, 780, 1,170, 2,310, 2,730, 6,630, 16,380, 25,740, 39,780, 90,090, 360,360, 540,540,$ and $900,900$. The prime factorizations of these values are $2, 2 \cdot 3 \cdot 13, 2 \cdot 3^2 \cdot 5 \cdot 7, 2^2 \cdot 3 \cdot 5 \cdot 13, 2 \cdot 3^2 \cdot 5 \cdot 13, 2 \cdot 3 \cdot 5 \cdot 7 \cdot 11, 2 \cdot 3 \cdot 5 \cdot 7 \cdot 13, 2 \cdot 3 \cdot 5 \cdot 13 \cdot 17, 2^2 \cdot 3^2 \cdot 5 \cdot 7 \cdot 13, 2^2 \cdot 3^2 \cdot 5 \cdot 11 \cdot 13, 2^2 \cdot 3^2 \cdot 5 \cdot 13 \cdot 17, 2 \cdot 3^2 \cdot 5 \cdot 7 \cdot 11 \cdot 13, 2^3 \cdot 3^2 \cdot 5 \cdot 7 \cdot 11 \cdot 13, 2^2 \cdot 3^3 \cdot 5 \cdot 7 \cdot 11 \cdot 13,$ and $2^2 \cdot 3^2 \cdot 5^2 \cdot 7 \cdot 11 \cdot 13$. The number of prime factors (counting powers of primes) is non-decreasing and odd. The corresponding minimum z_x values are $0.091944, -0.079490, -0.086033, -0.095726, -0.133309, -0.168437, -0.193491, -0.205926, -0.269875, -0.317359, -0.339756, -0.615993, -0.715986, -0.913493, -1.359183,$ and -1.385499 . See Figure (95) for a plot of the minima of the z_x distributions for x less than or equal to 5,000.

Let z'_x denote the Dirichlet inverse of $\theta'_{x+2} - \theta'_x$. For a normal probability fit of z'_x for x less than or equal to 9,999, the mean is -0.0013 with a 95% confidence interval of $(-0.0025, -0.0001)$ and the standard deviation is 0.0614 with a 95% confidence interval of $(0.0605, 0.0622)$. See Figure (96) for a plot of z'_x for x less than or equal to 9,999. See Figure (97) for a plot of the sorted z'_x values and $F^{-1}(p) = \mu + \sigma\Phi^{-1}(p)$ (where $\mu = -0.0013$ and $\sigma = 0.0614$) for $p = 0.0001, 0.0002, 0.0003, \dots, 0.9999$. The minimum and maximum z'_x values are -0.652787 and 0.721099 and the minimum and maximum F^{-1} values are -0.1972 and 0.1946 . In general, the z'_x values bound the F^{-1} values. See Figure

(98) for a plot of the means of the distributions of z'_x for x less than or equal to 1,000, 2,000, 3,000, ..., 60,000. Other than being small, there isn't much pattern to the means. See Figure (99) for a plot of the standard deviations of the distributions of z'_x for x less than or equal to 1,000, 2,000, 3,000, ..., 60,000. The standard deviations slowly decrease. See Figure (100) for a plot of the reciprocals of the standard deviations and $\log(x) \cdot 1.925726 + 1.0/0.0853$ for $x = 1, 2, 3, \dots, 60$. The standard deviations are accurately modeled.

For x less than or equal to 1,000,000, the maximum z'_x values increase at $x = 390, 2,340, 6,930, 13,260, 30,030, 80,010, 119,340,$ and $180,180$. The number of prime factors (counting powers of primes) is non-decreasing and even. The corresponding maximum z'_x values are 0.442263, 0.548131, 0.721099, 0.813133, 0.958113, 1.082810, 1.345843, and 2.081319.

For x less than or equal to 1,000,000, the minimum z'_x values decrease at $x = 2, 780, 1,170, 2,310, 2,730, 6,630, 16,380, 25,740, 39,780, 90,090, 360,360, 510,510, 540,540,$ and $900,900$. The number of prime factors (counting powers of primes) is non-decreasing and odd. The corresponding minimum z'_x values are $-0.339049, -0.369013, -0.466524, -0.508299, -0.542218, -.652787, -0.731160, -0.768962, -1.295561, -1.468219, -1.623613, -1.632653, -2.428308,$ and -2.471748 .

See Cox [5] for the software used to determine the above results.

References

- [1] Odlyzko, A. M., “www.dtc.umn.edu/~odlyzko/zeta_tables/index.html”
- [2] Hutchinson, J. I. On the roots of the Riemann zeta-function. *Trans. Amer. Math. Soc.* 27, 49-60 (1925)
- [3] Gram, J.-P. Sur les Zéros de la Fonction $\zeta(s)$ de Riemann. *Acta Math.* 27, 289-304 (1903)
- [4] Steinbrecher, G., Shaw, W.T., Quantile mechanics. *European Journal of Applied Mathematics* 19 (2): 87-112 (2008)
- [5] Cox, D., “www.darrellcox.website/riemann.htm”

Figure 1

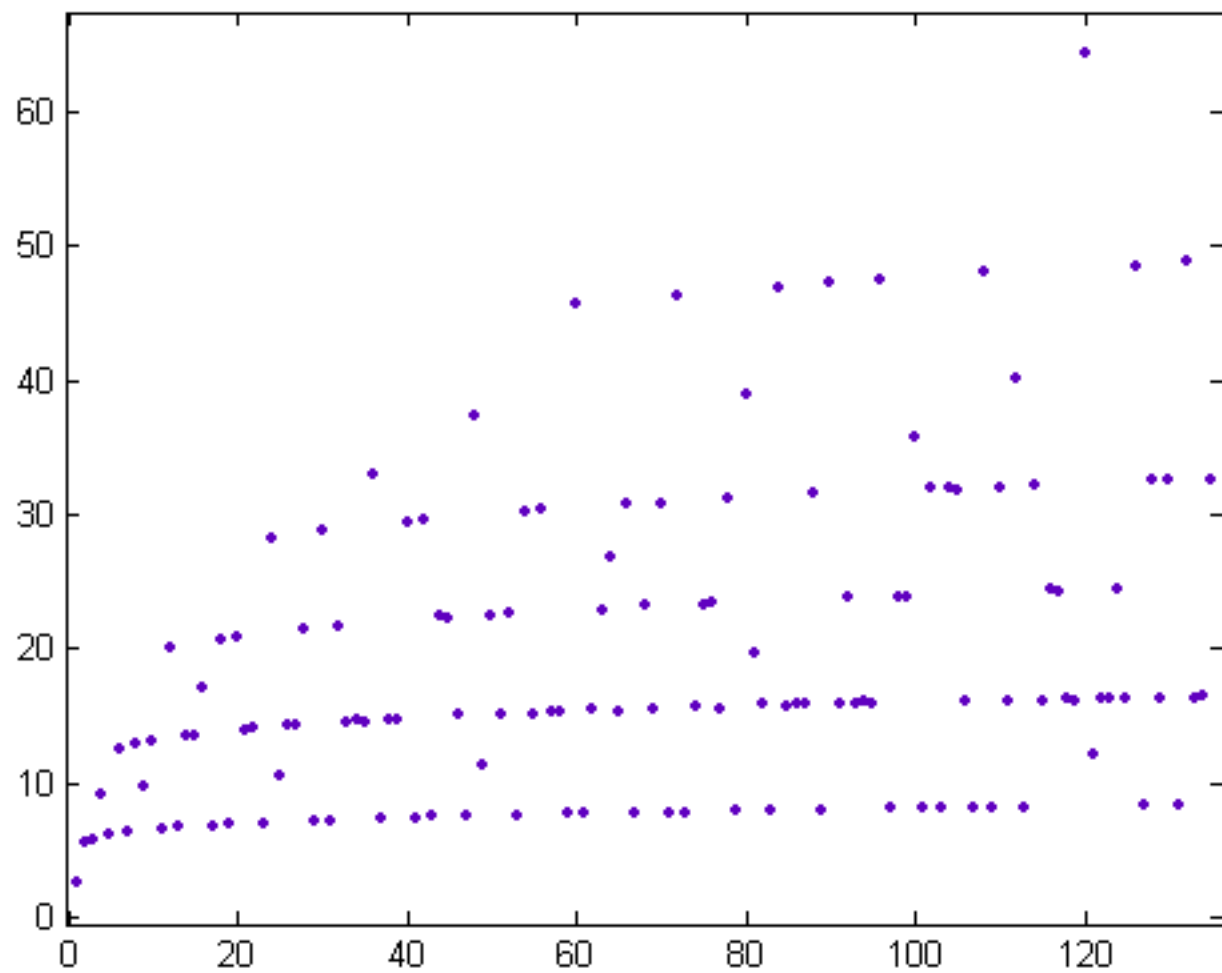


Figure 2

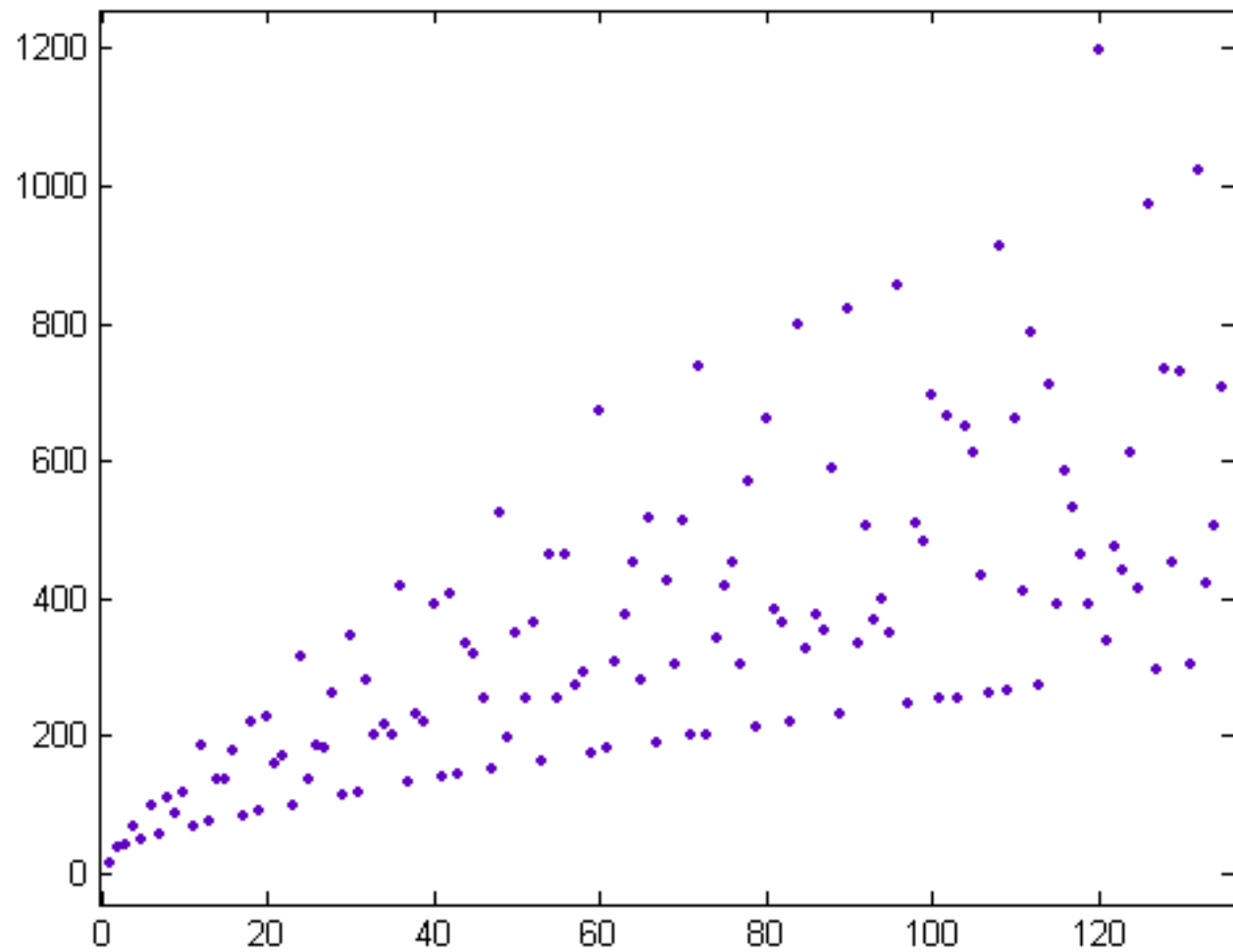


Figure 3

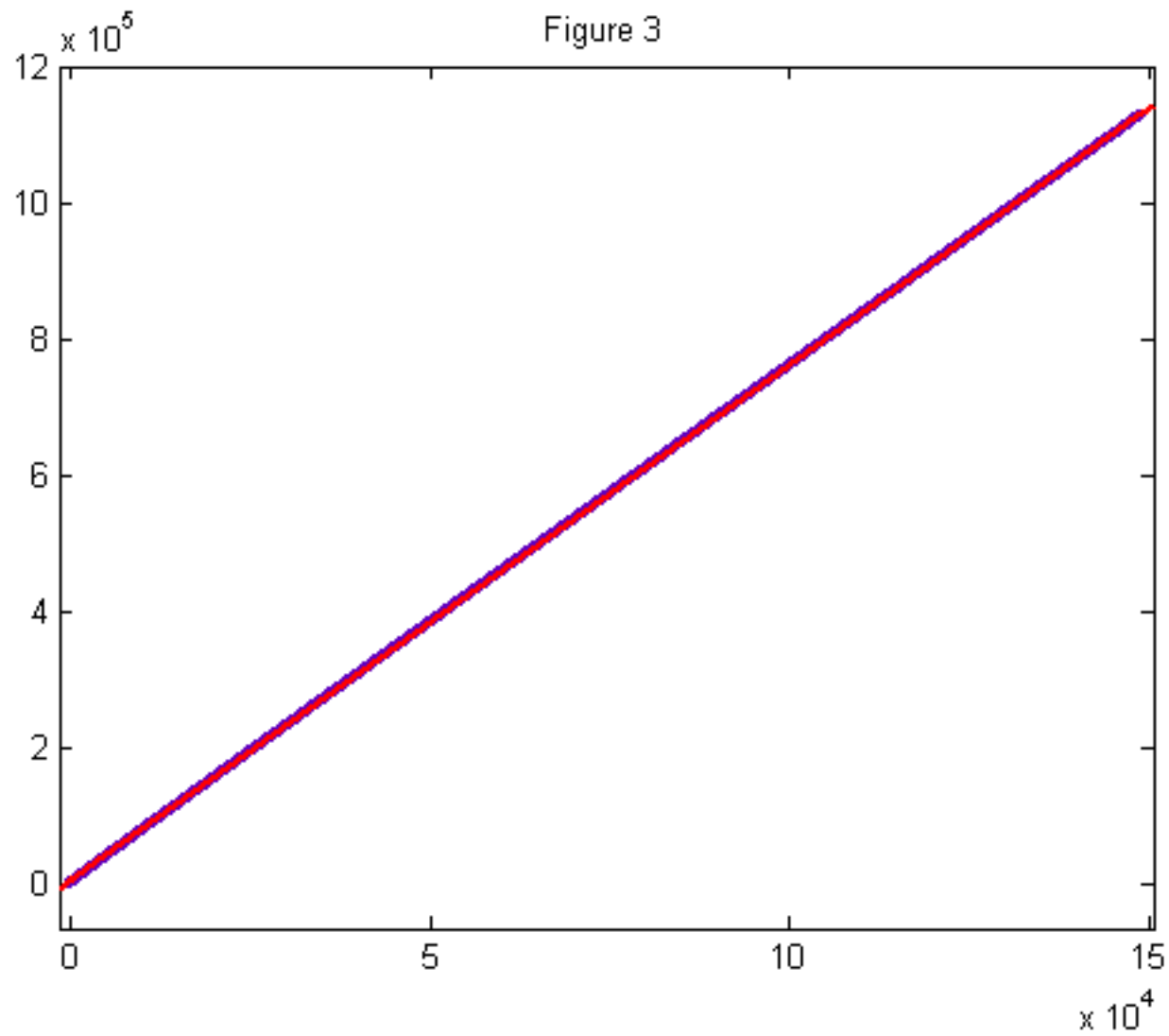


Figure 4

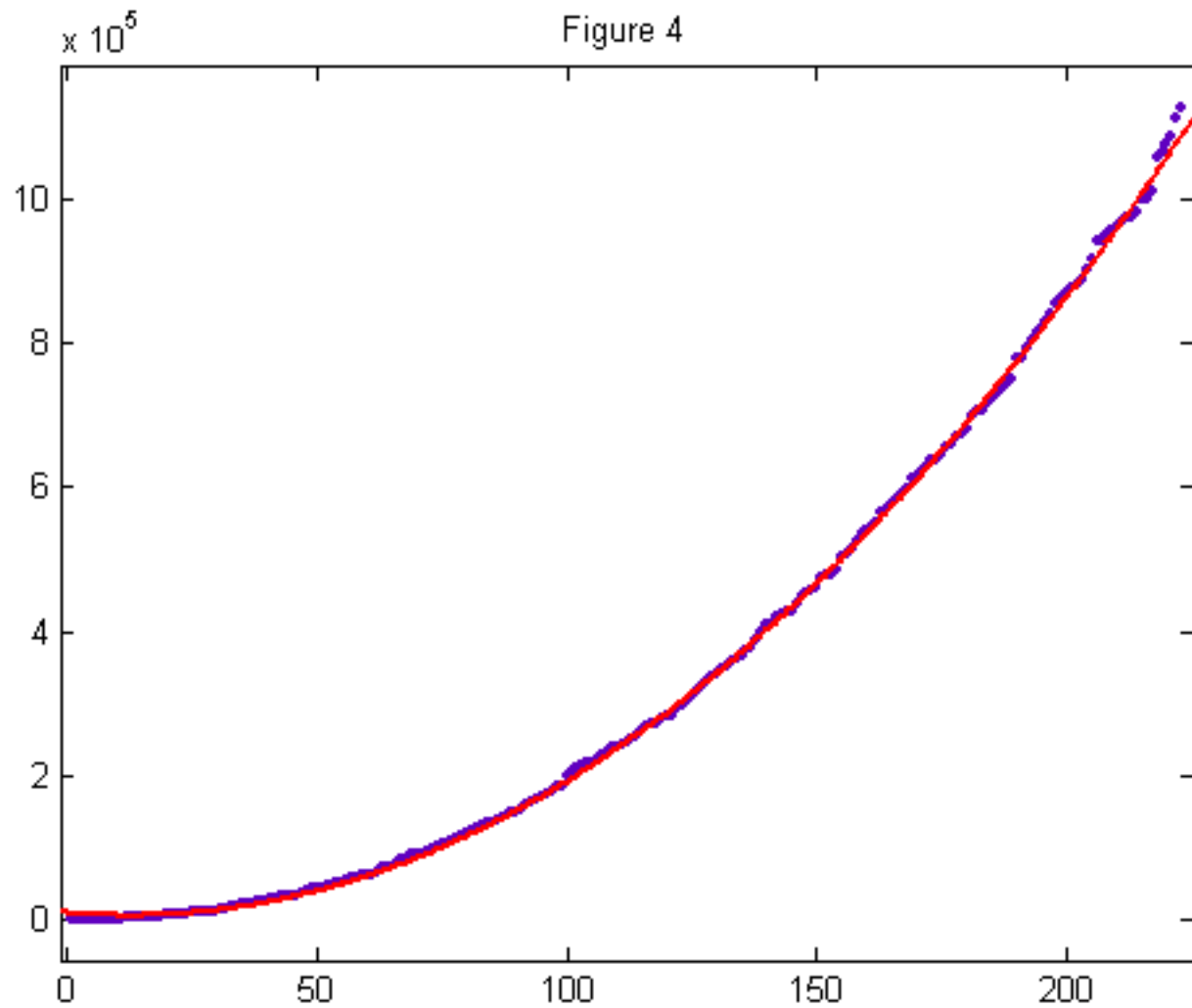


Figure 5

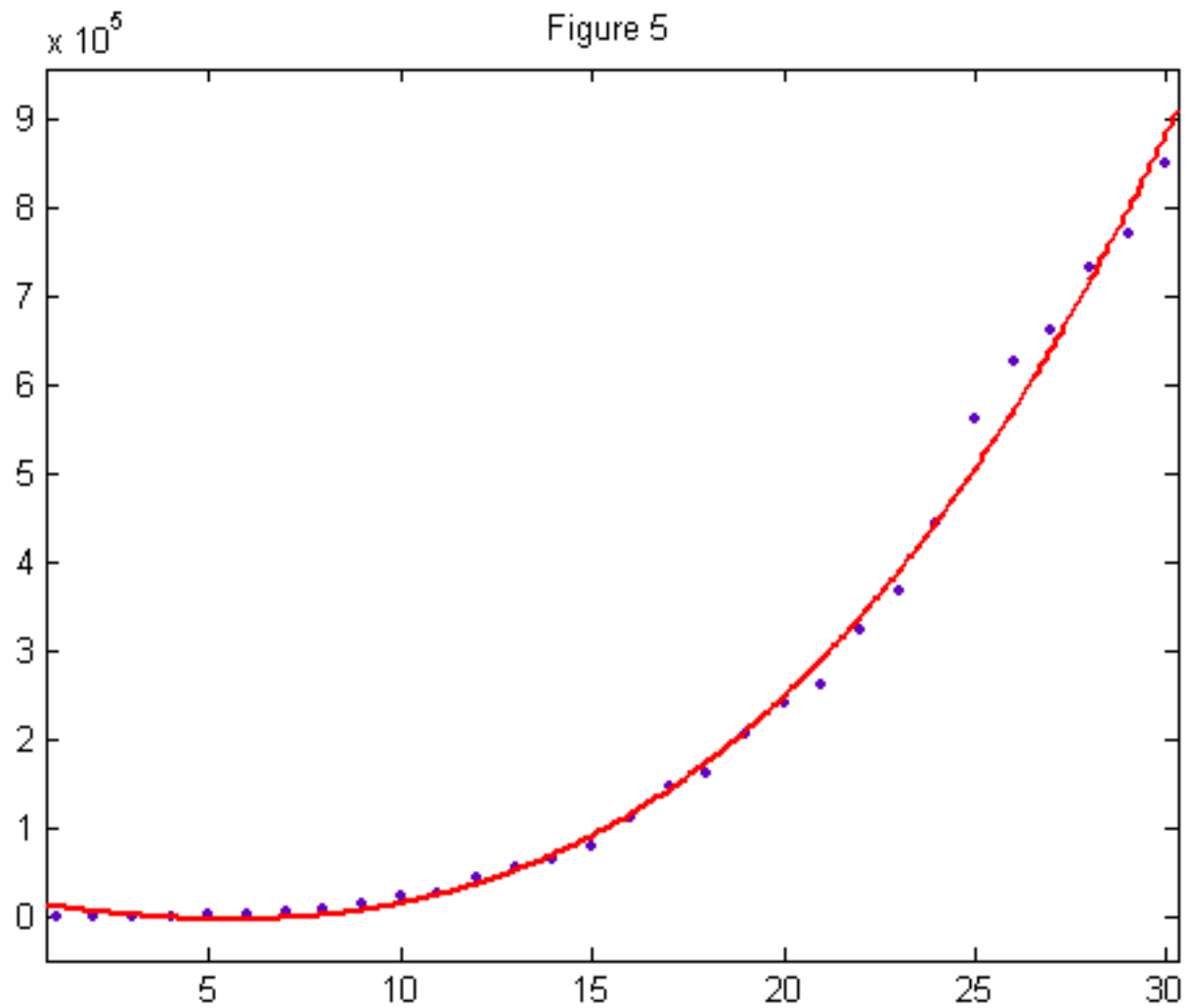


Figure 6

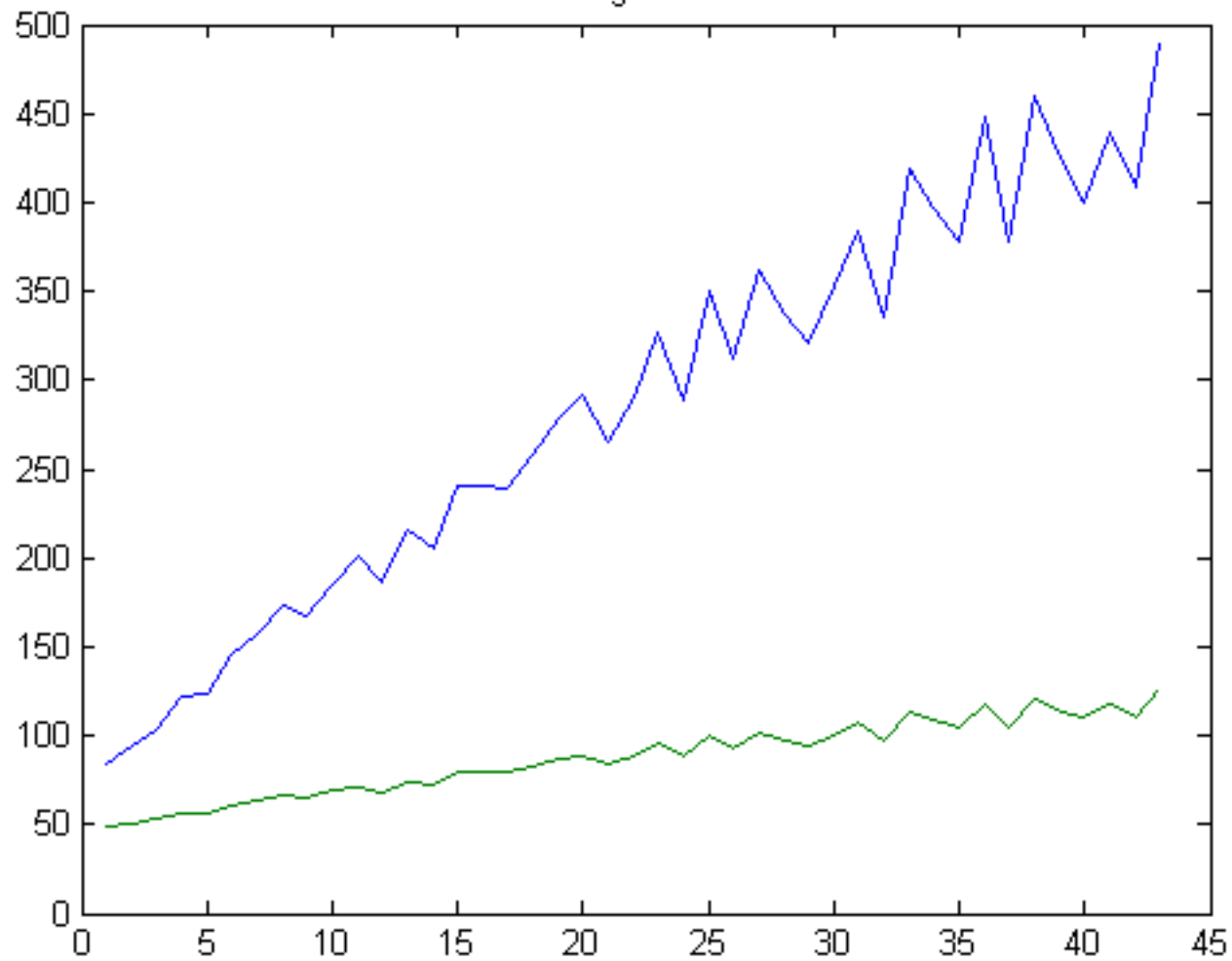


Figure 7

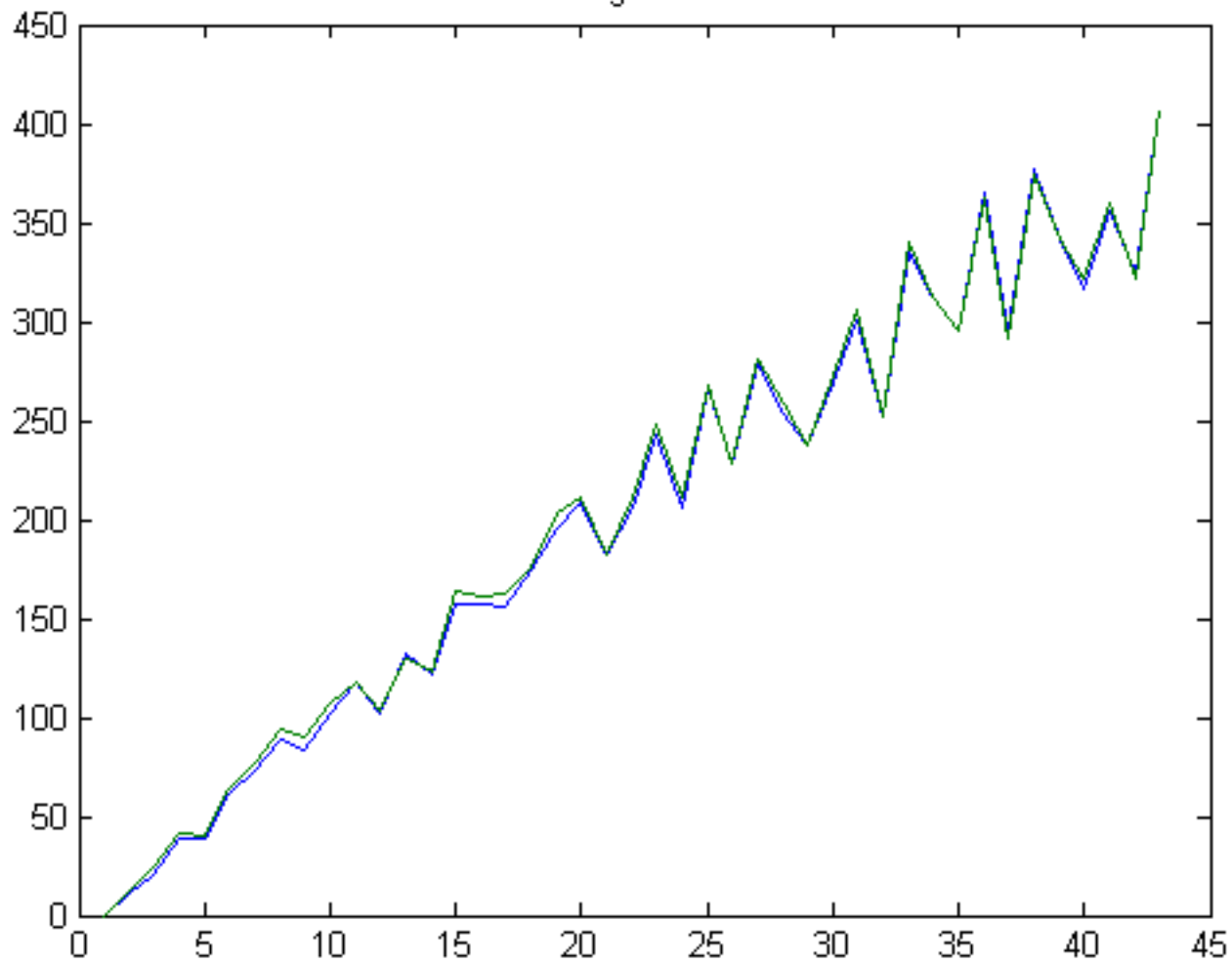


Figure 8

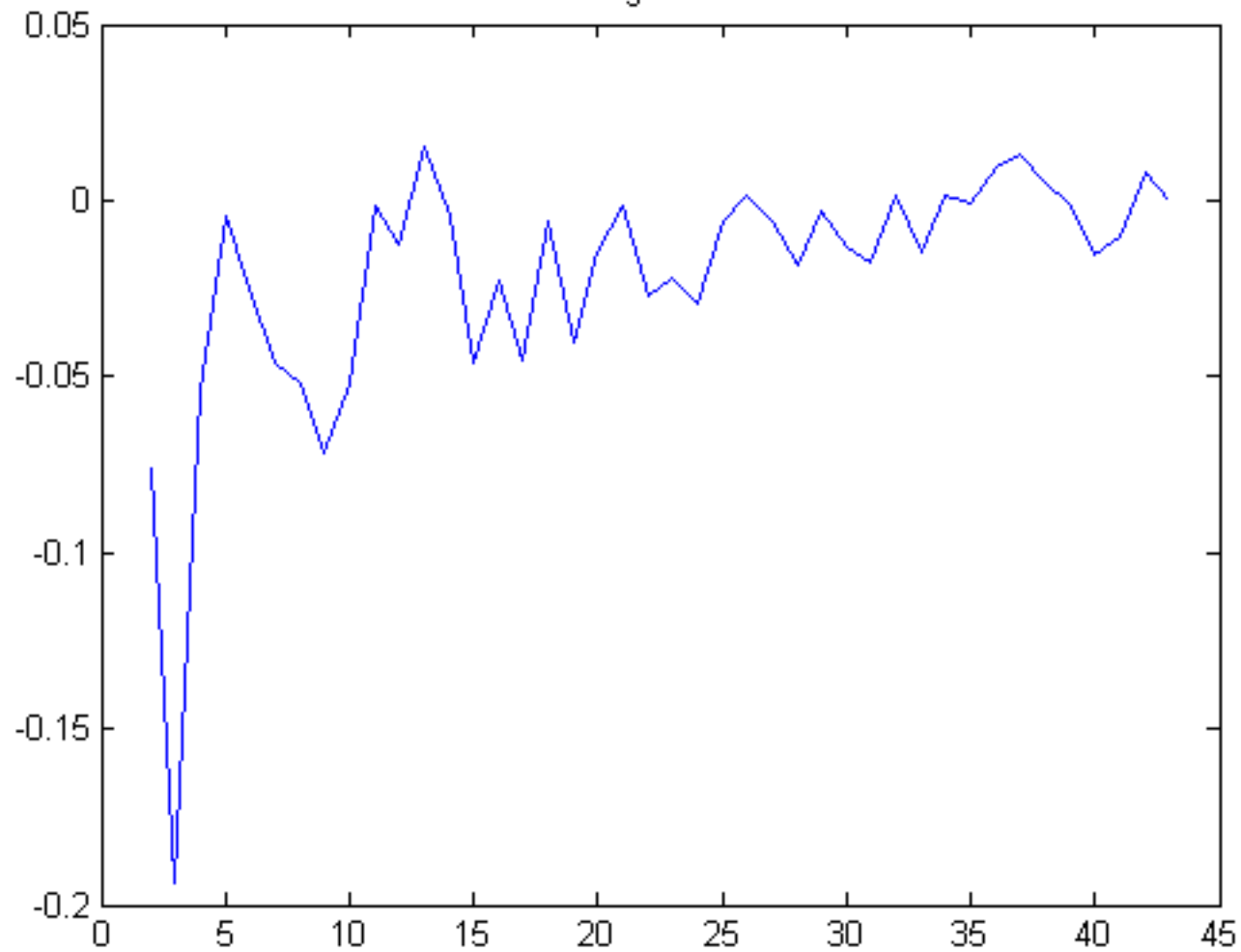


Figure 9

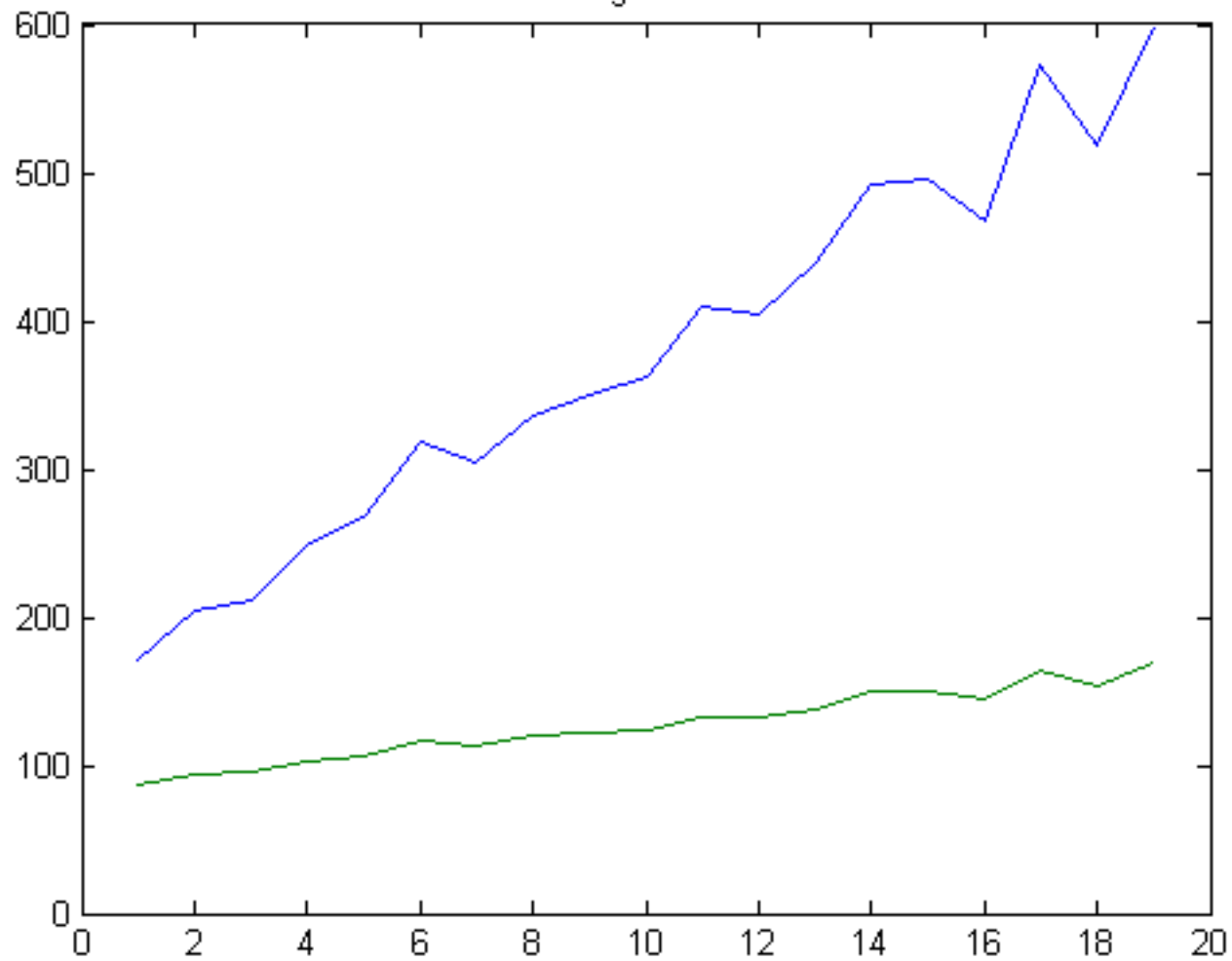


Figure 10

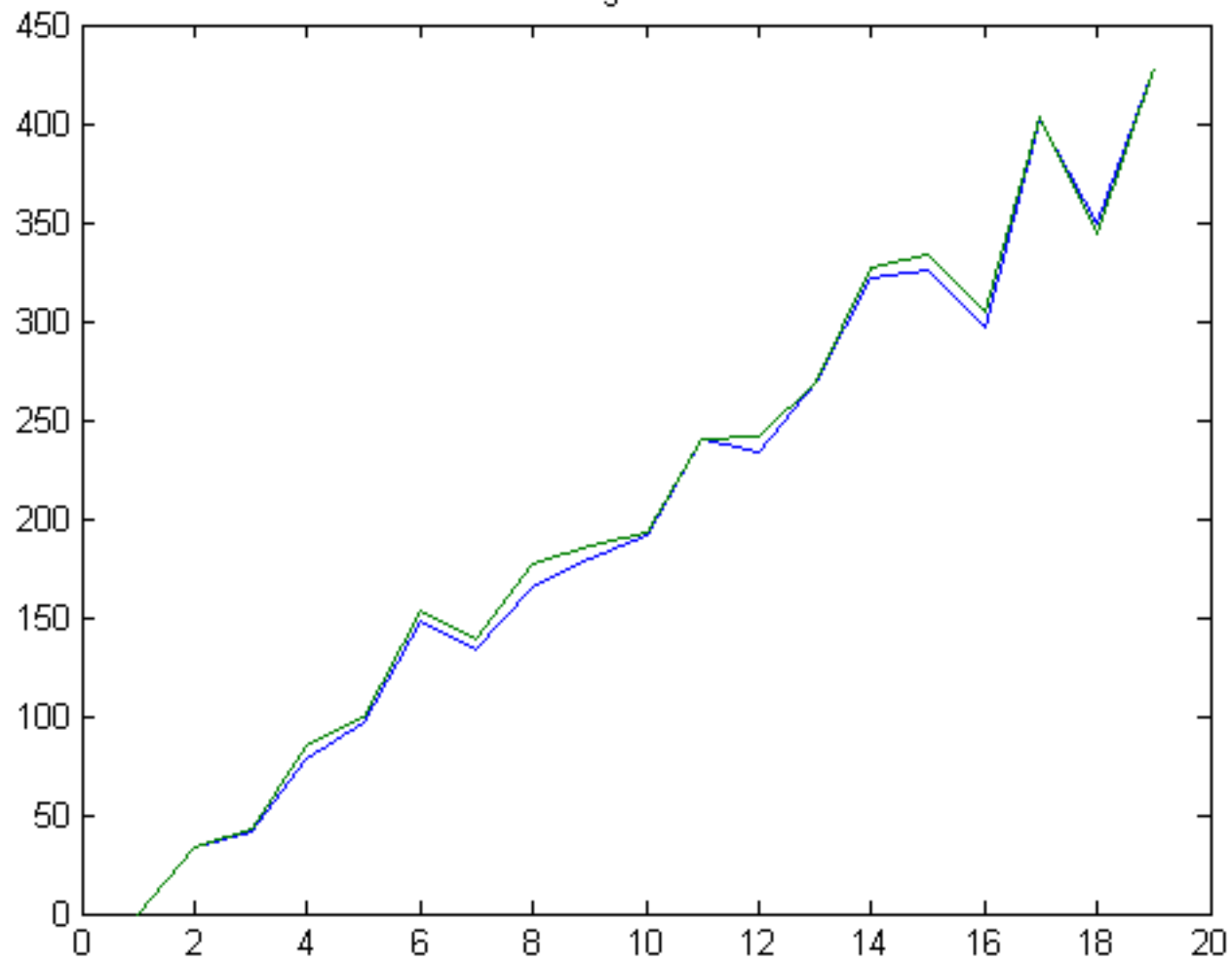


Figure 11

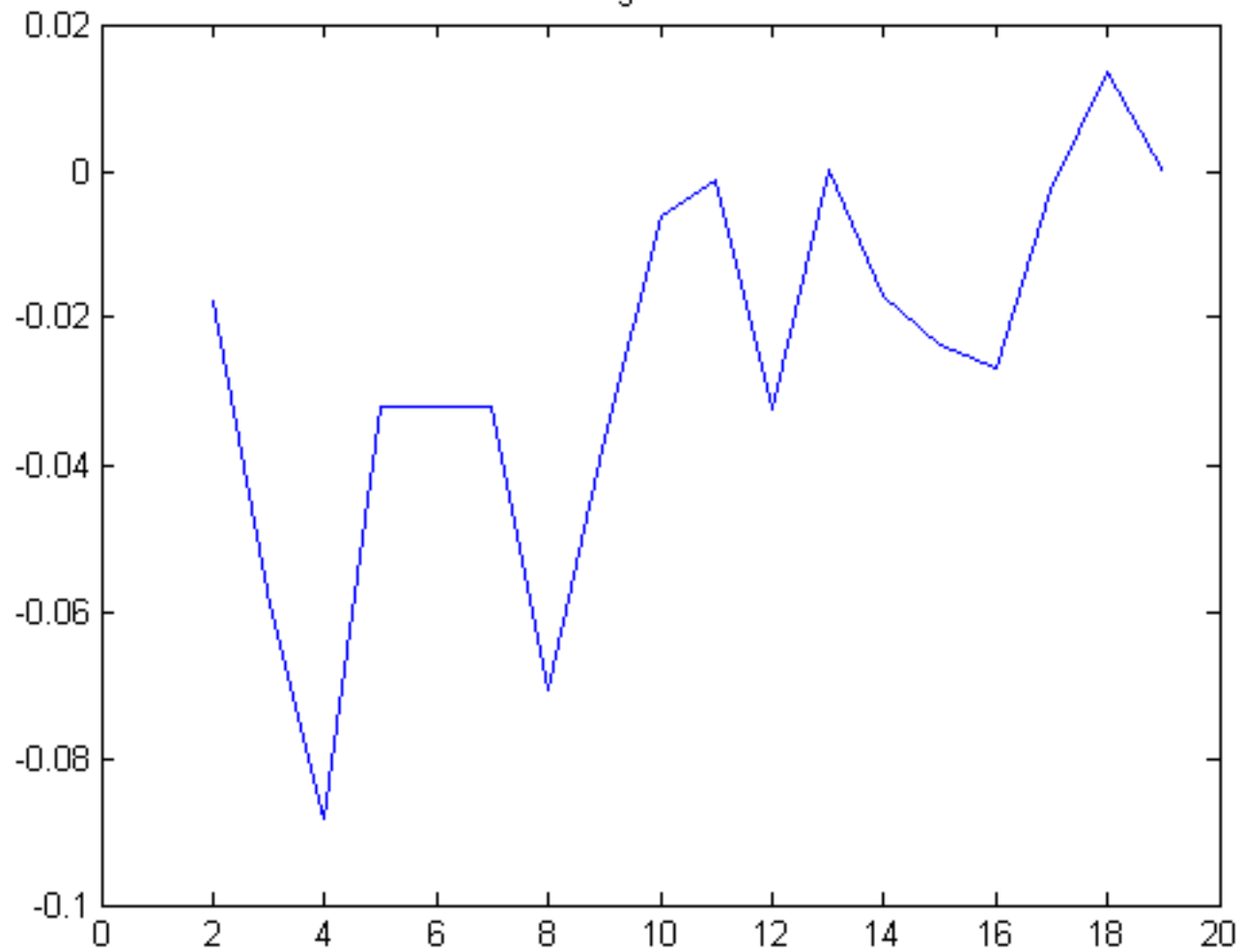


Figure 12

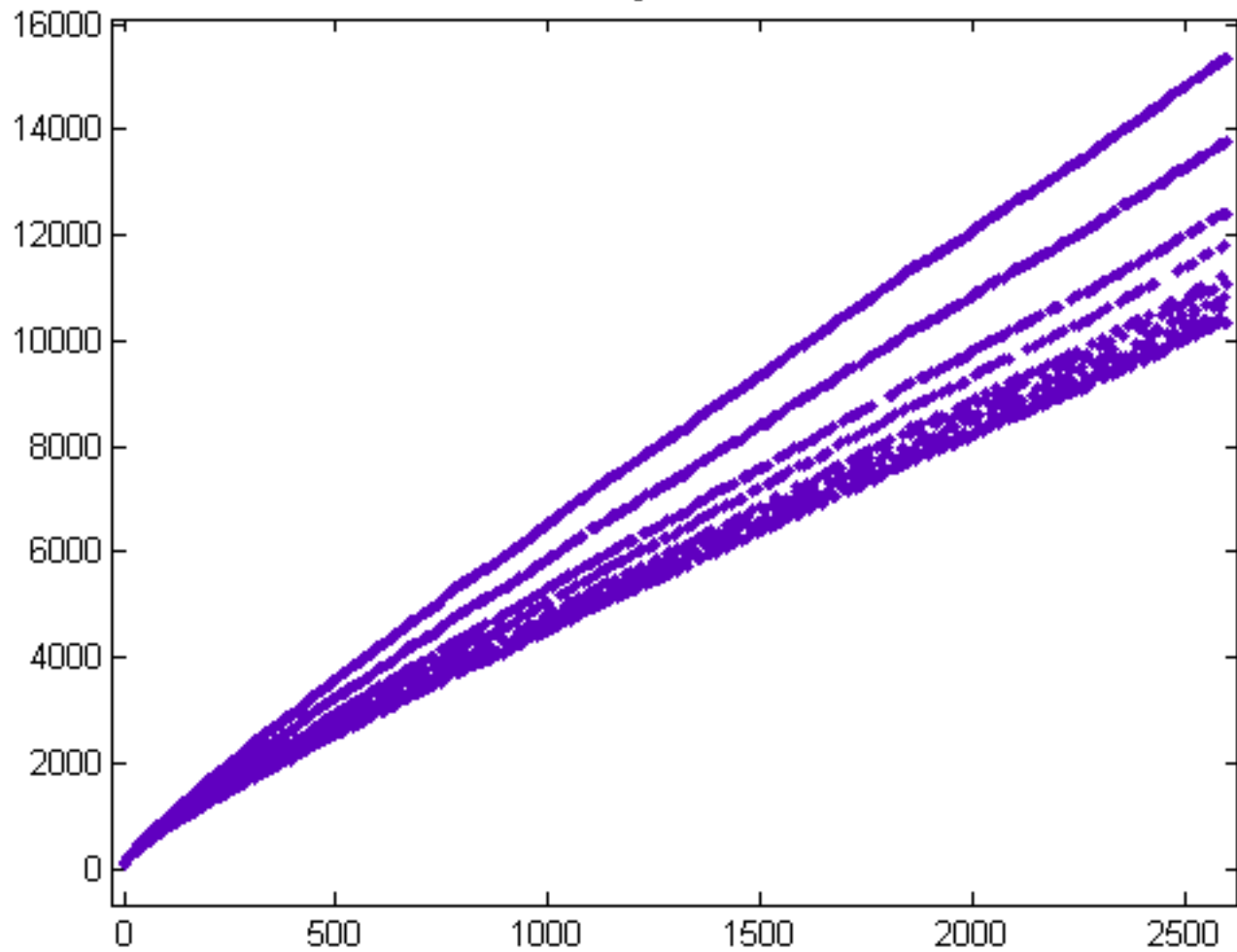


Figure 13

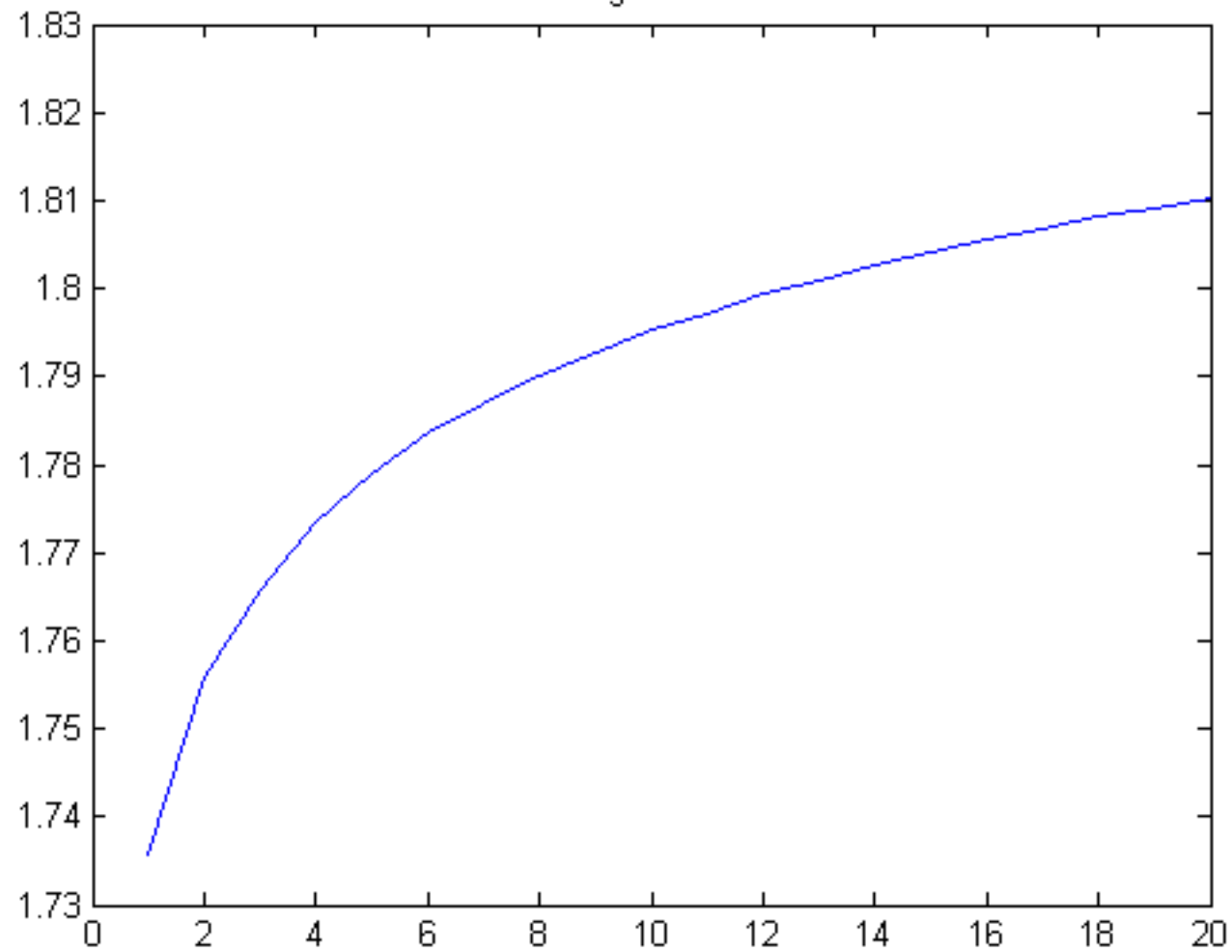


Figure 14

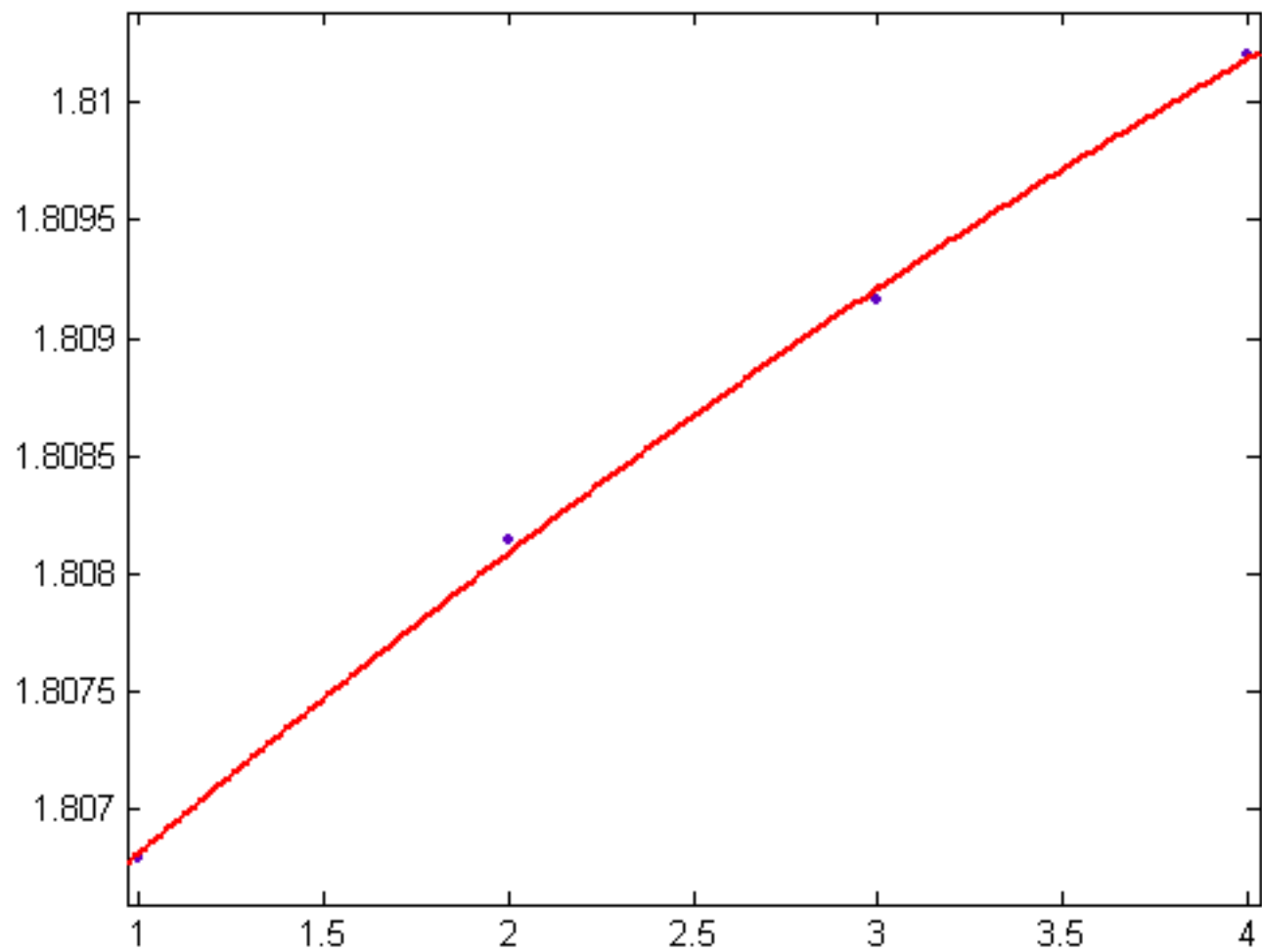


Figure 15

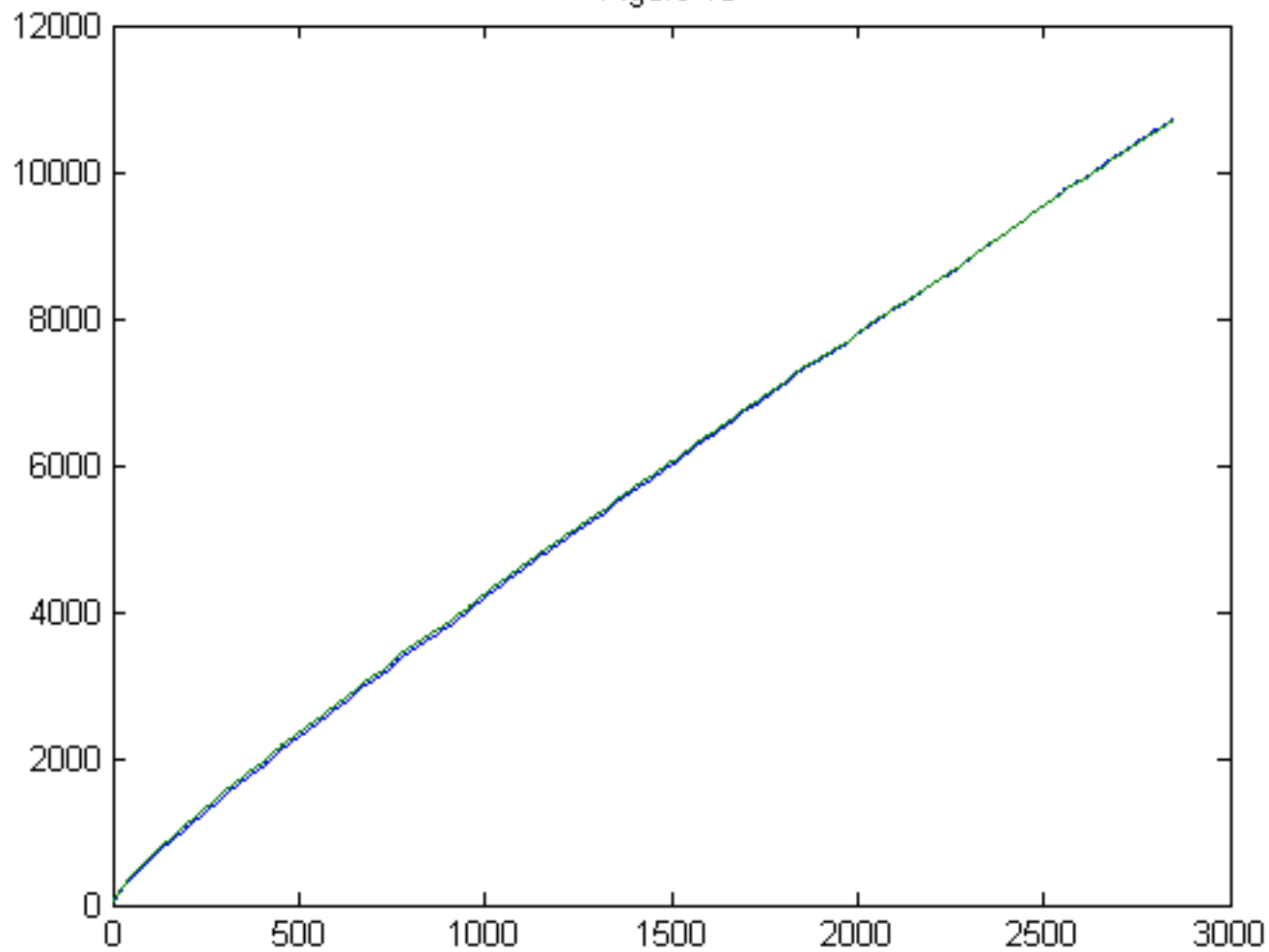


Figure 16

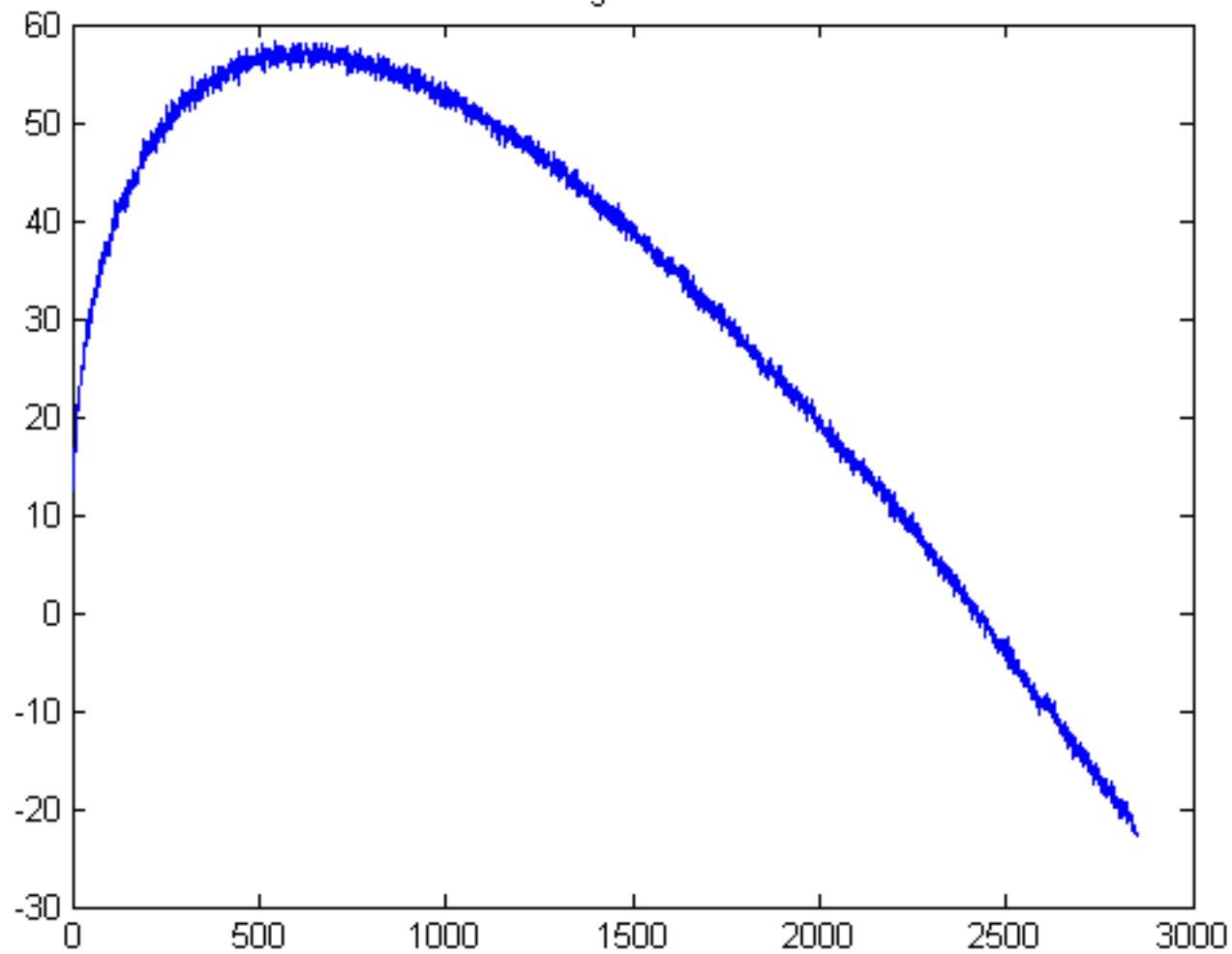


Figure 17

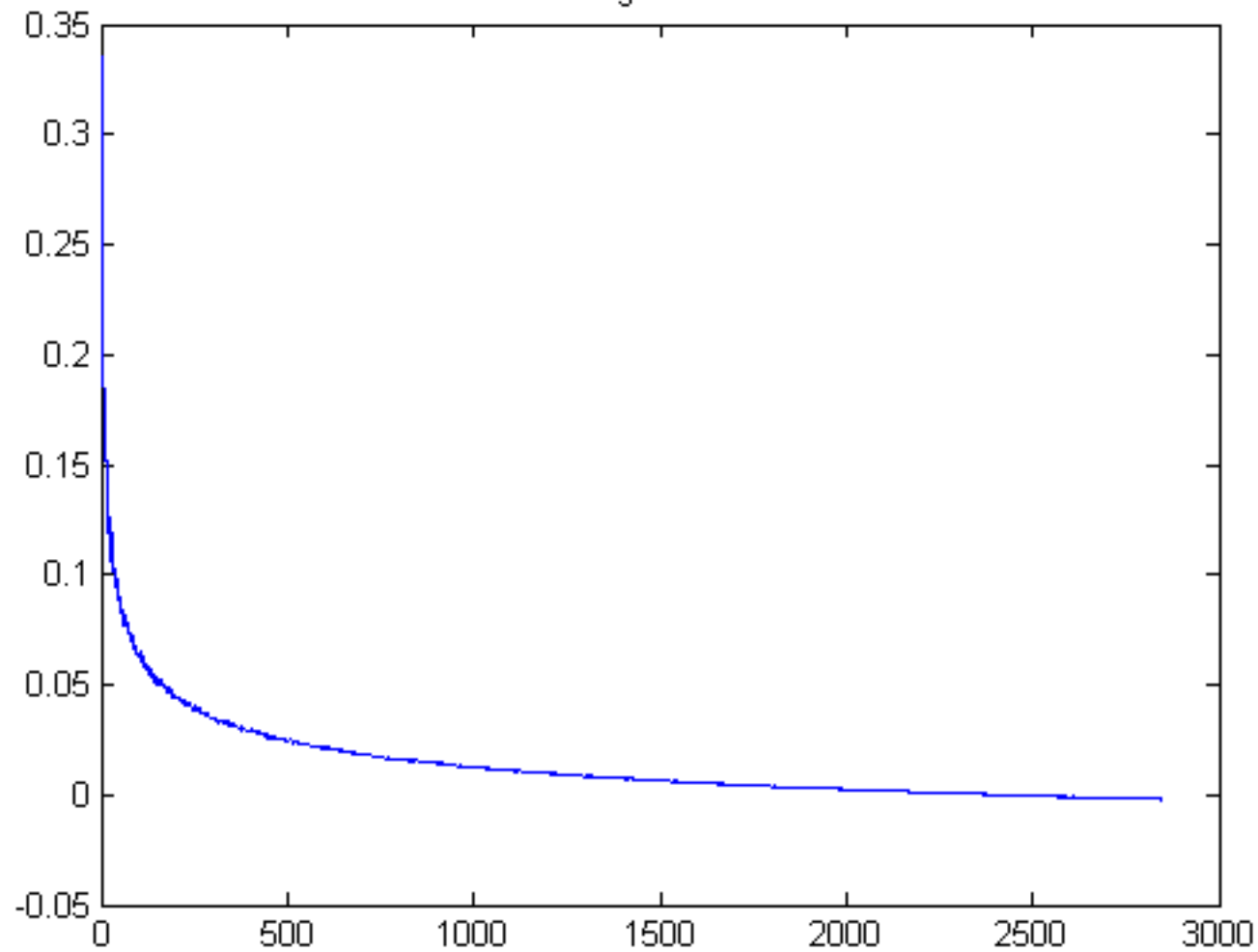


Figure 18

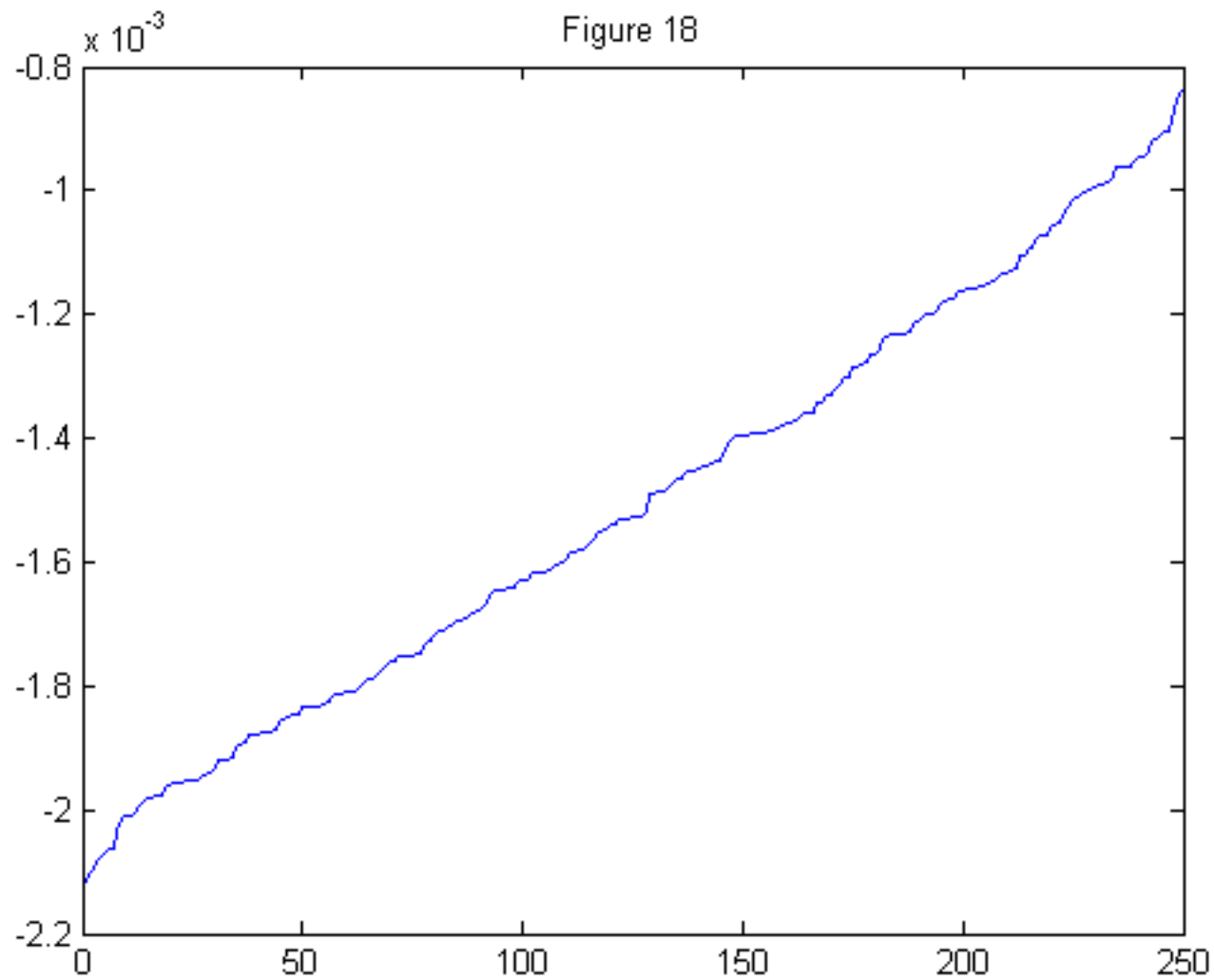


Figure 19

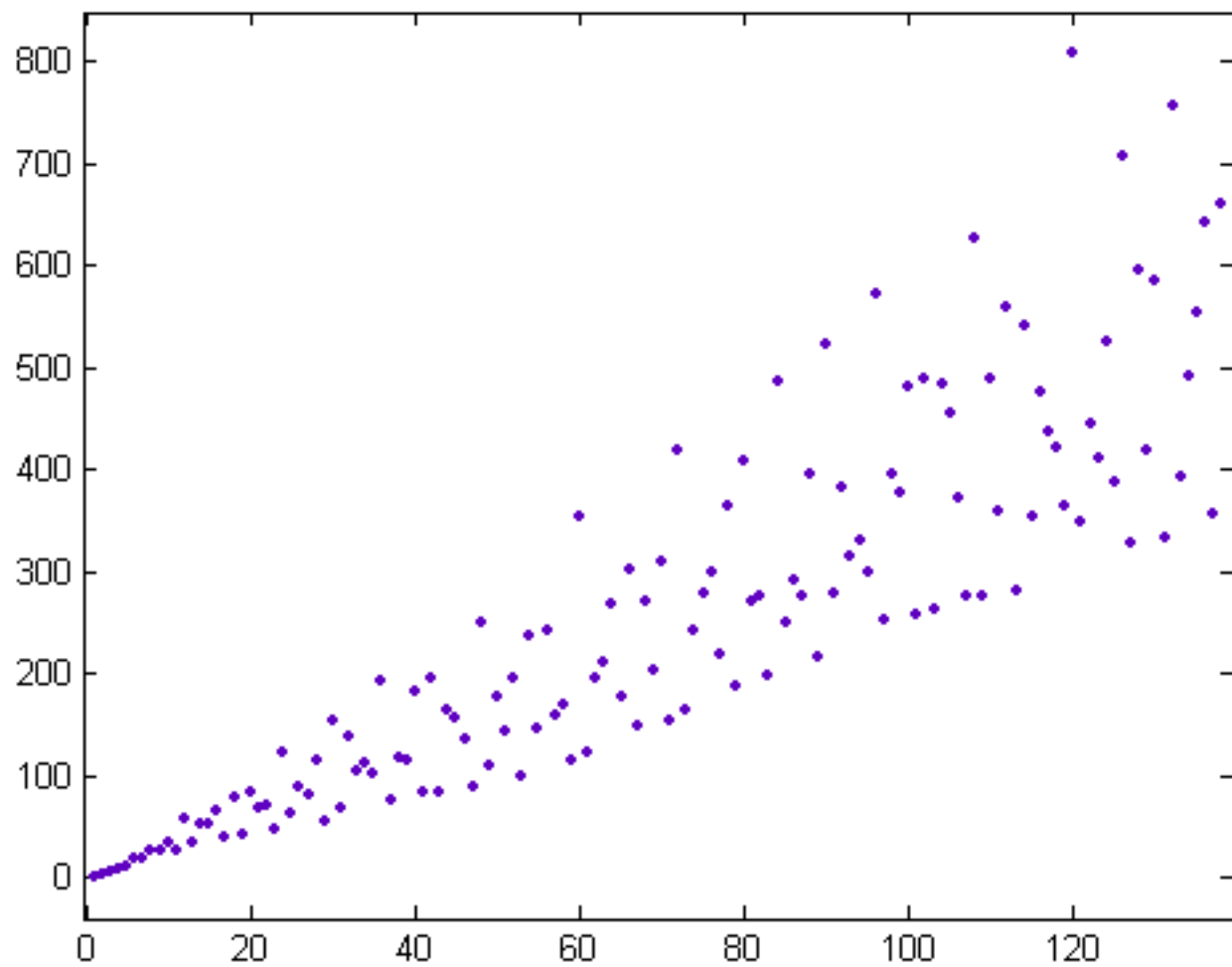


Figure 20

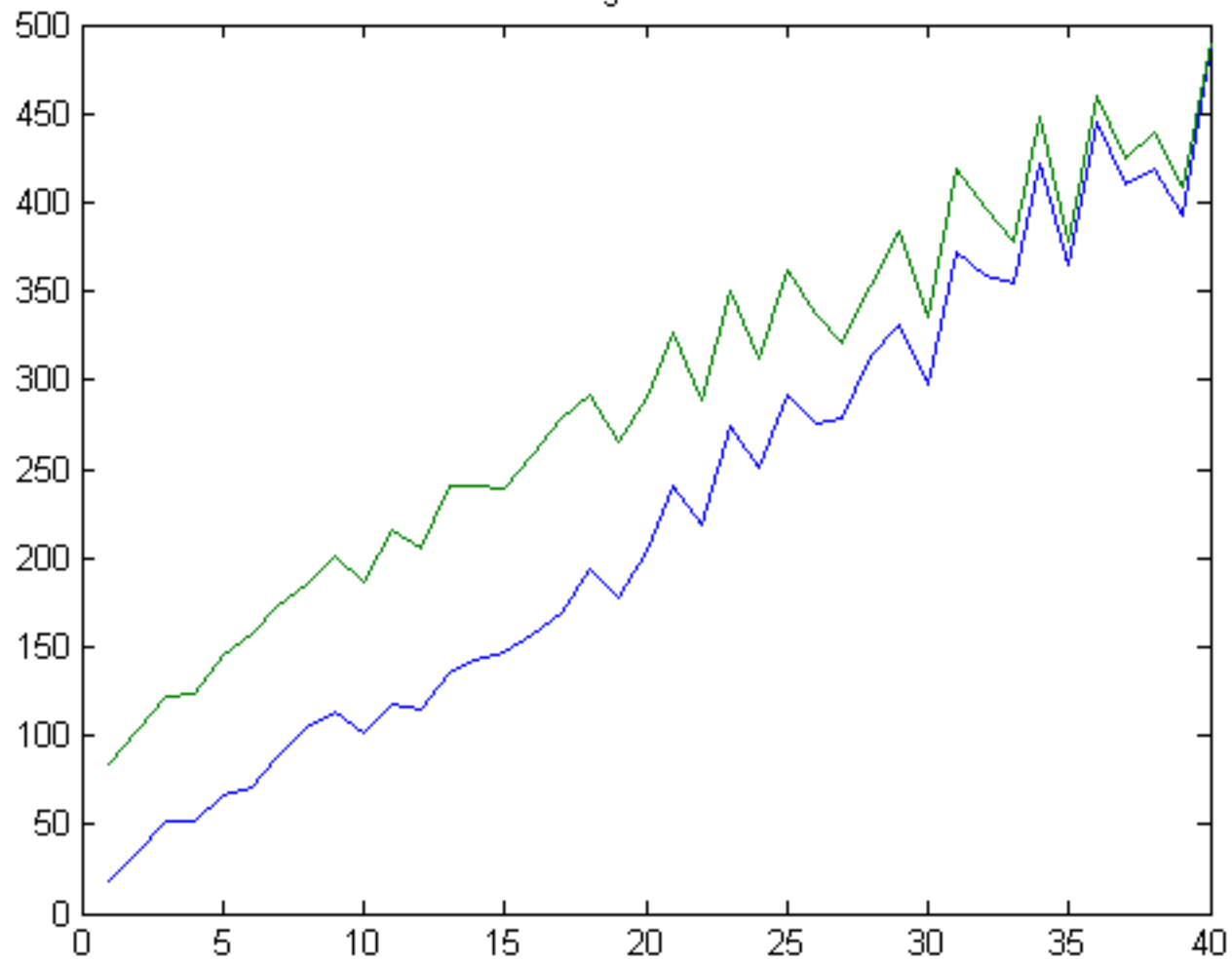


Figure 21

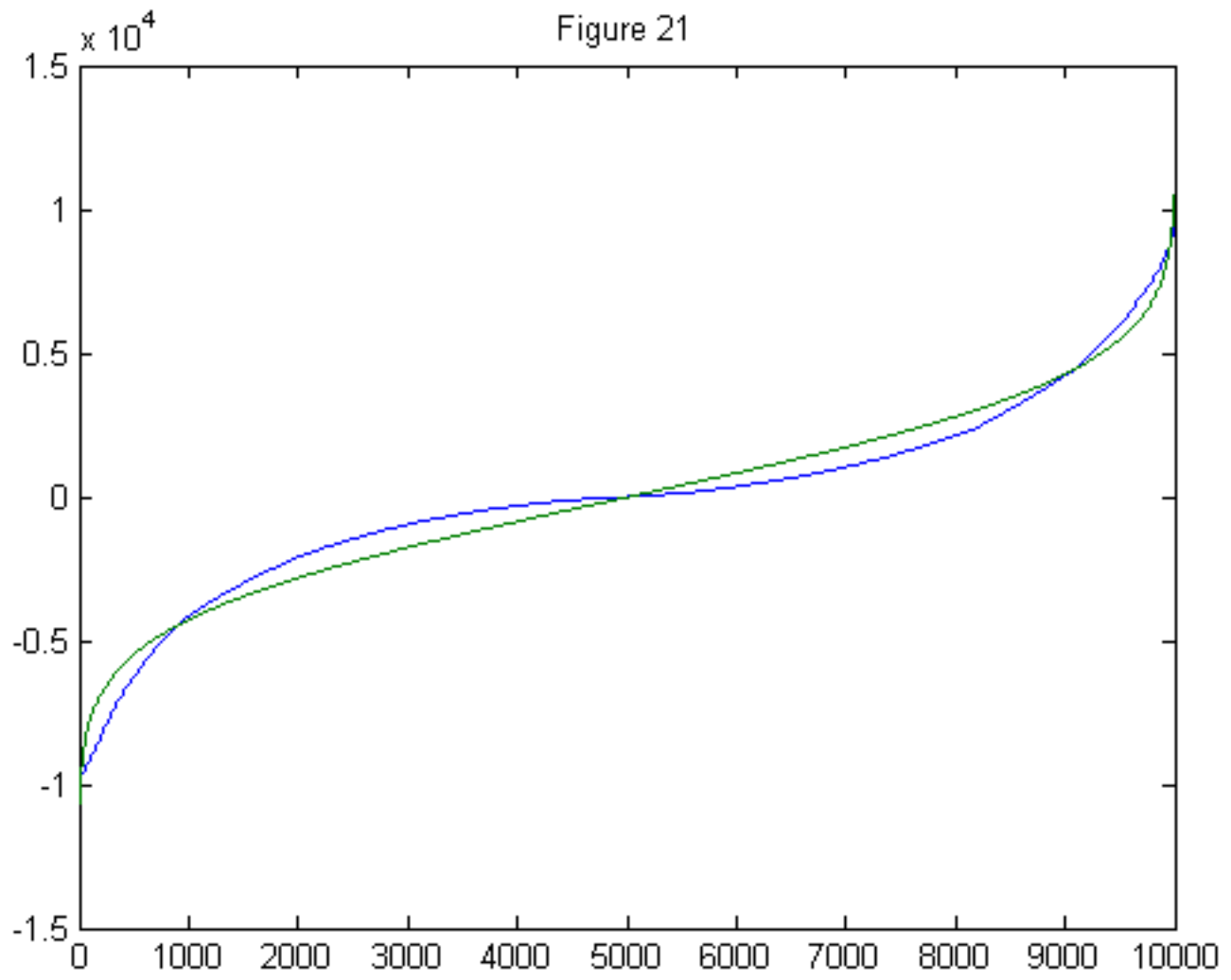


Figure 22

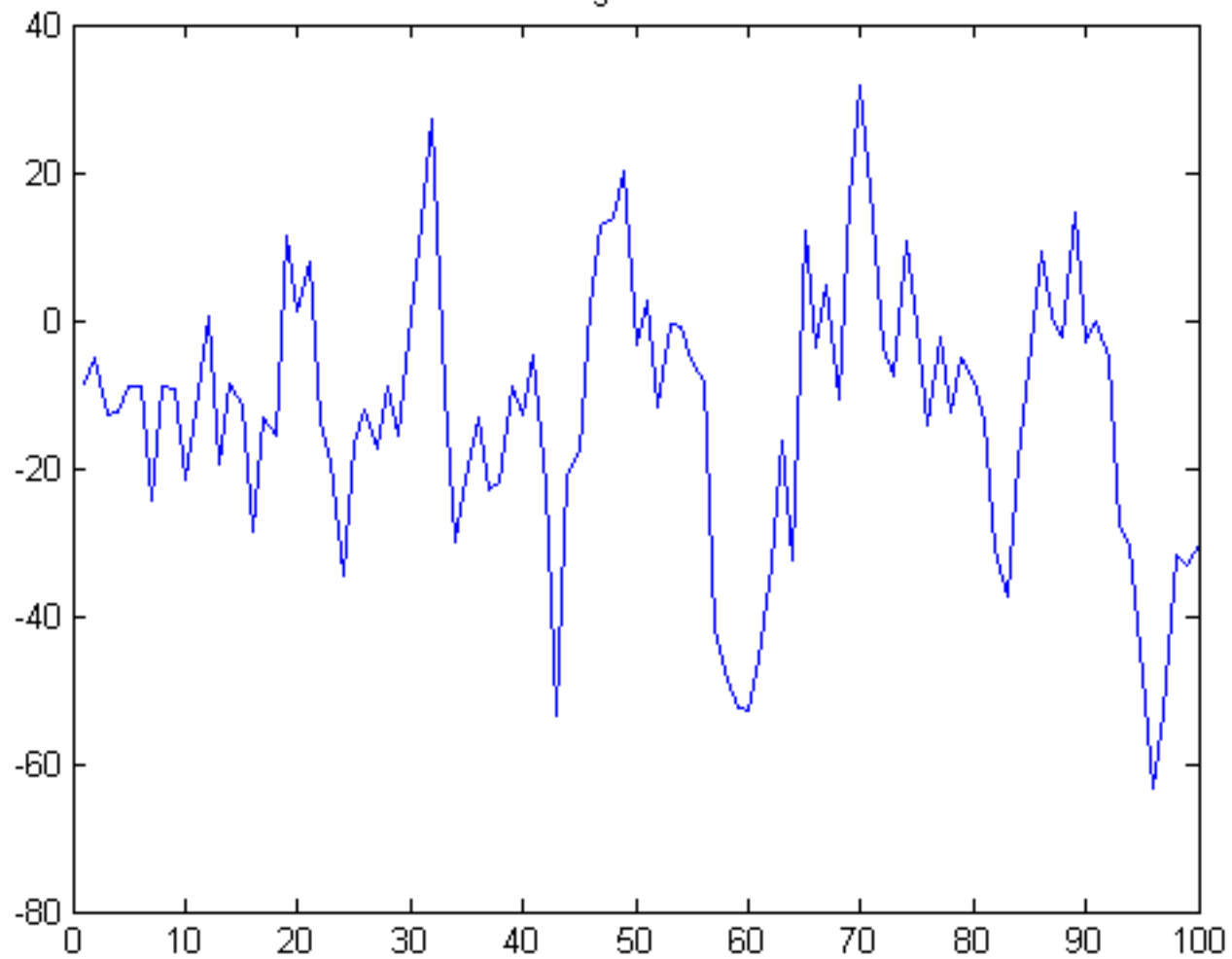


Figure 23

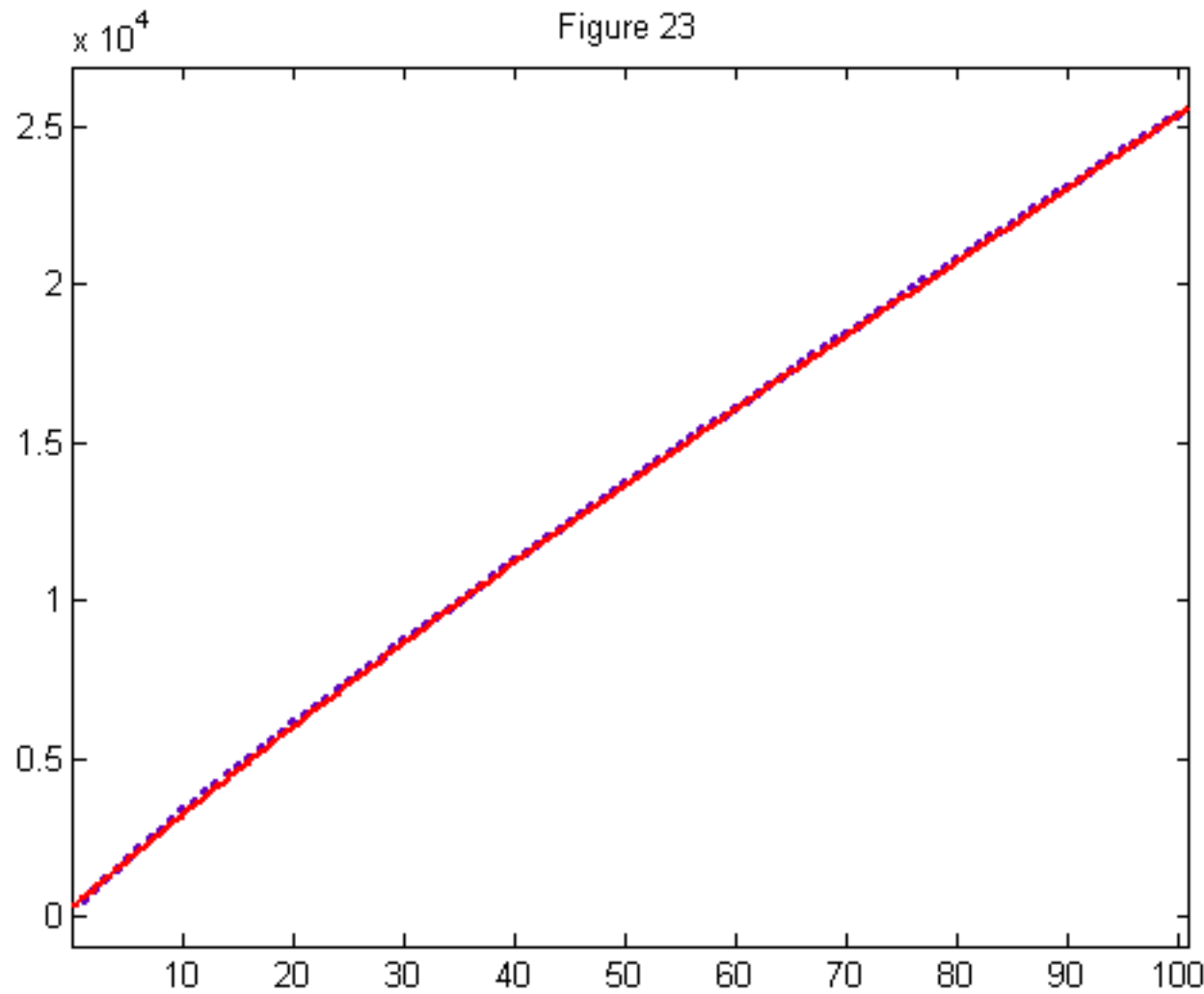


Figure 24

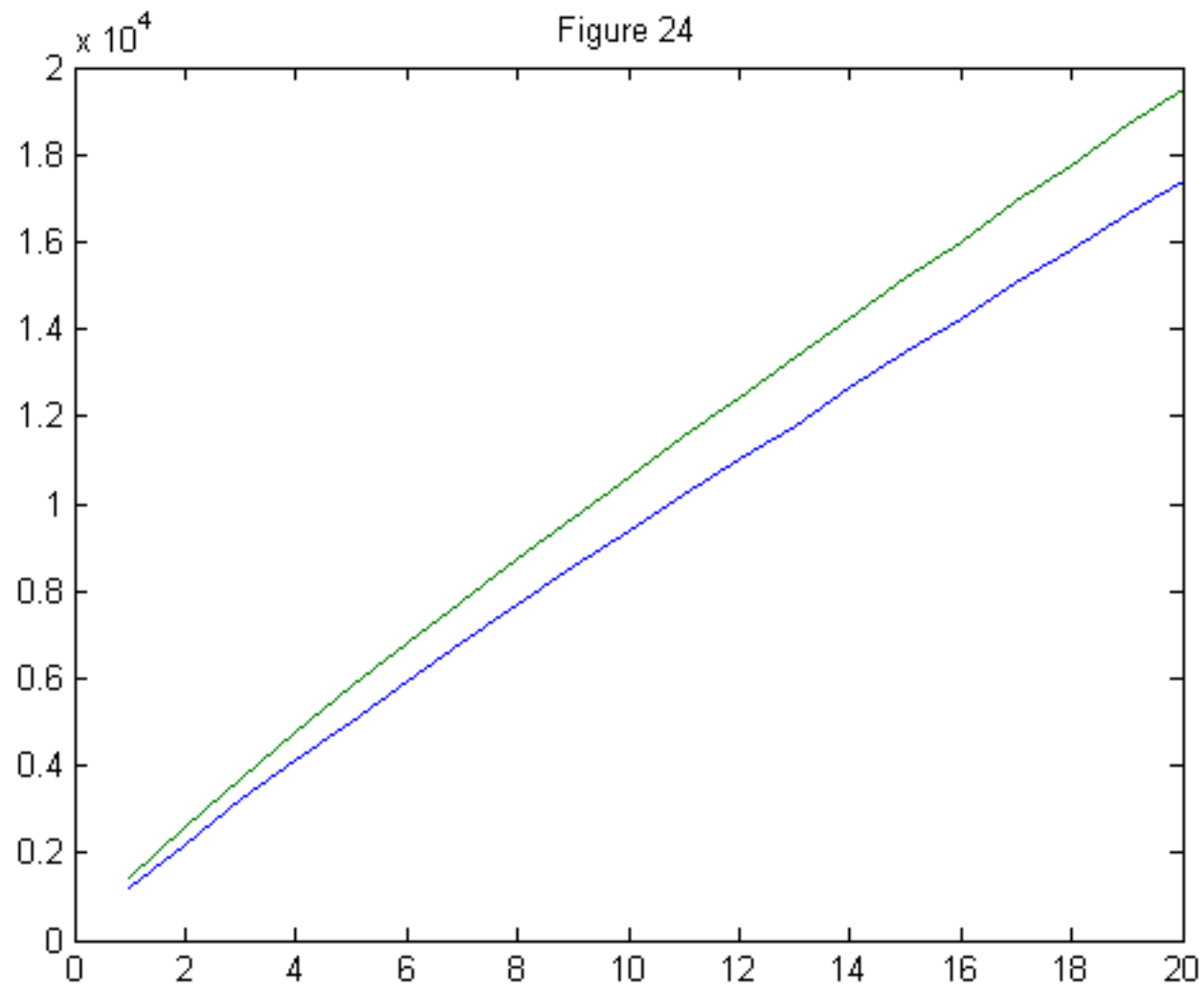


Figure 25

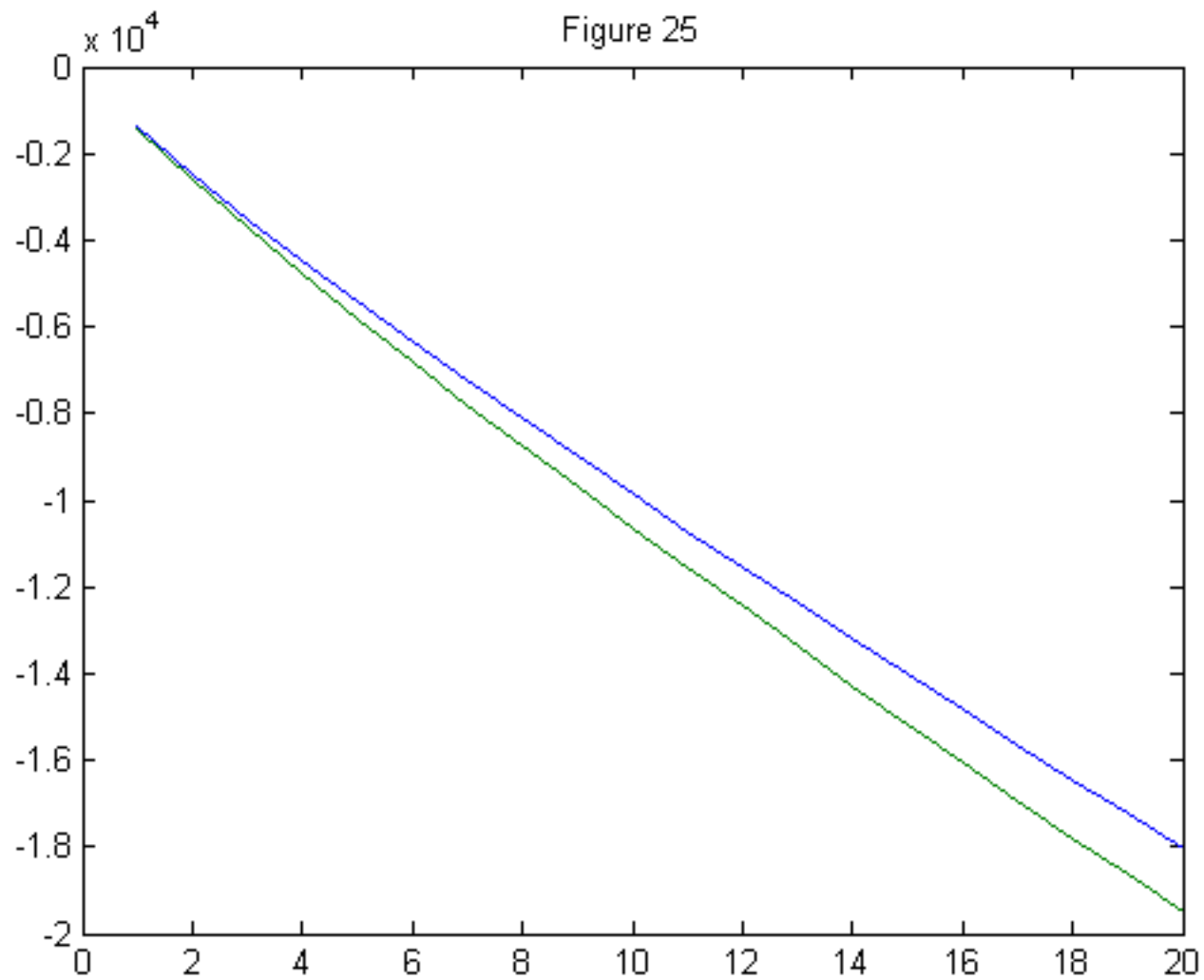


Figure 26

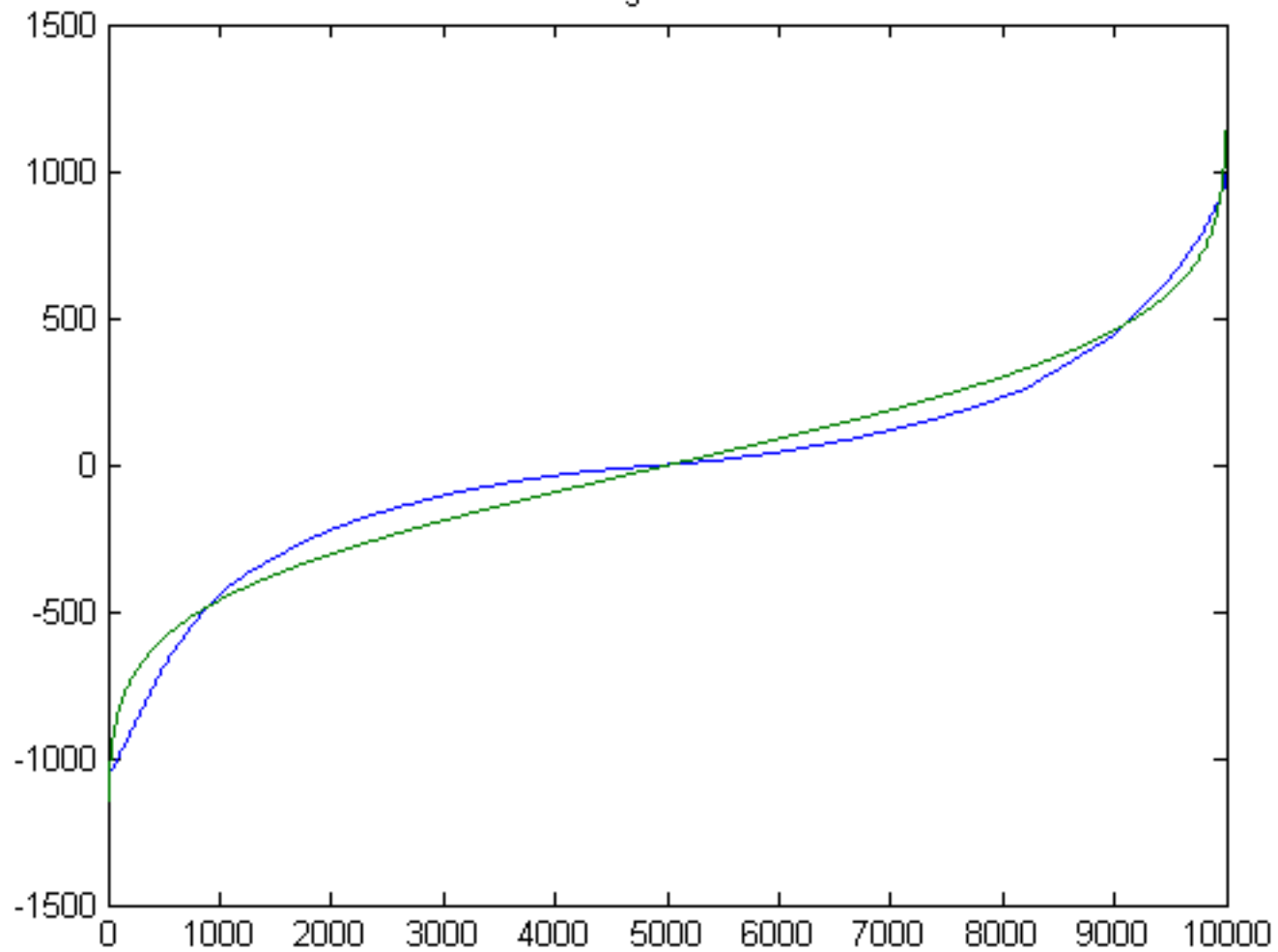


Figure 27

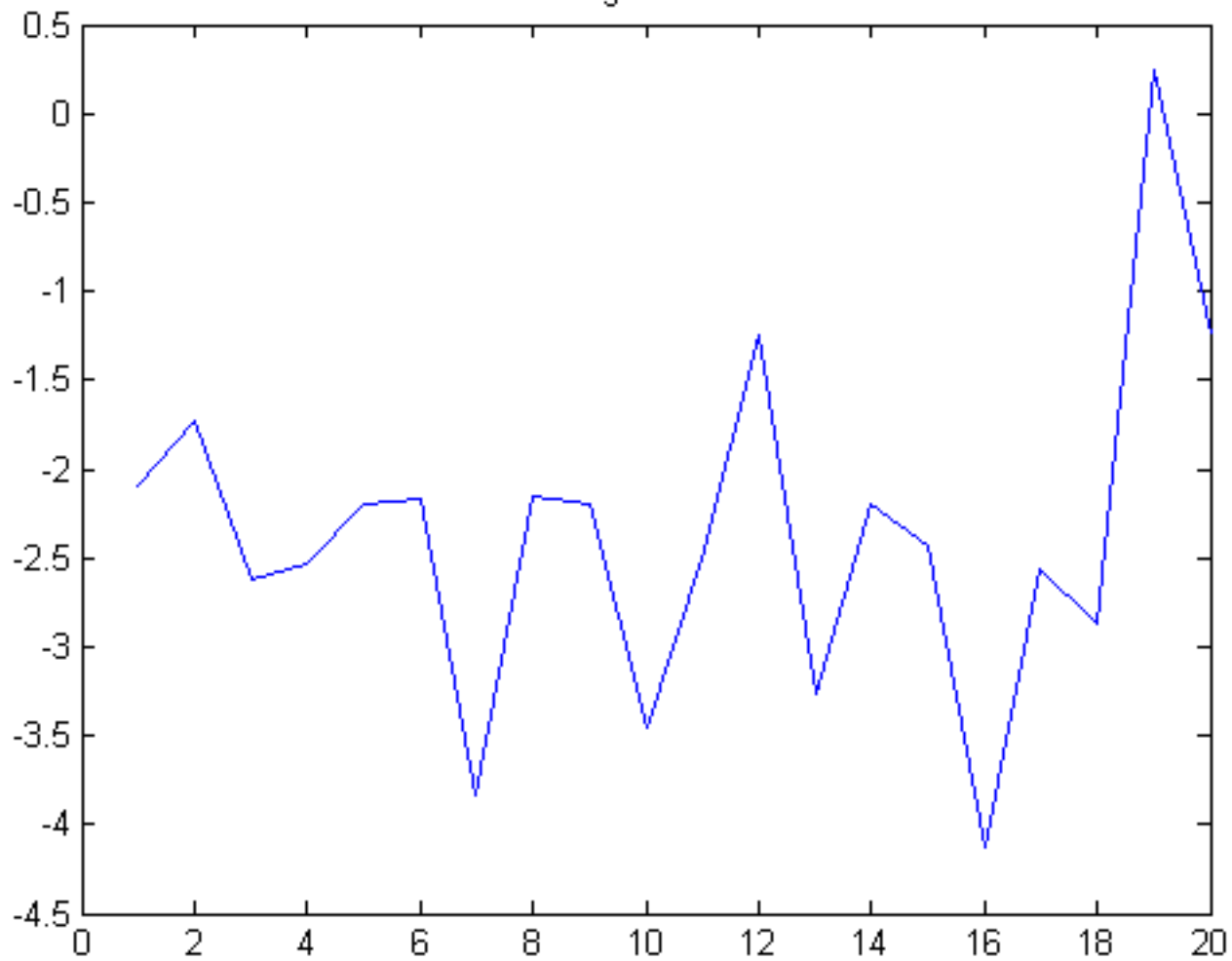


Figure 28

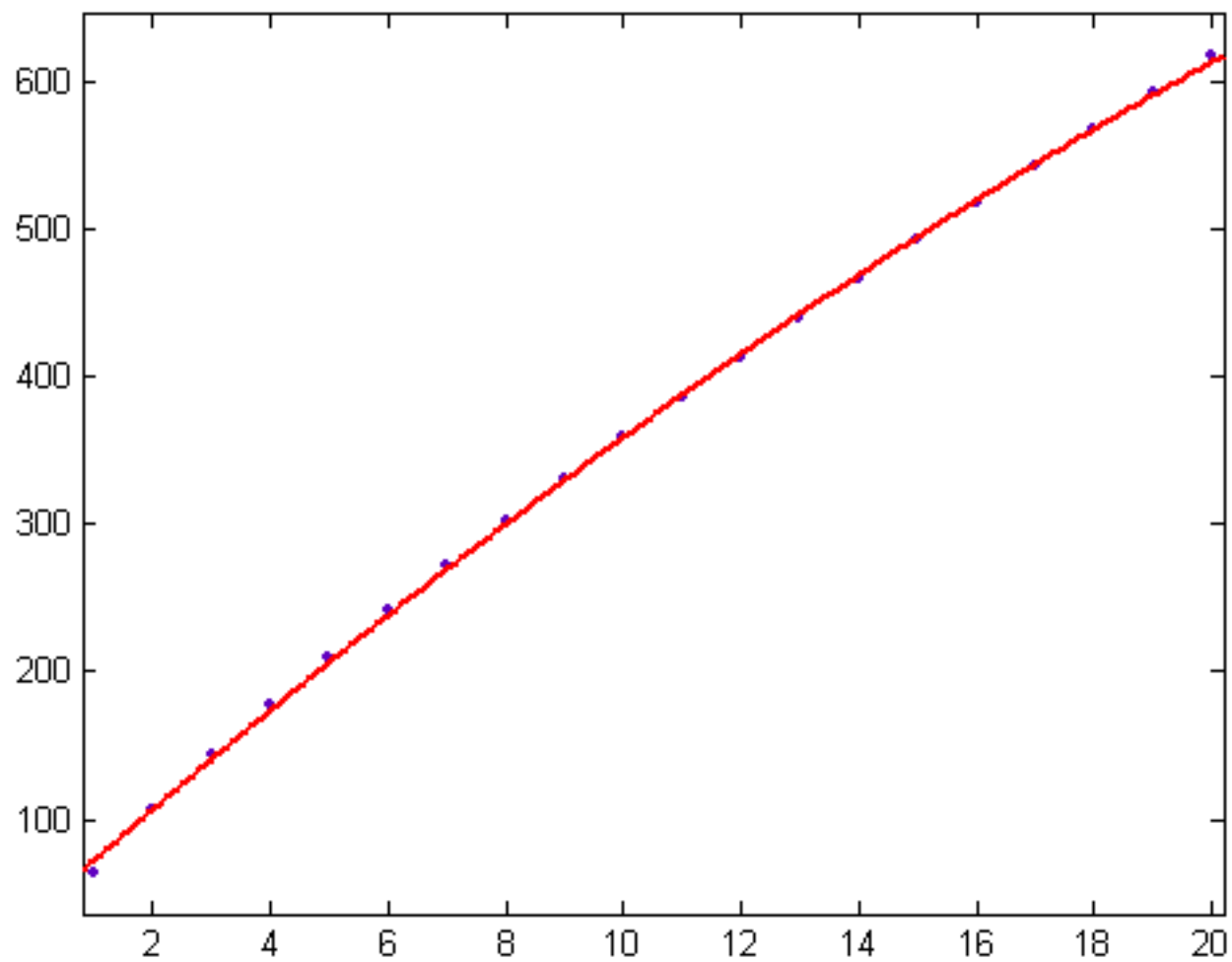


Figure 29

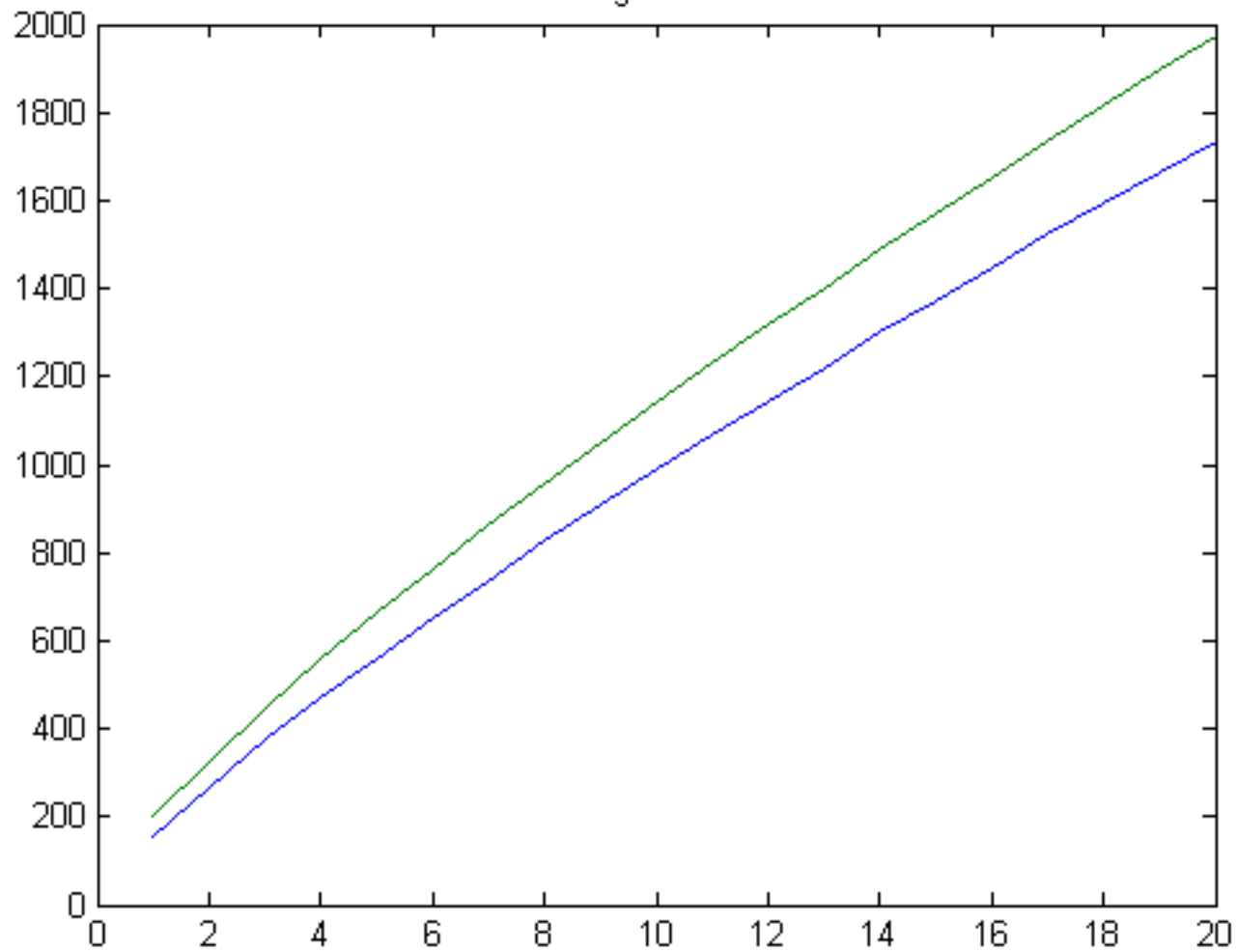


Figure 30

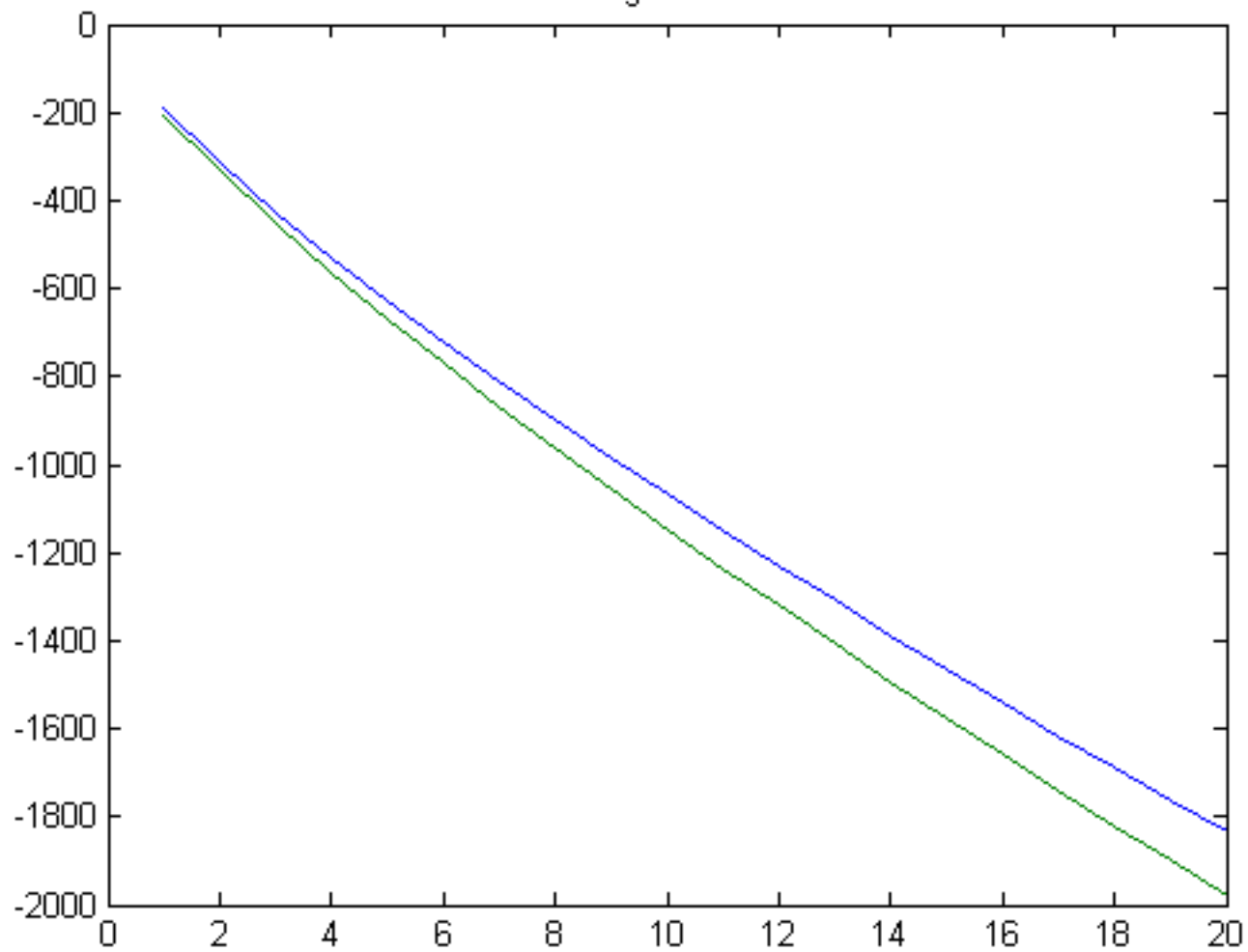


Figure 31

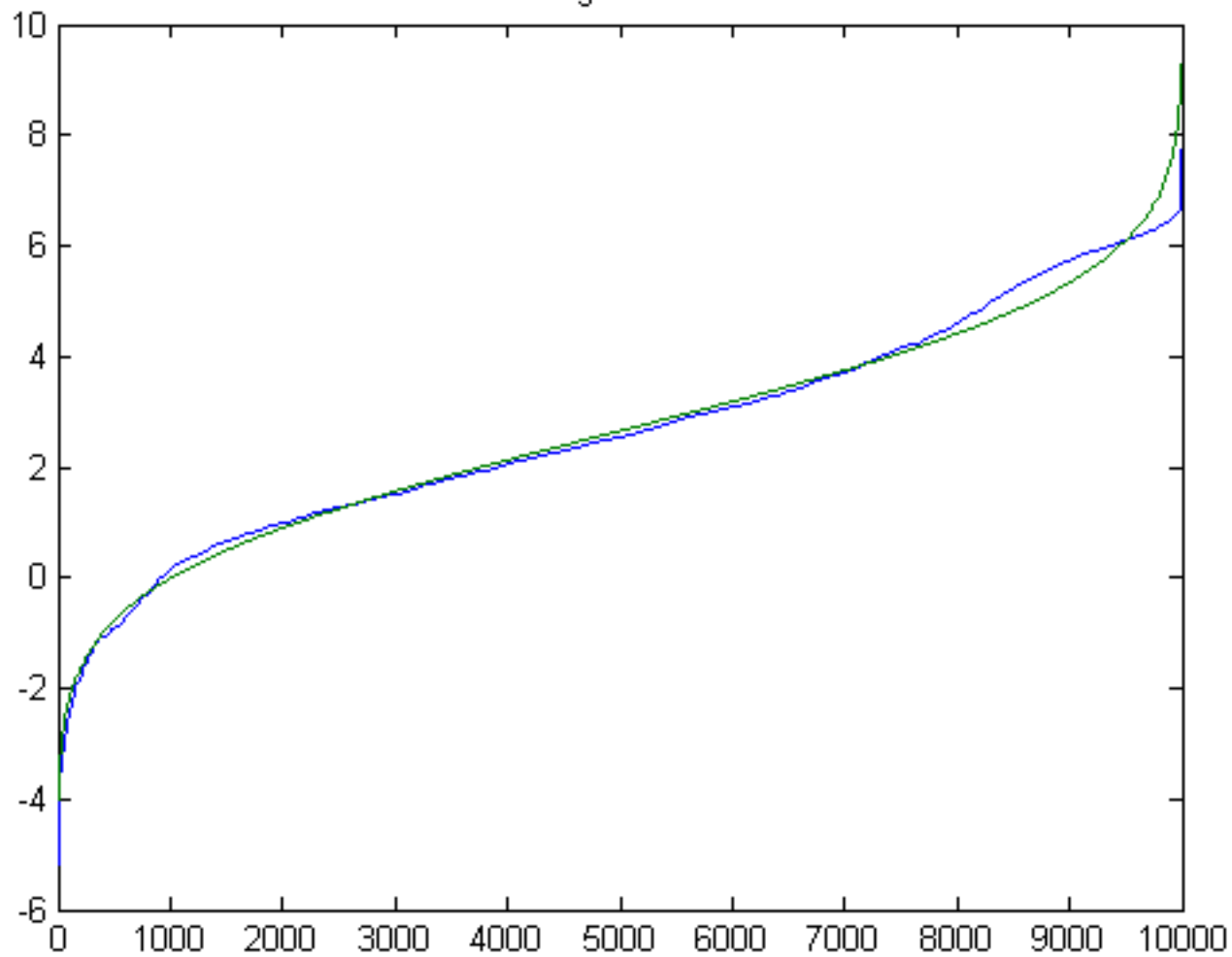


Figure 32

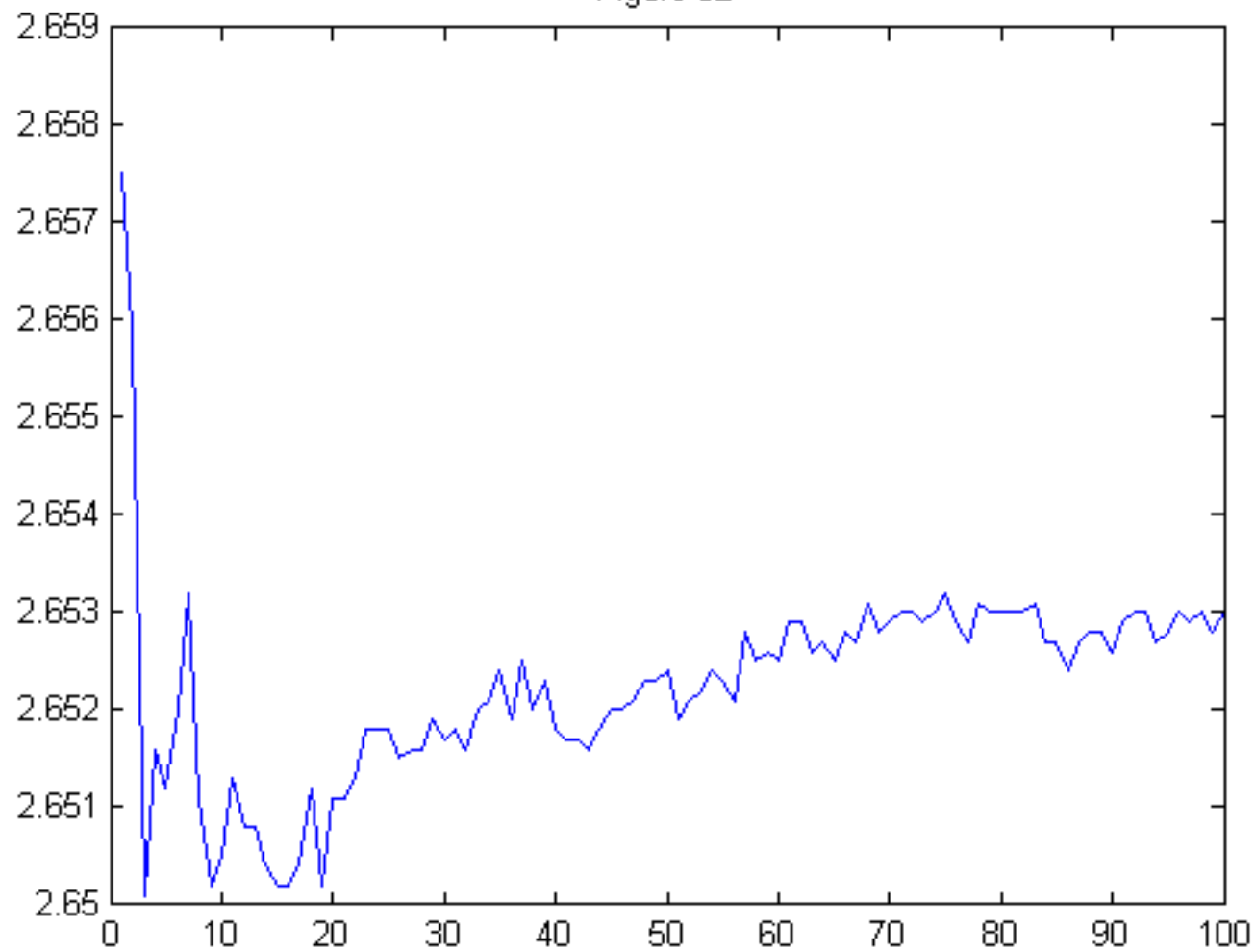


Figure 33

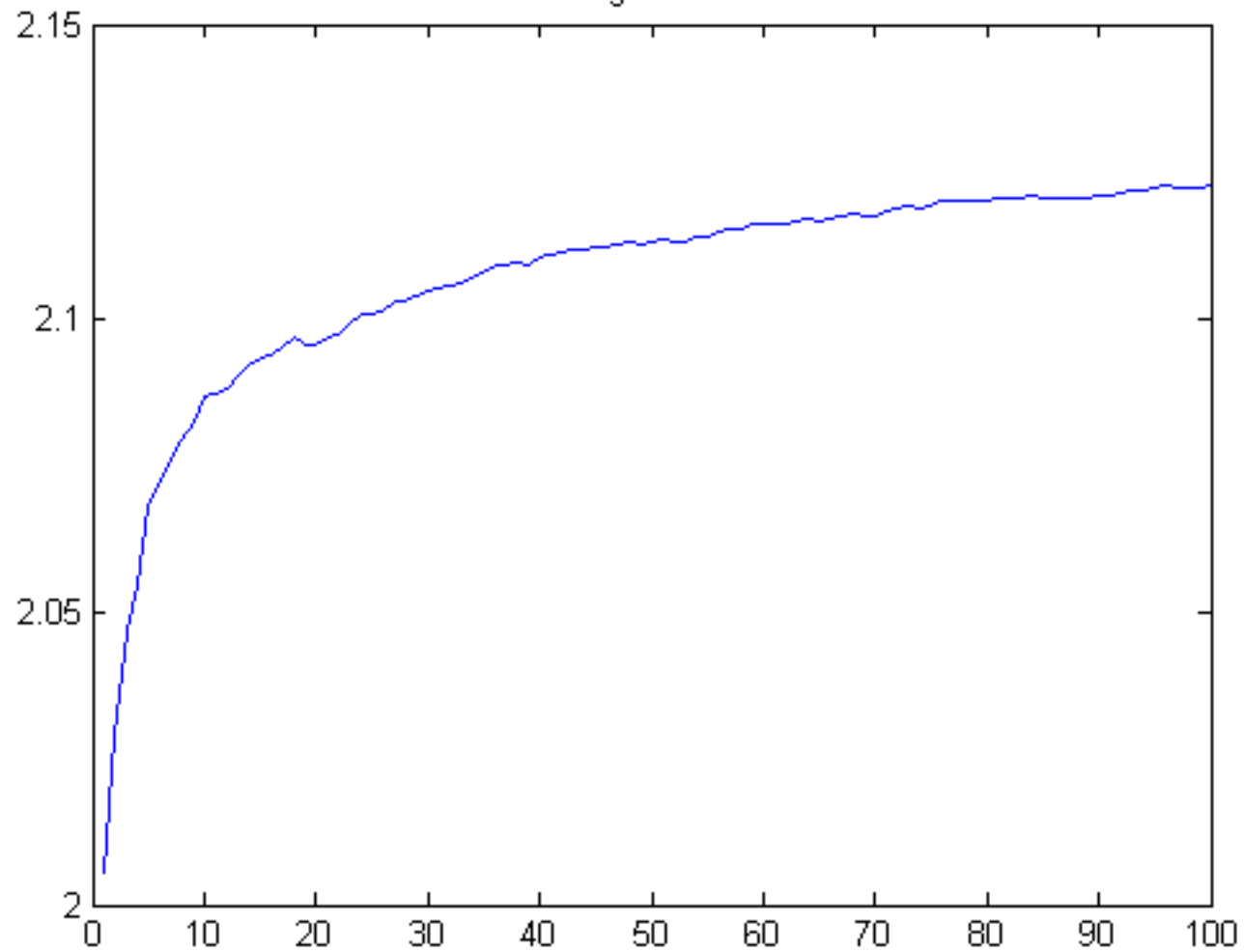


Figure 34

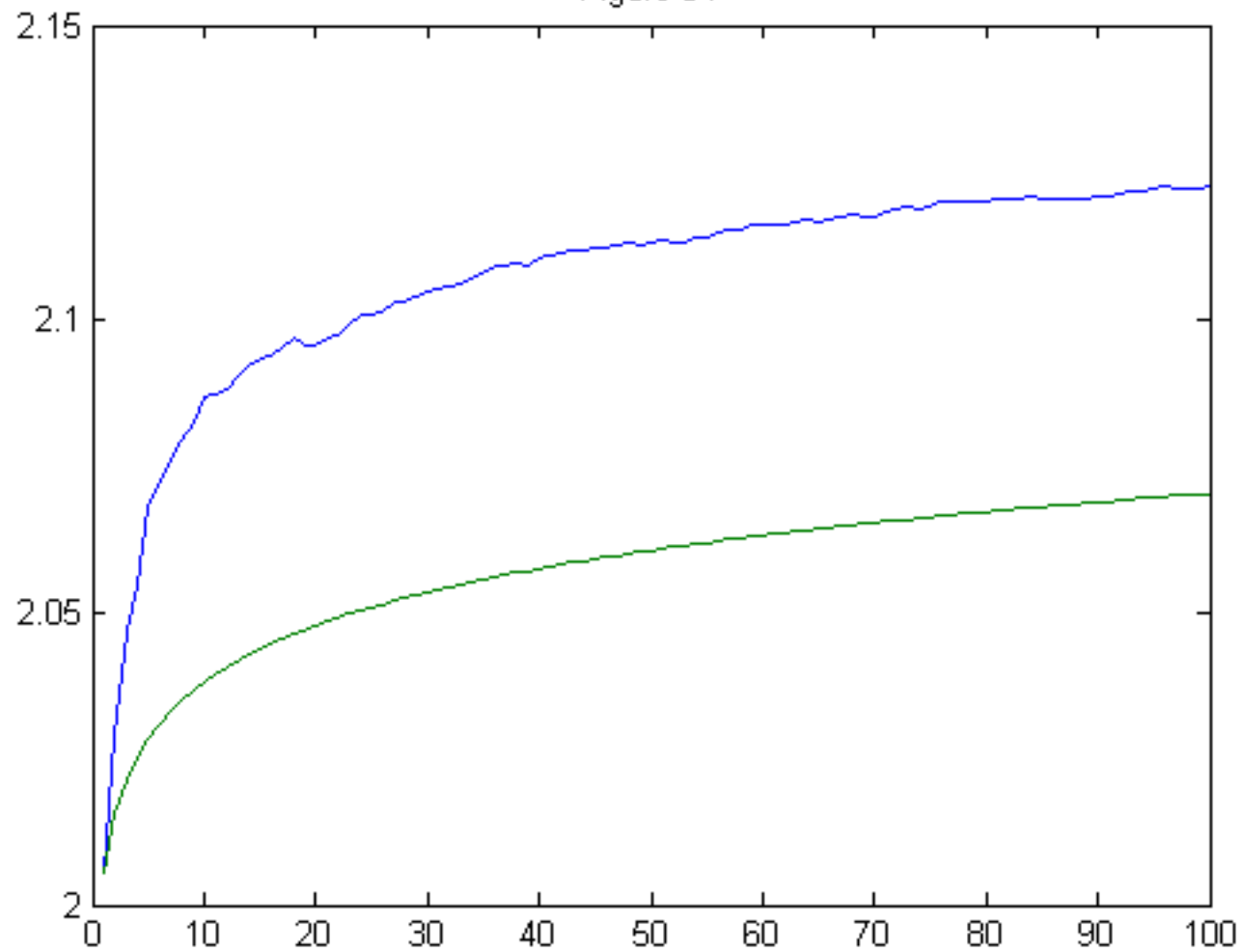


Figure 35

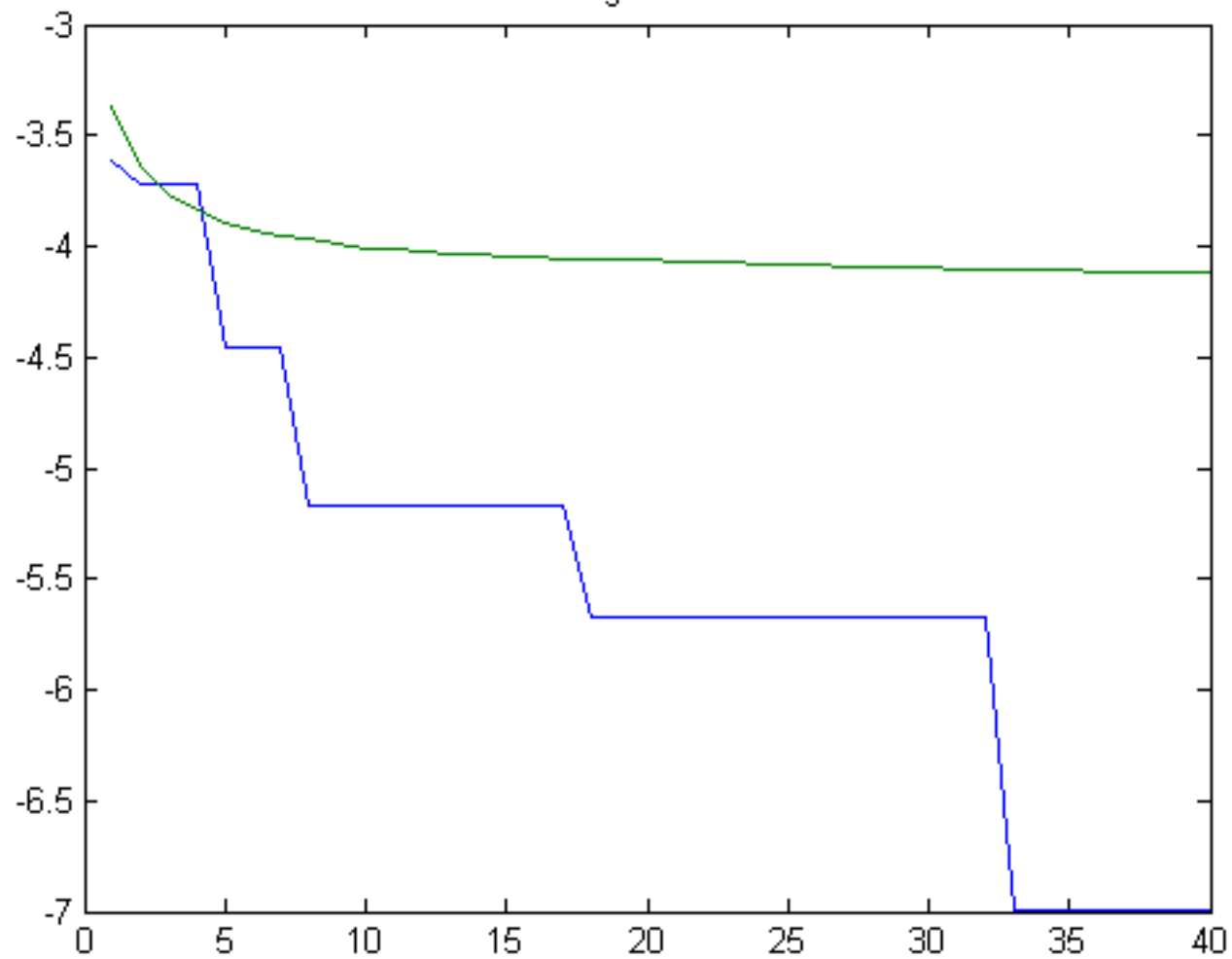


Figure 36

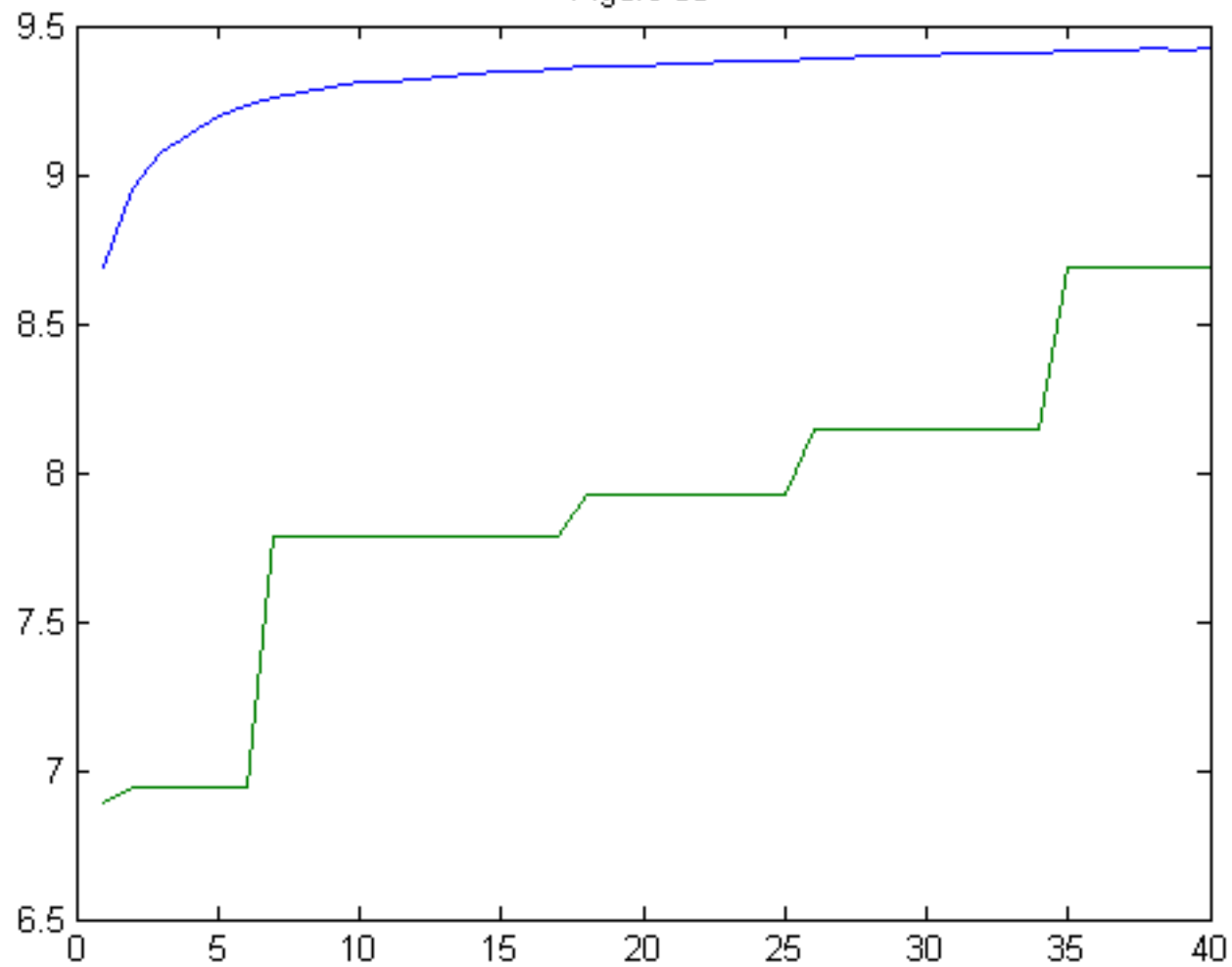


Figure 37

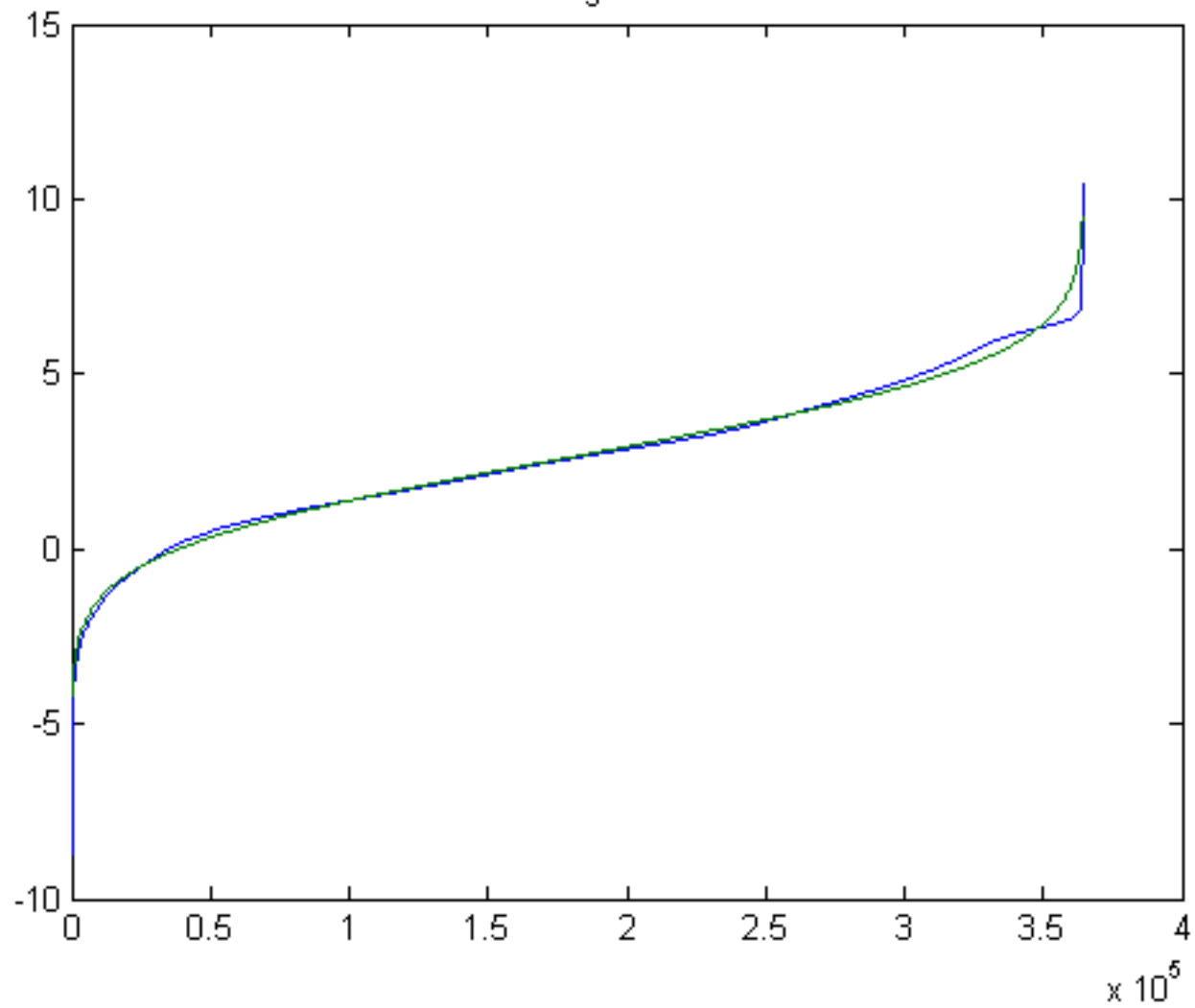


Figure 38

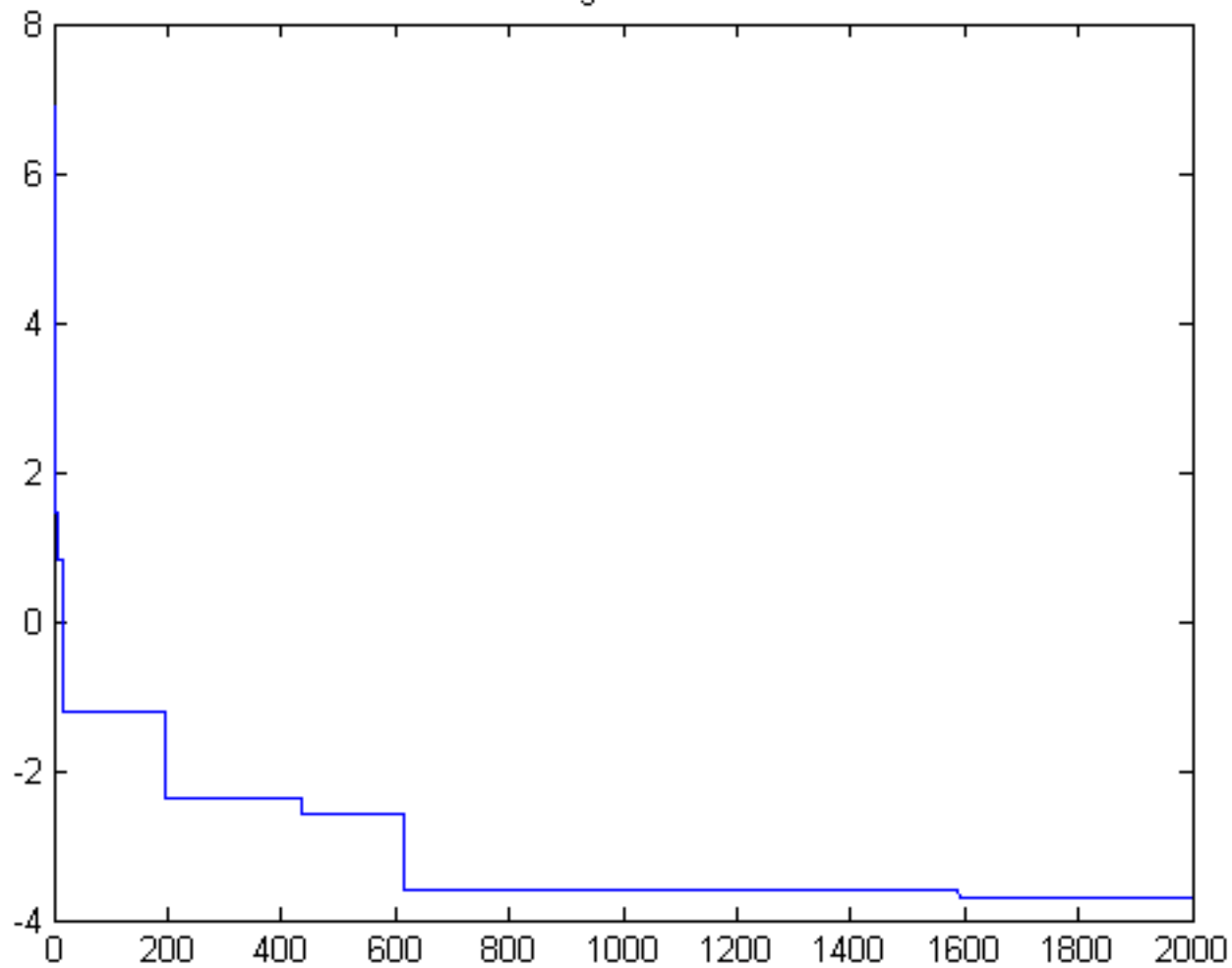


Figure 39

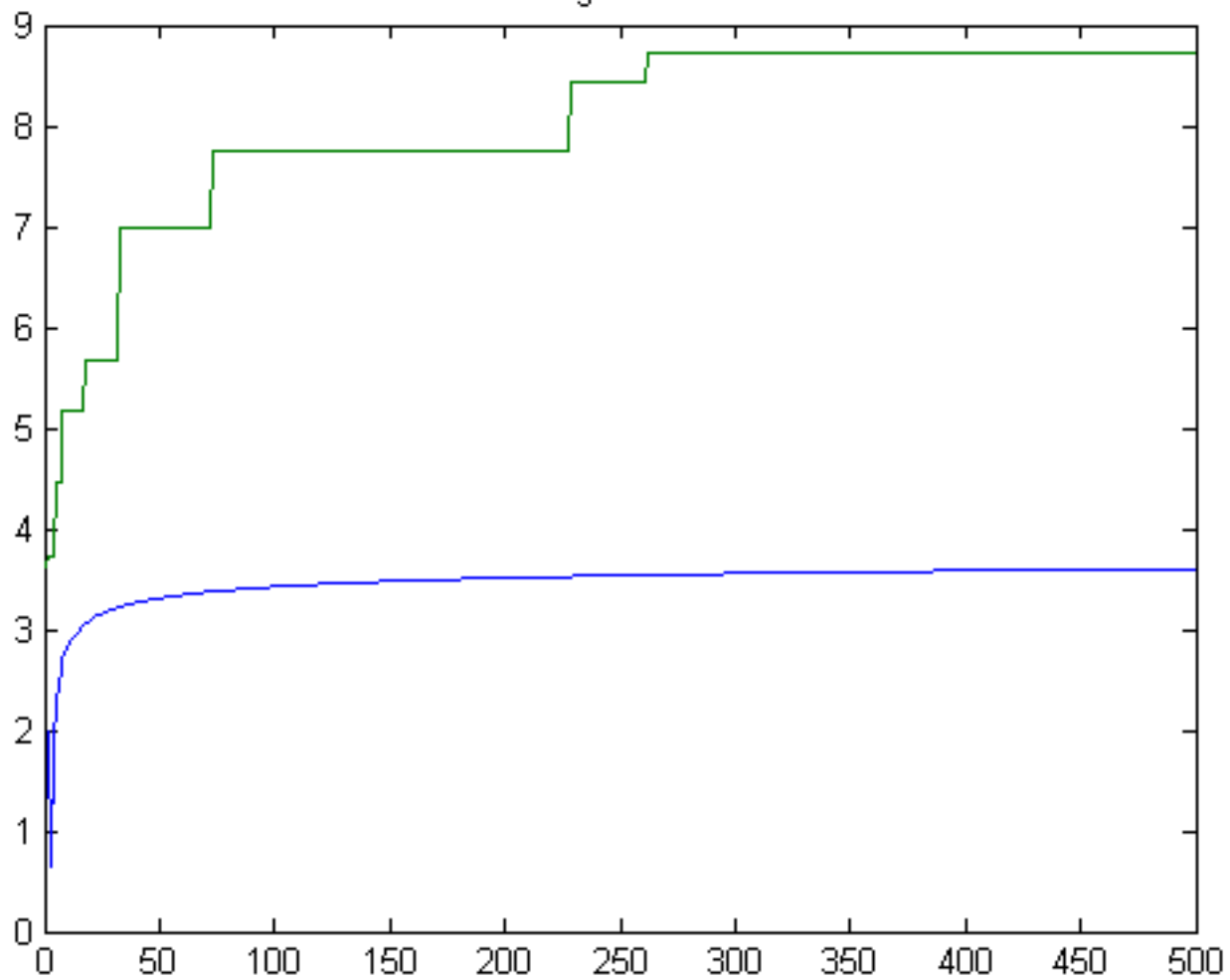


Figure 40

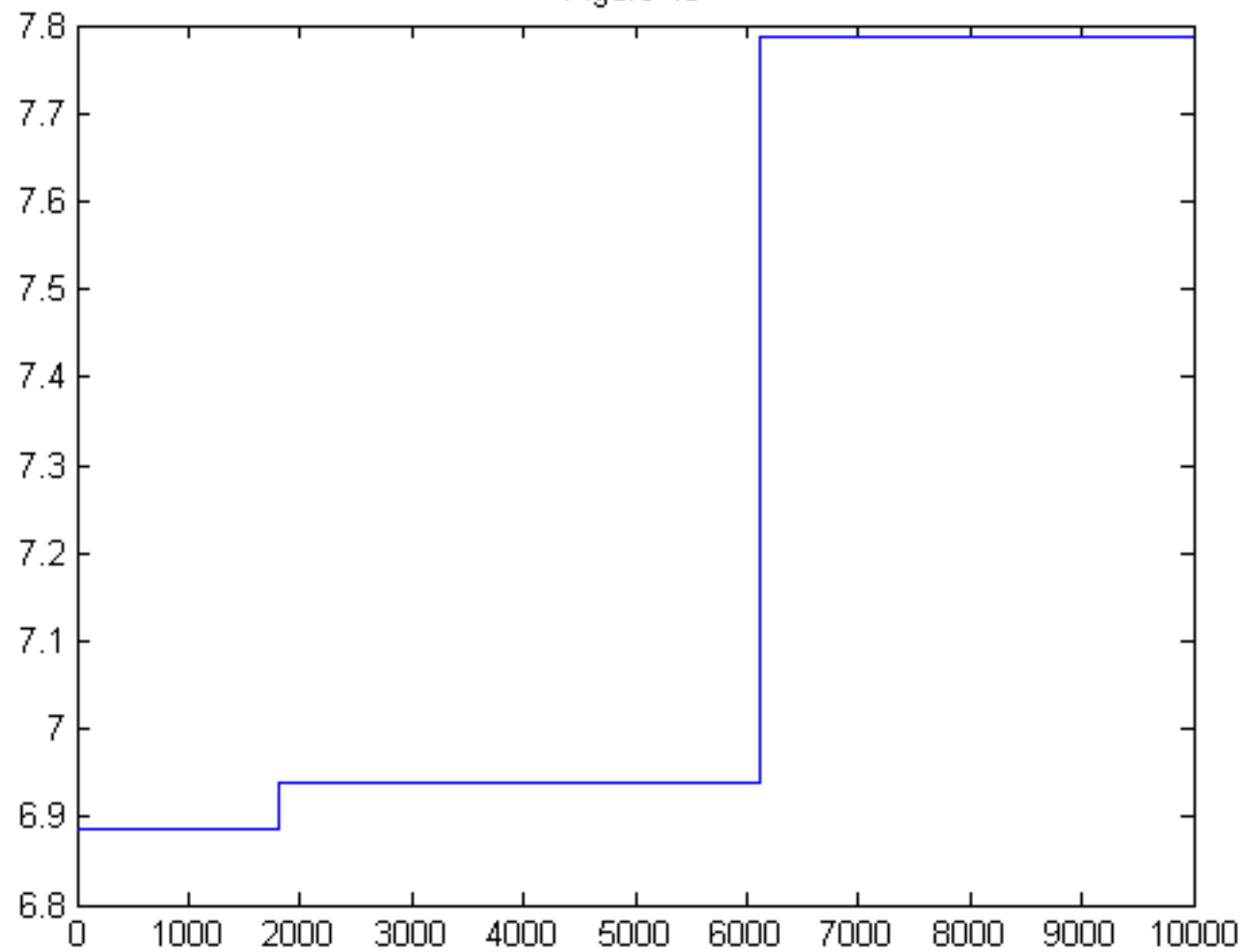


Figure 41

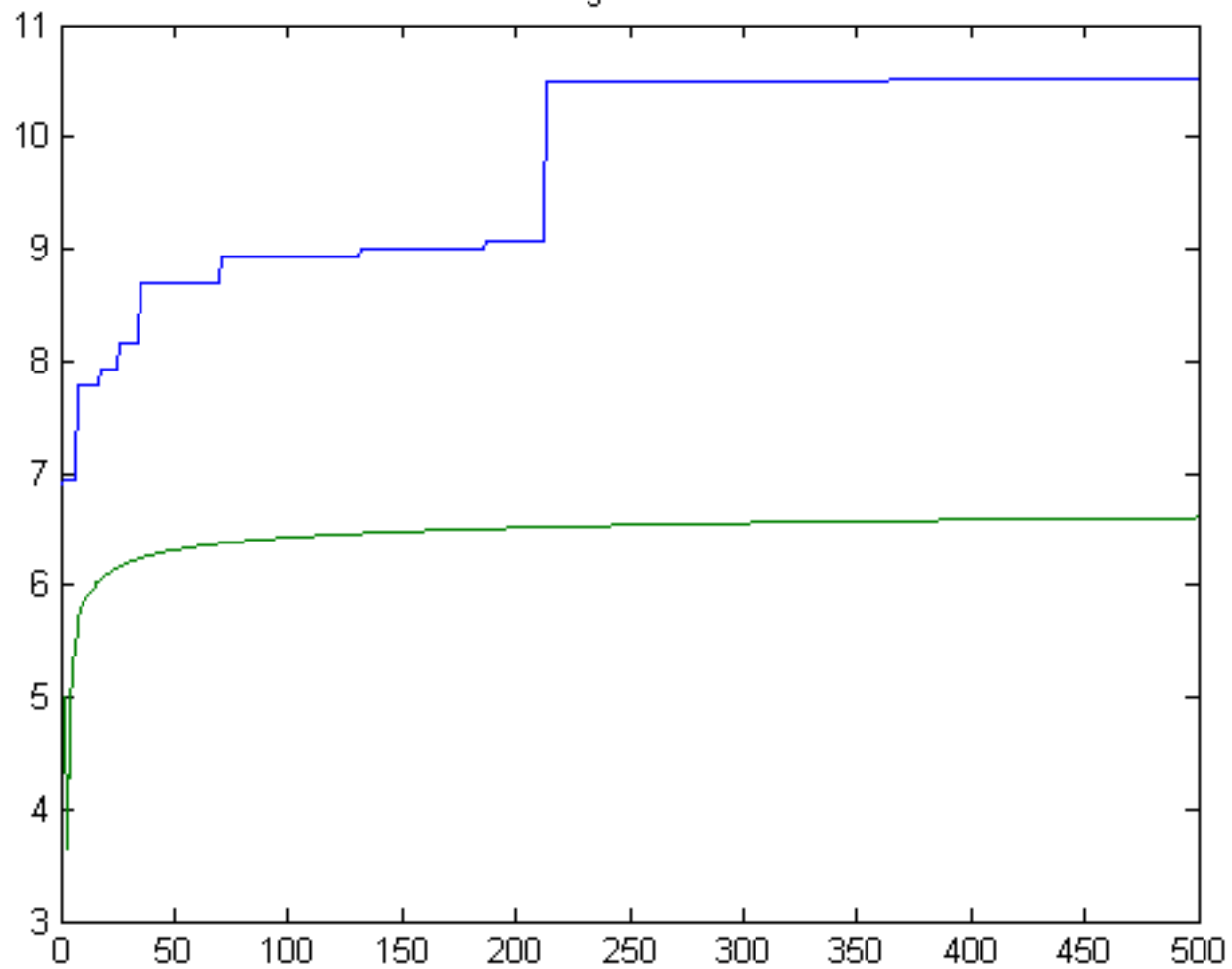


Figure 42

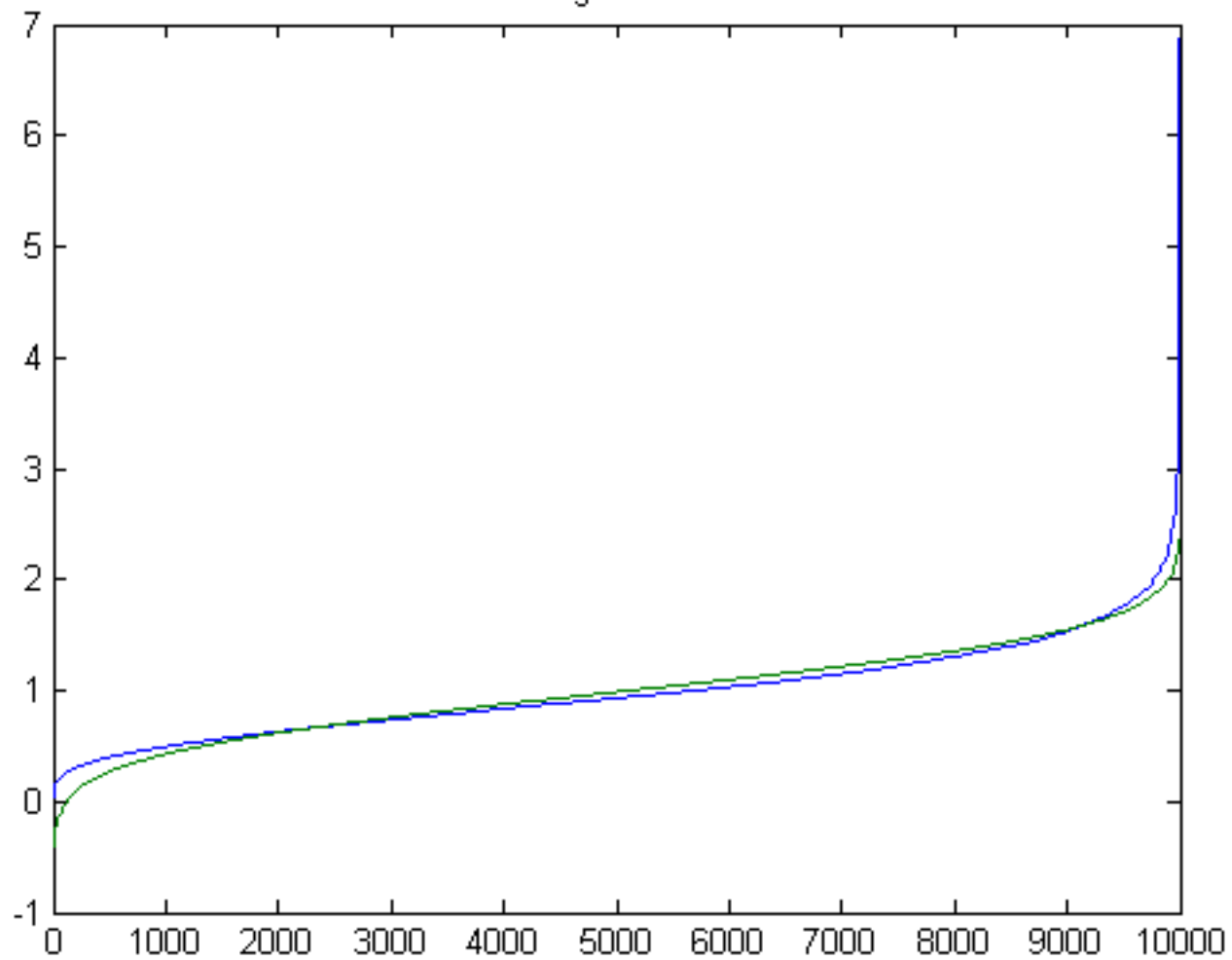


Figure 43

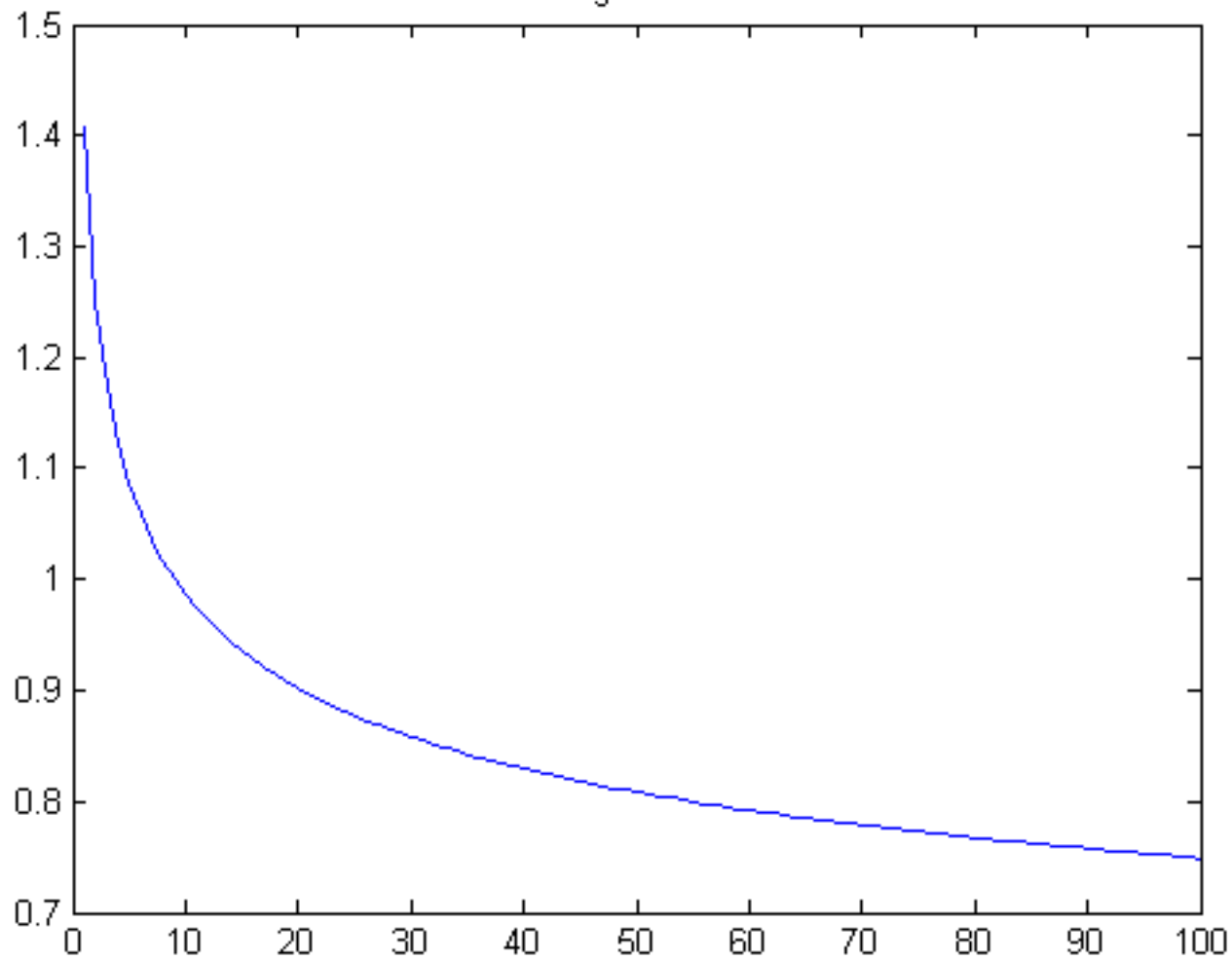


Figure 44

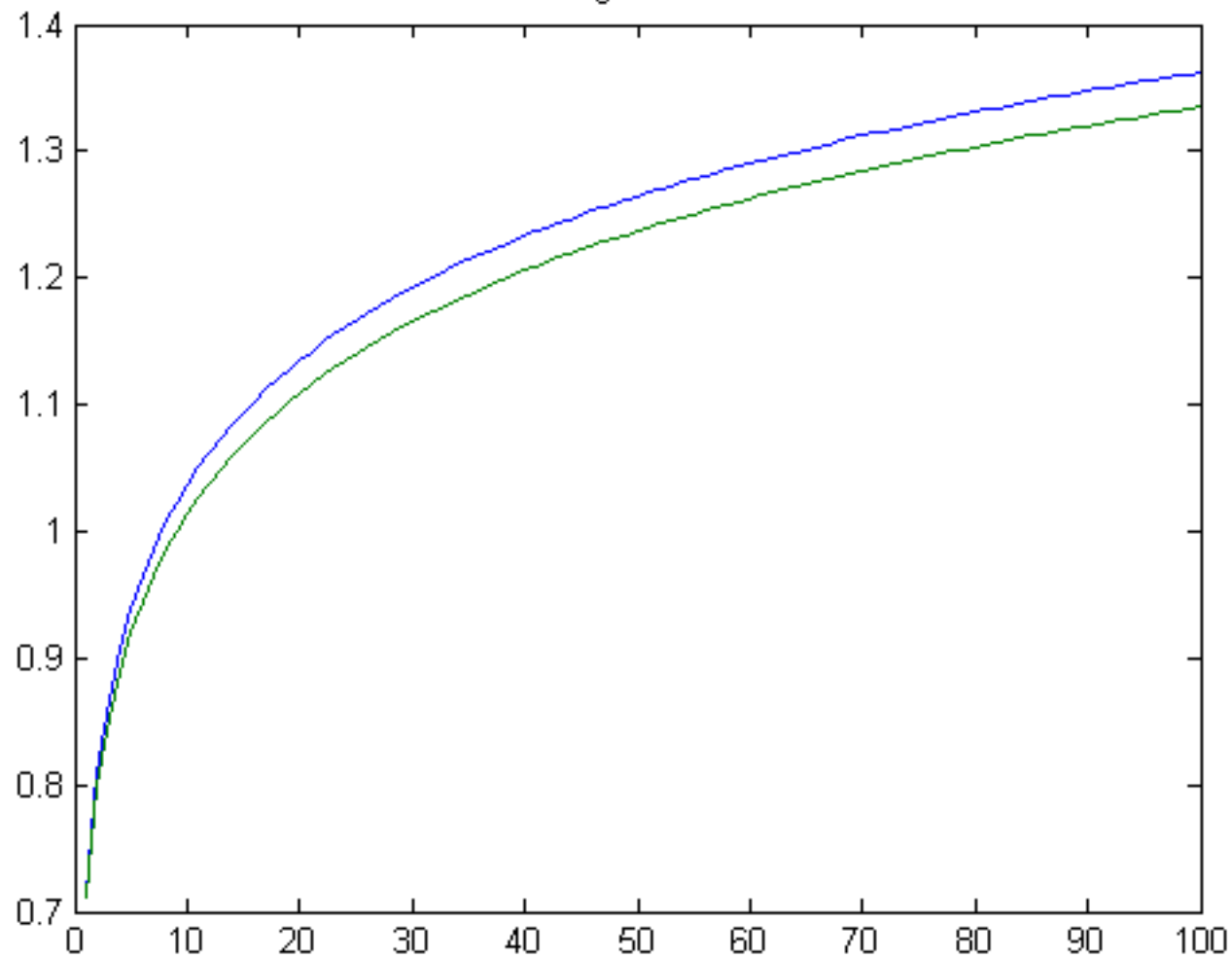


Figure 45

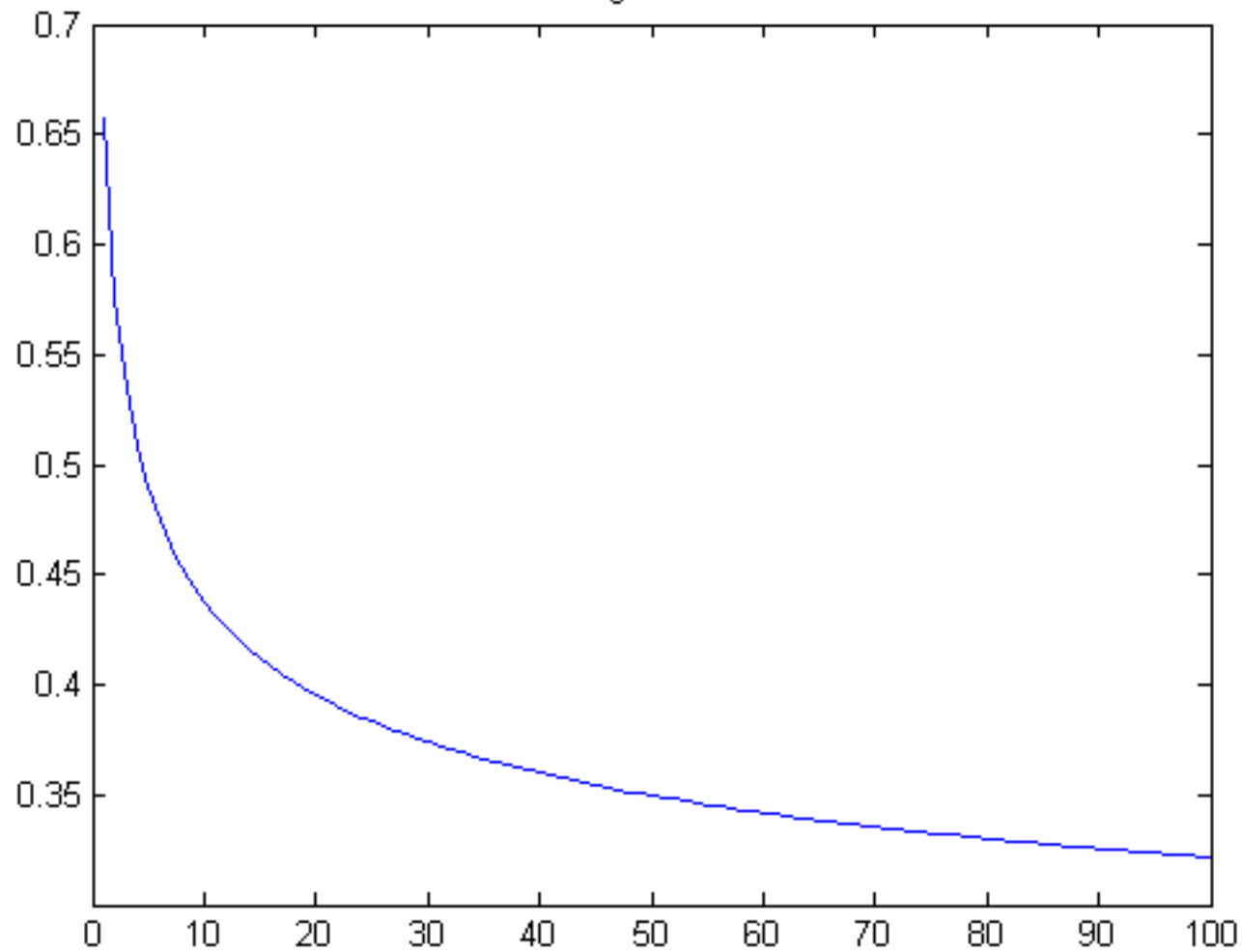


Figure 46

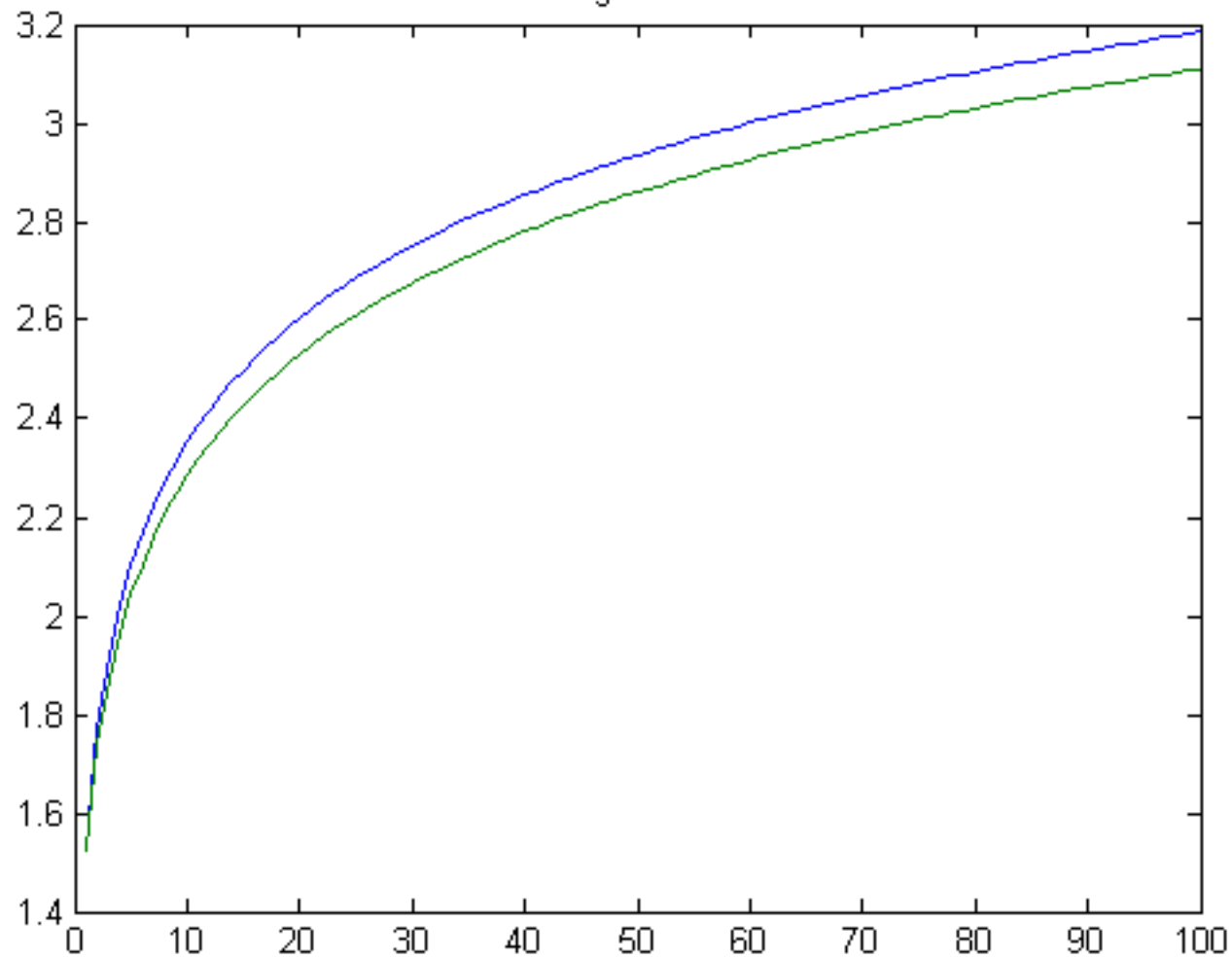


Figure 47

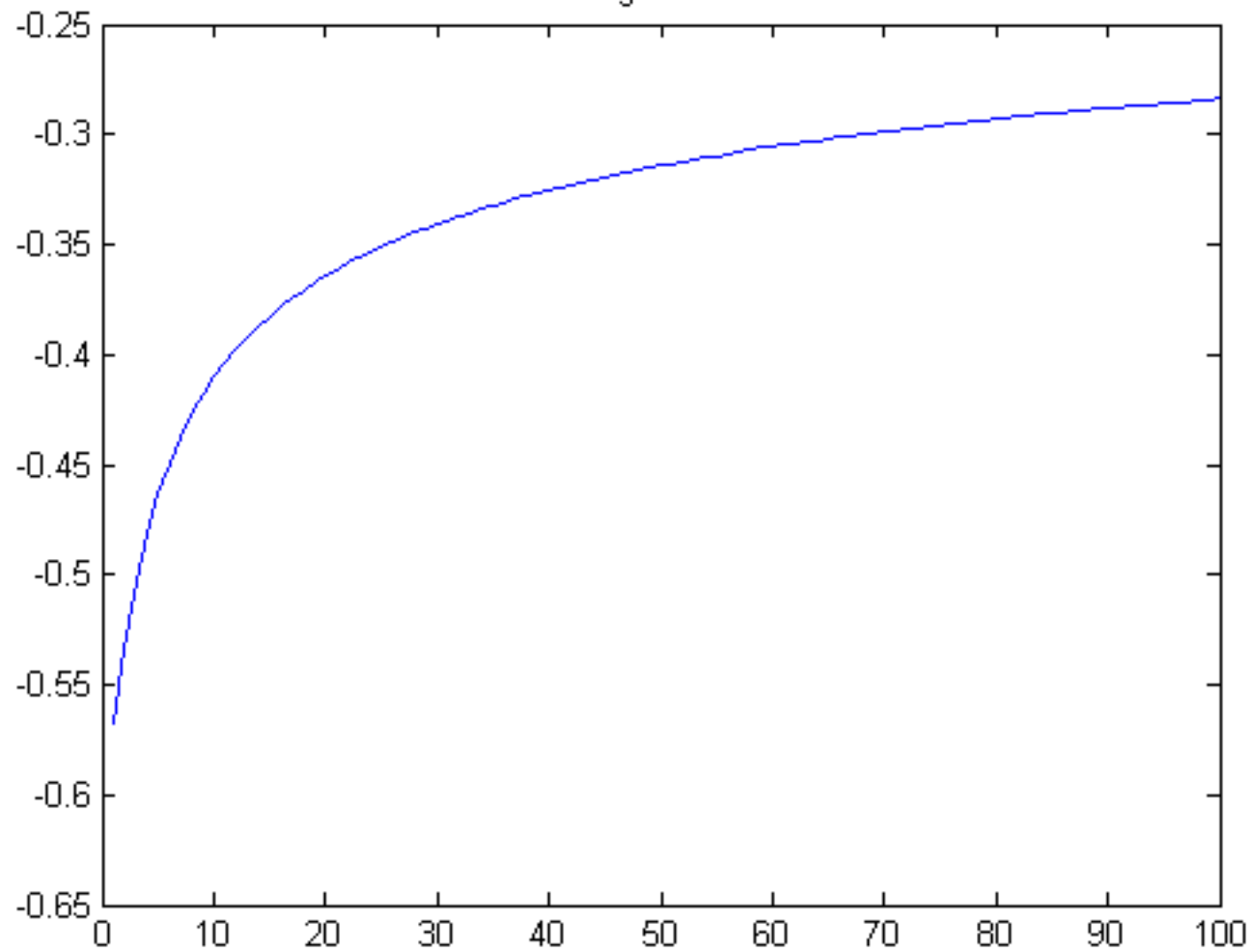


Figure 48

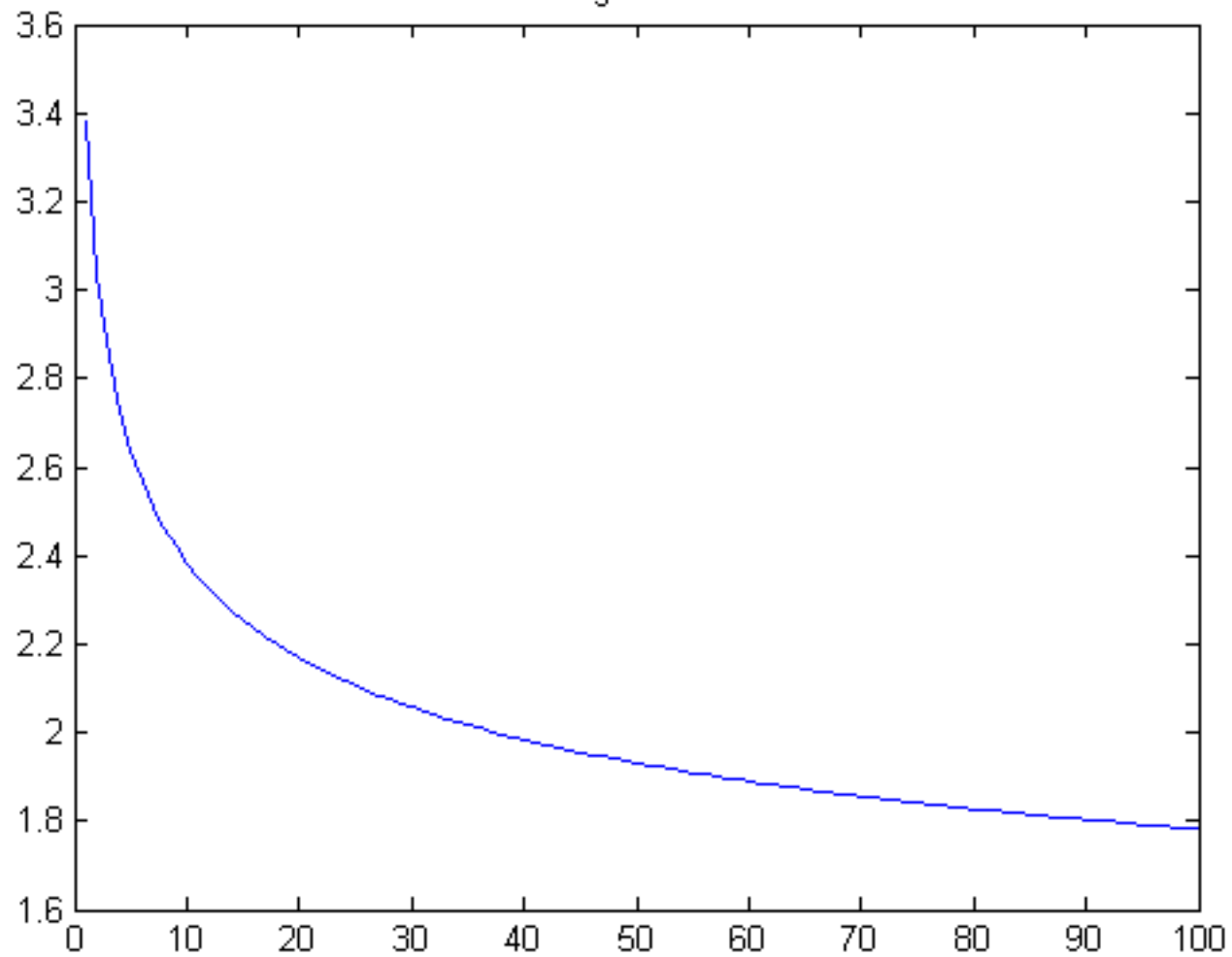


Figure 49

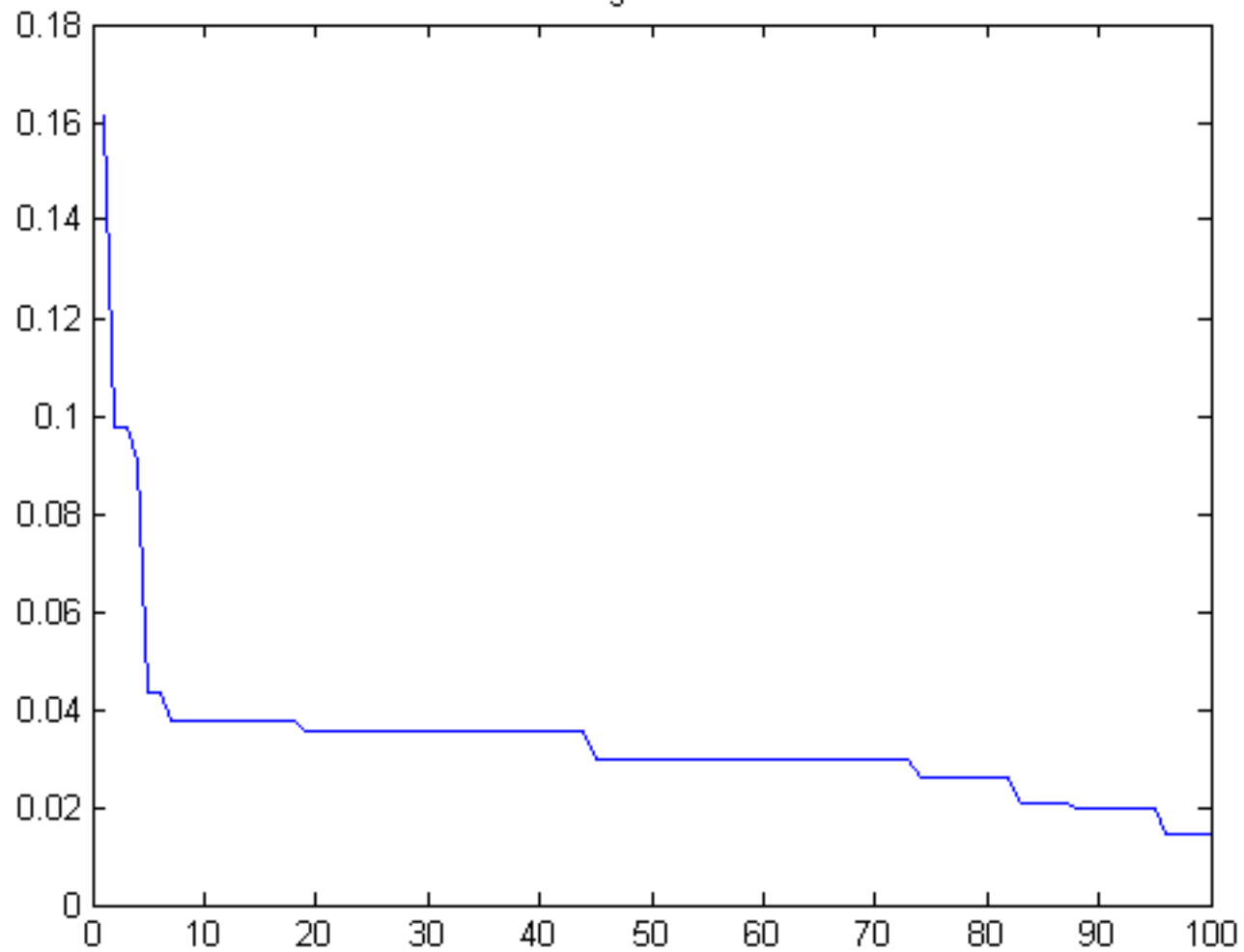


Figure 50

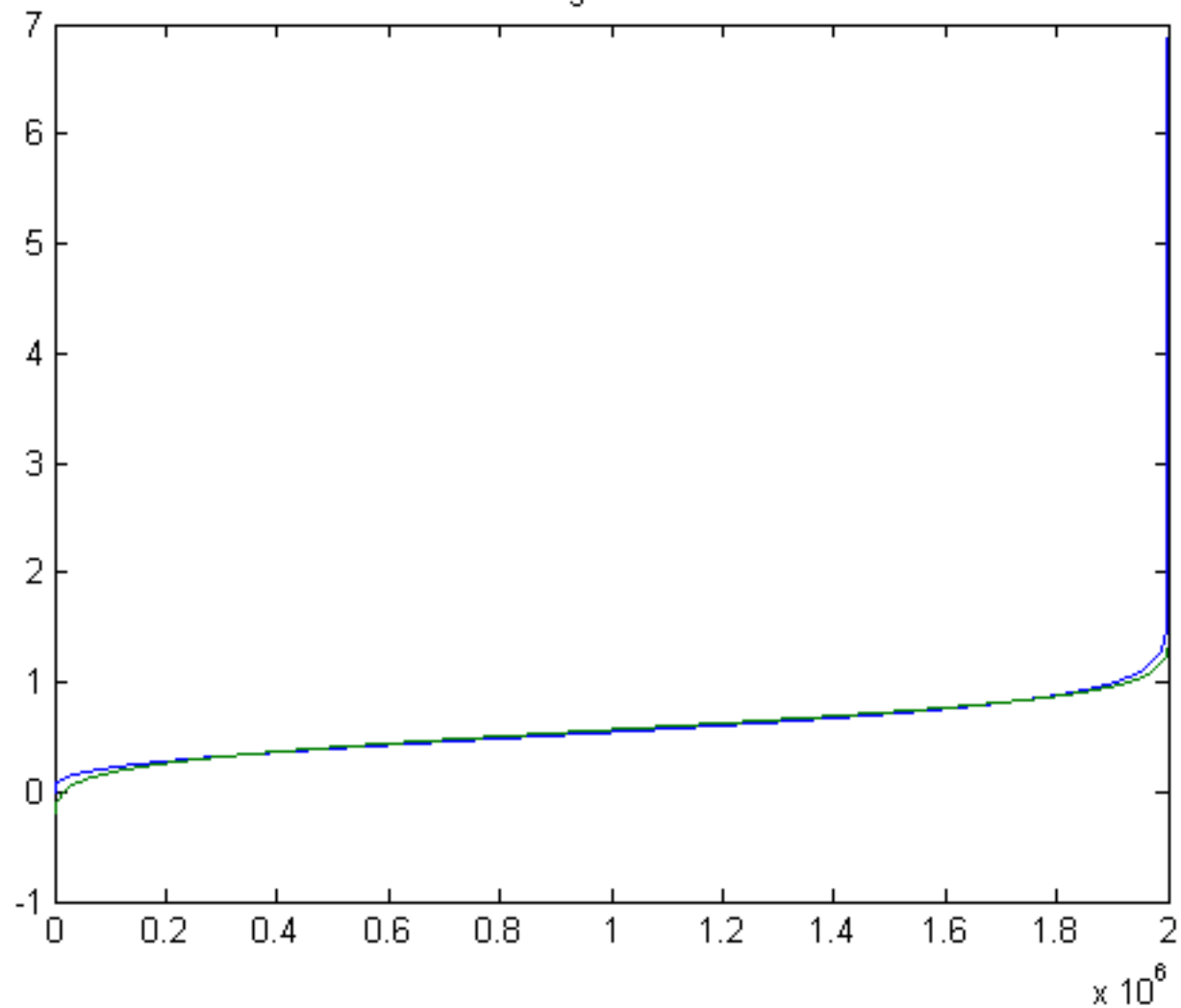


Figure 51

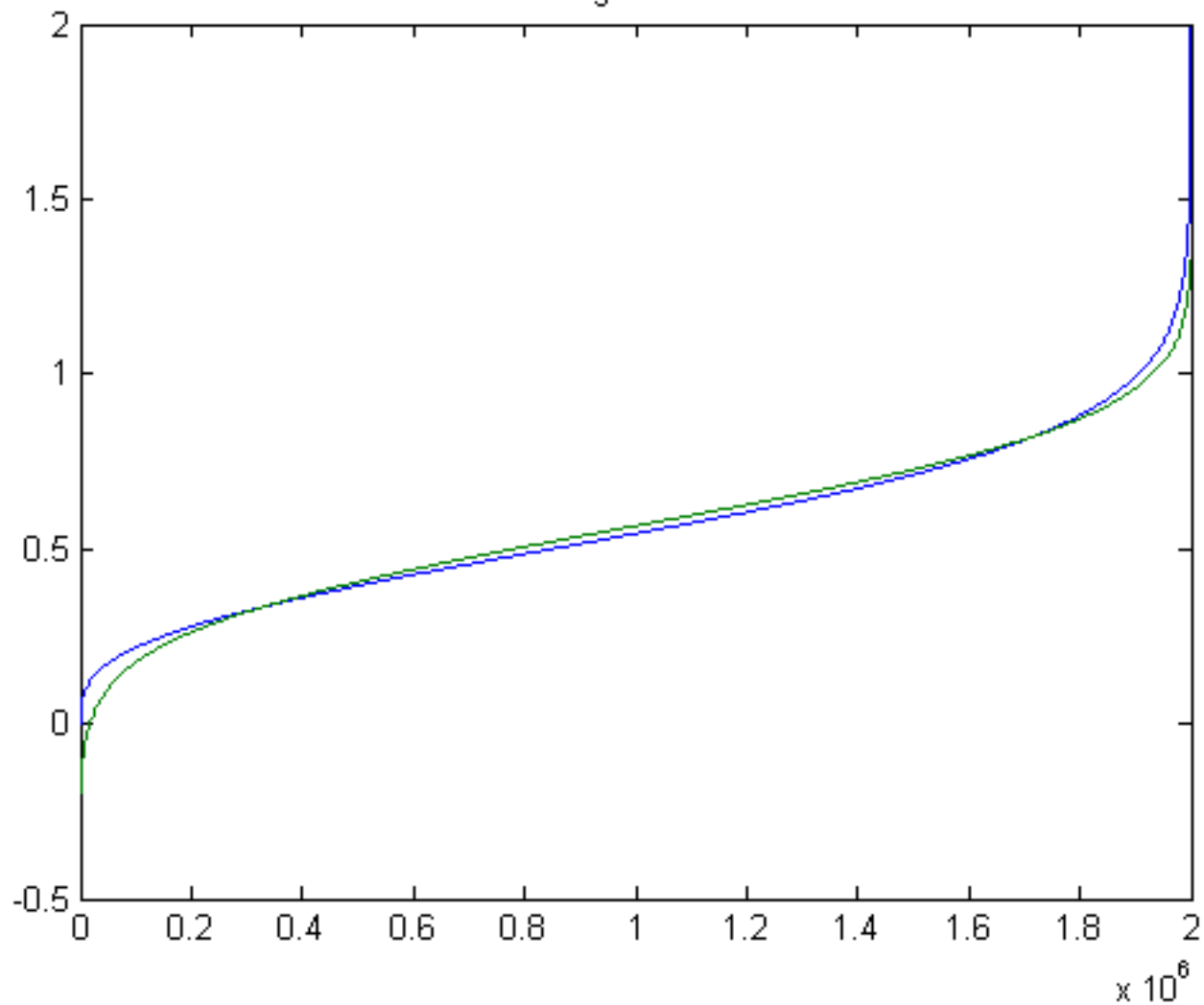


Figure 52

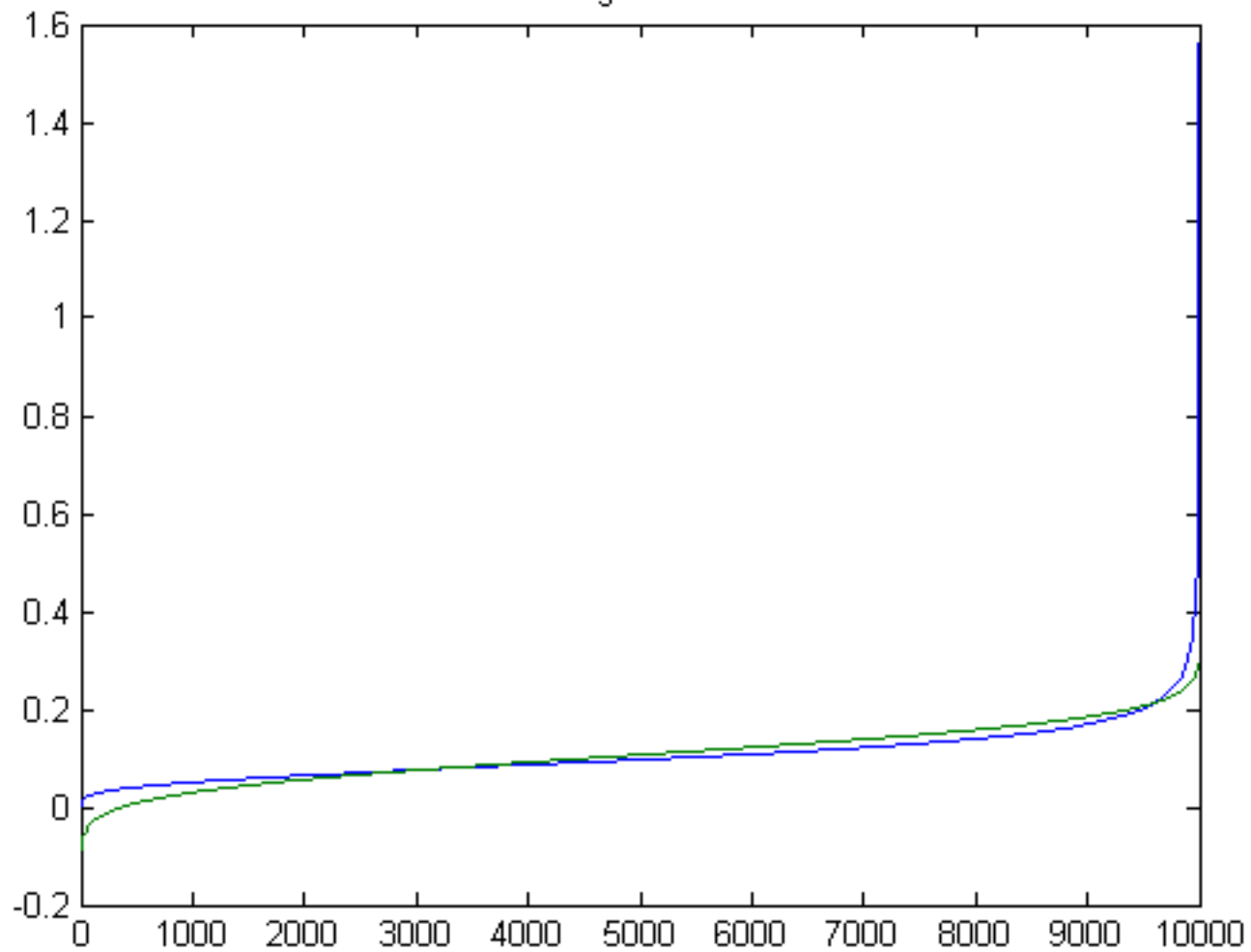


Figure 53

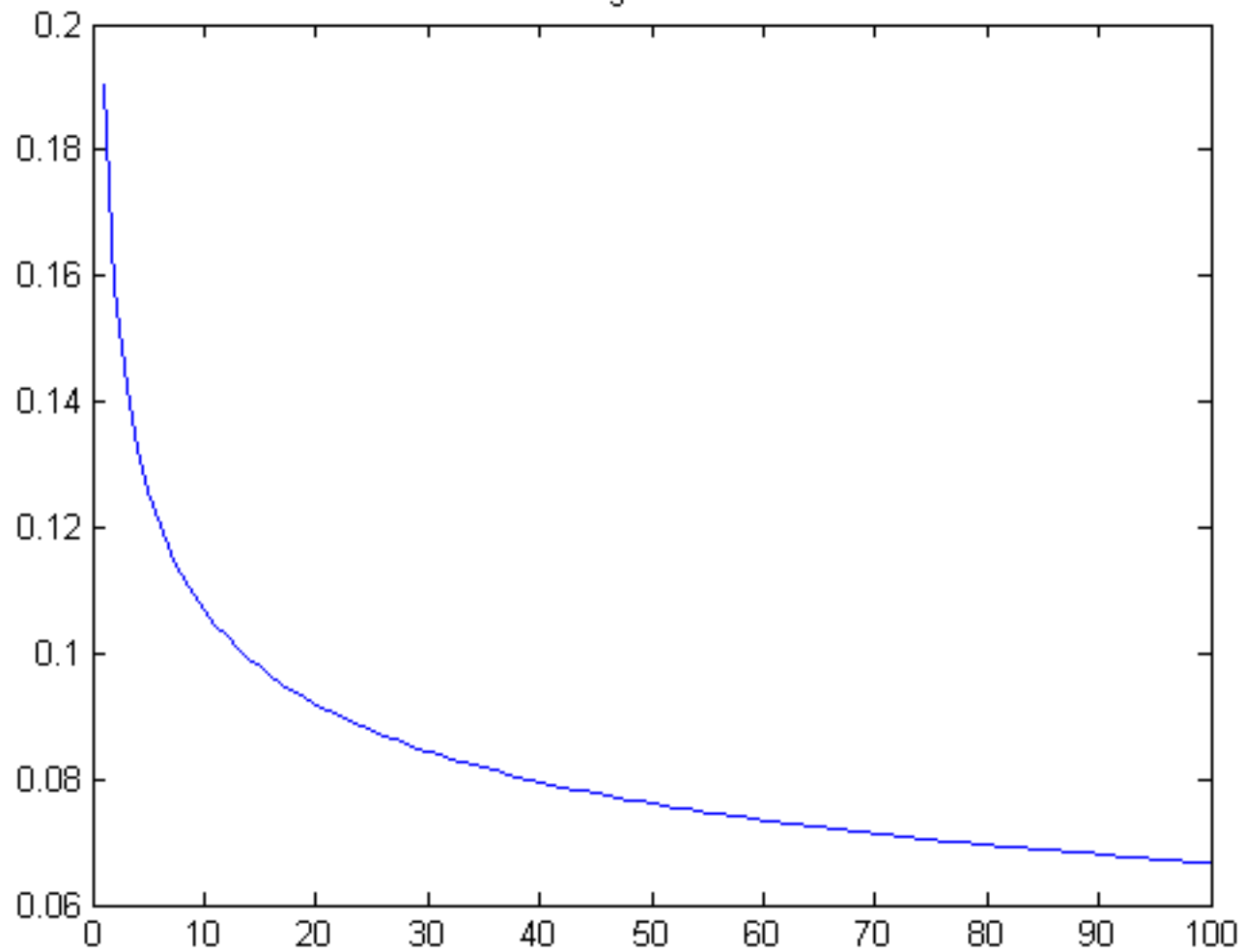


Figure 54

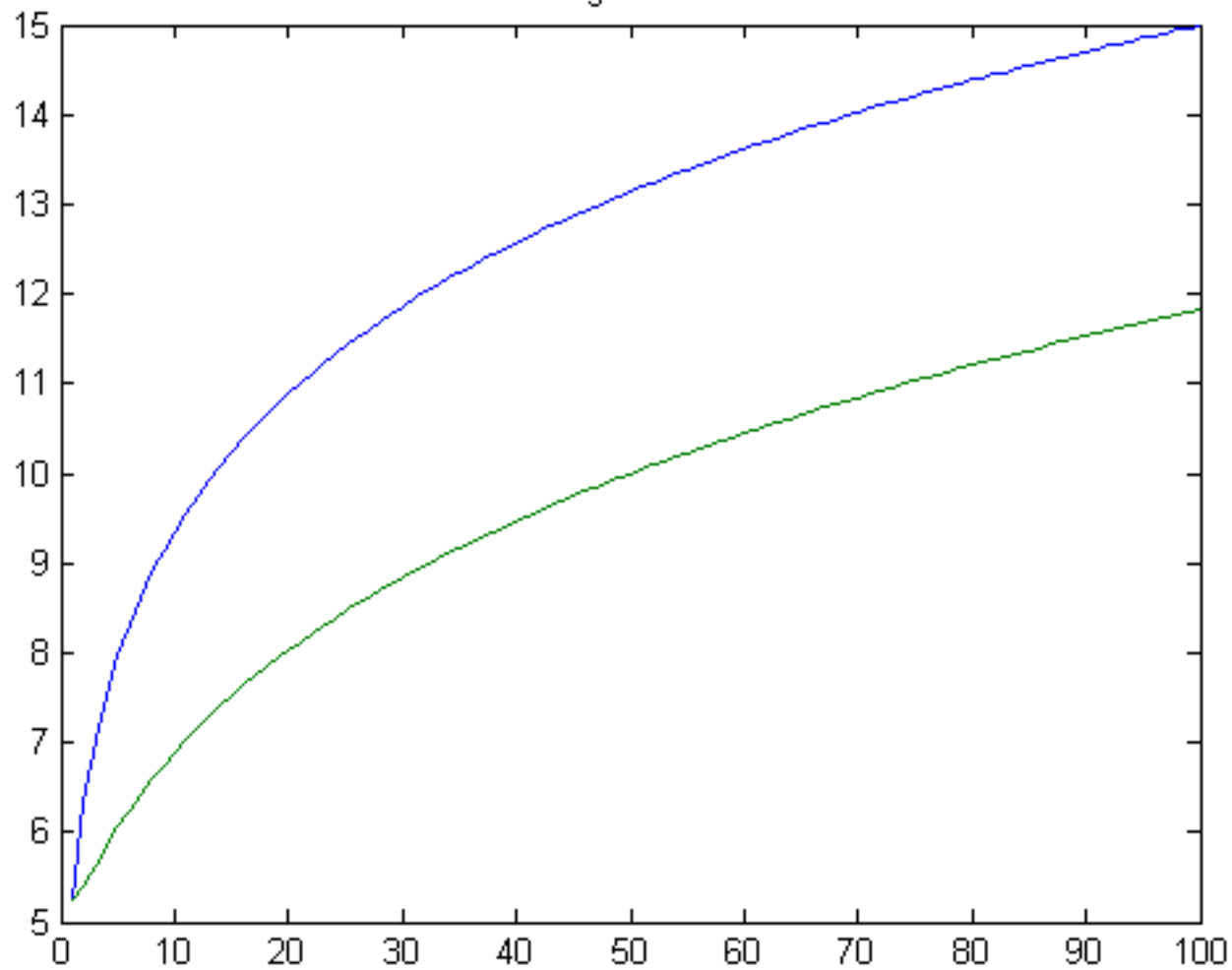


Figure 55

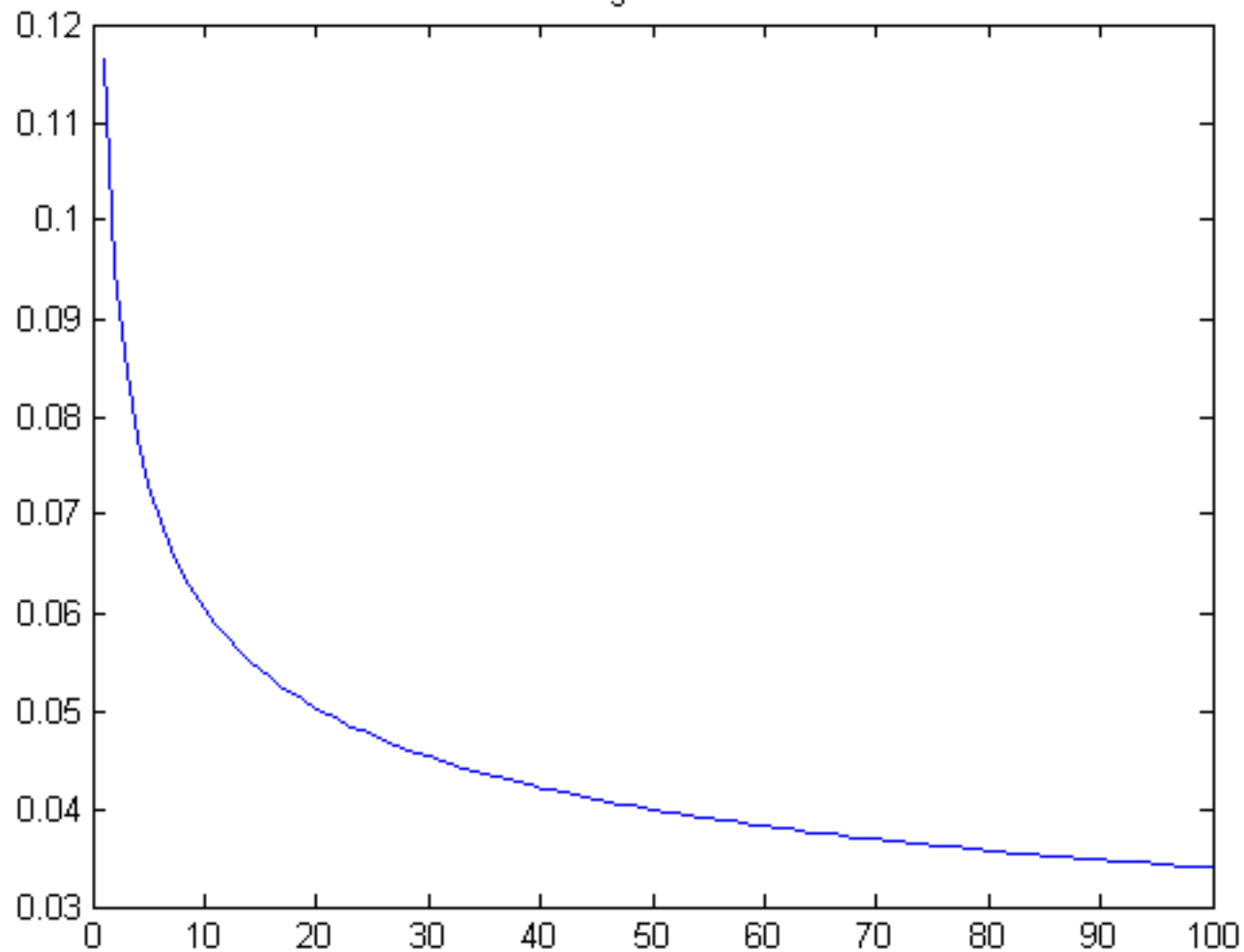


Figure 56

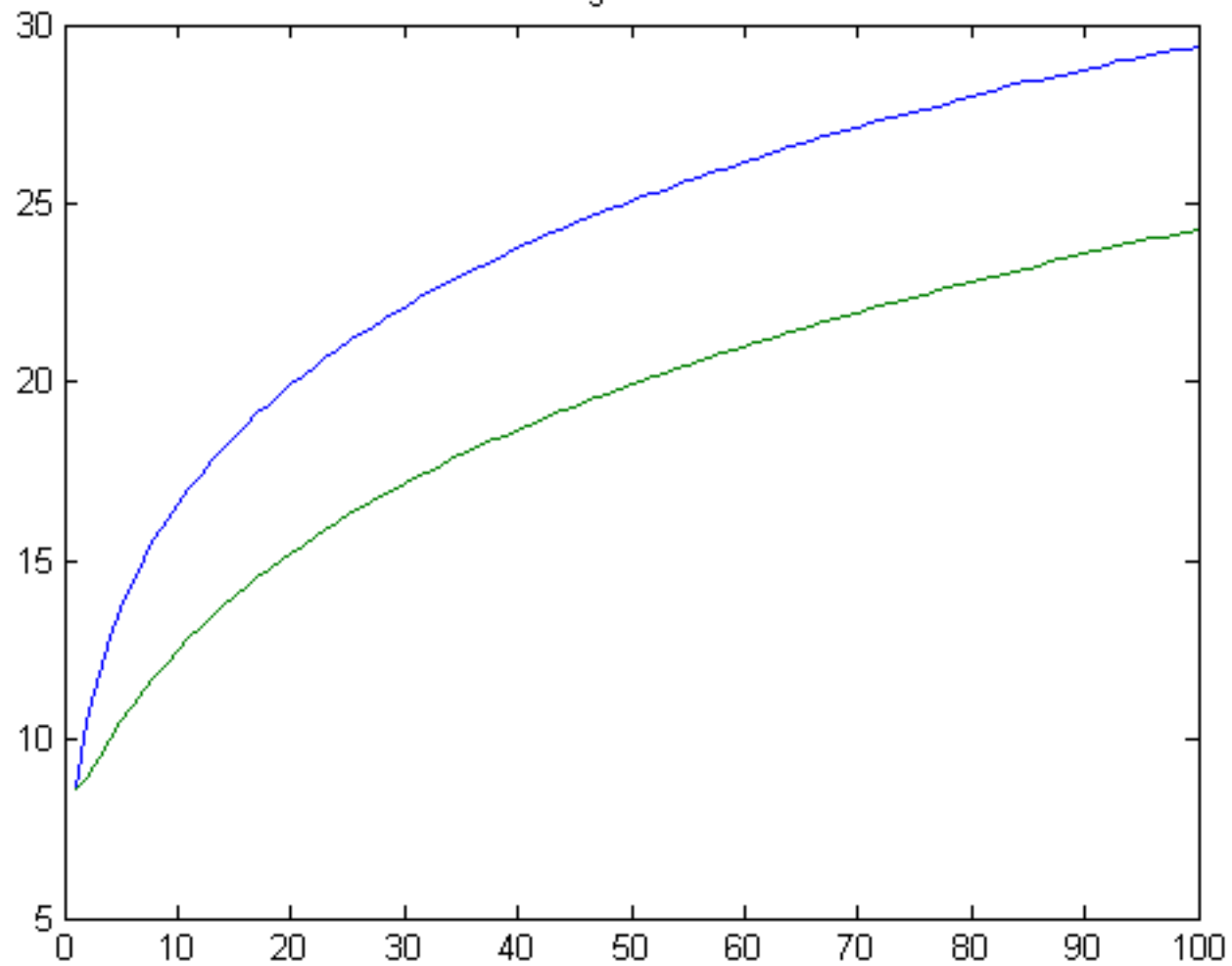


Figure 57

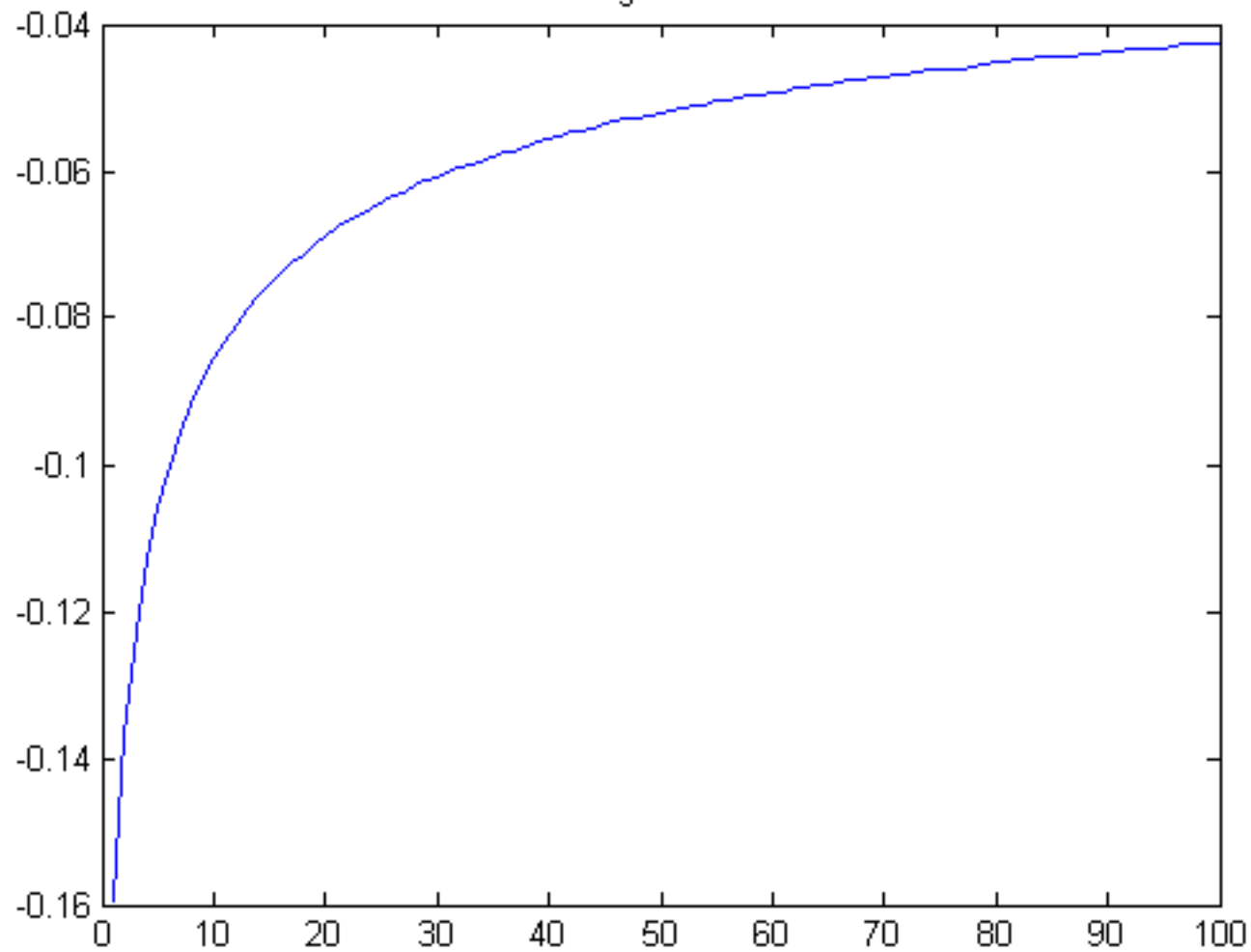


Figure 58

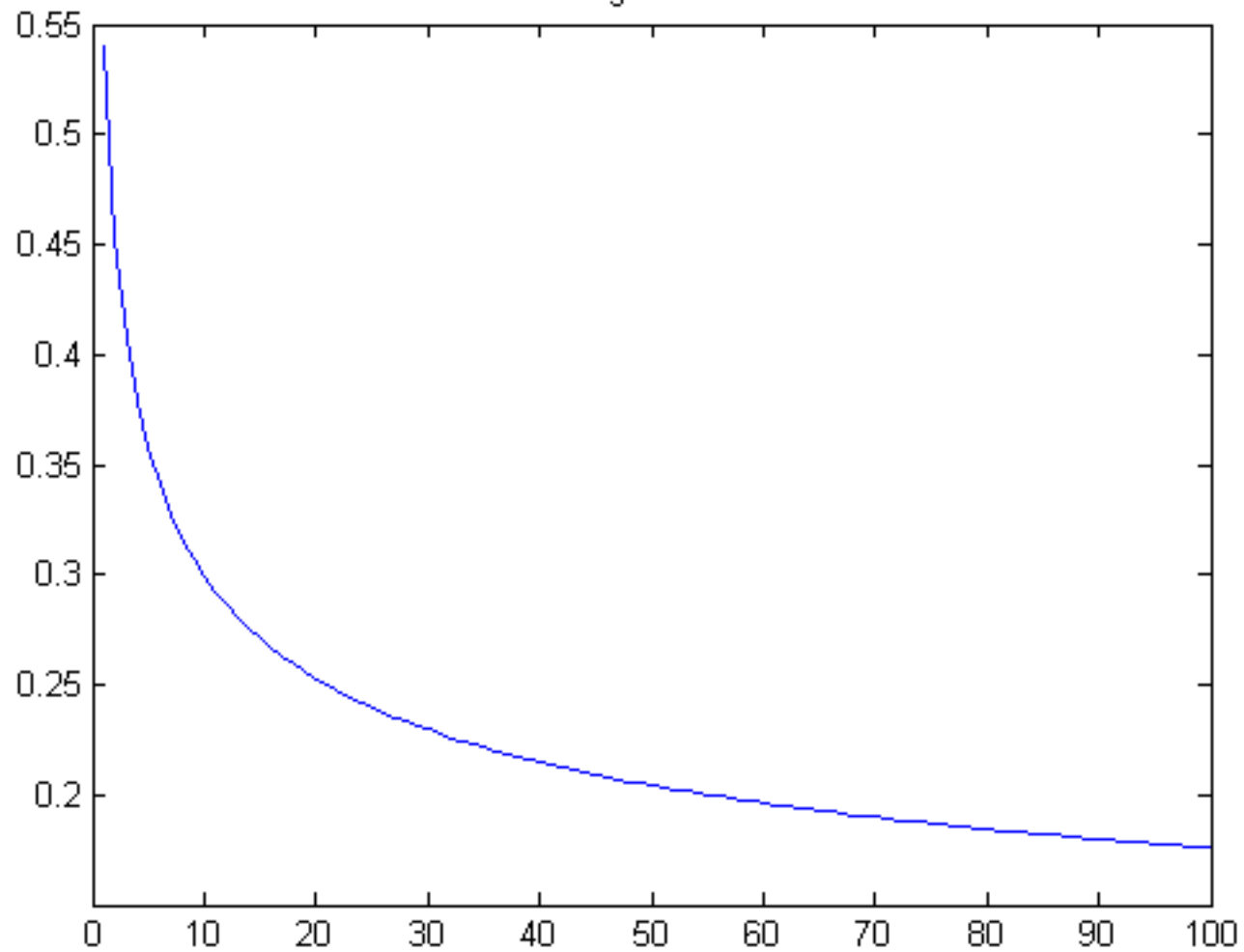


Figure 59

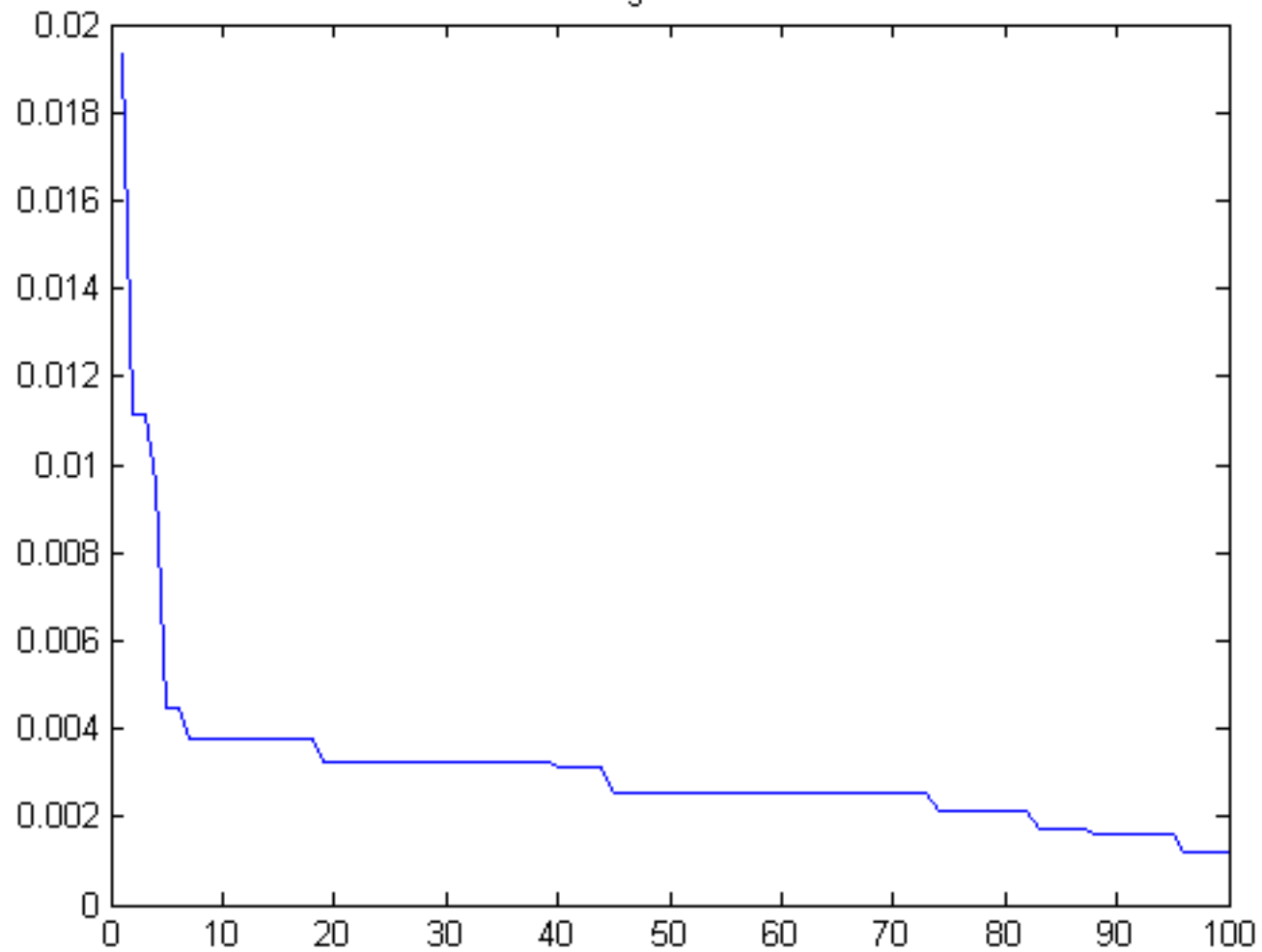


Figure 60

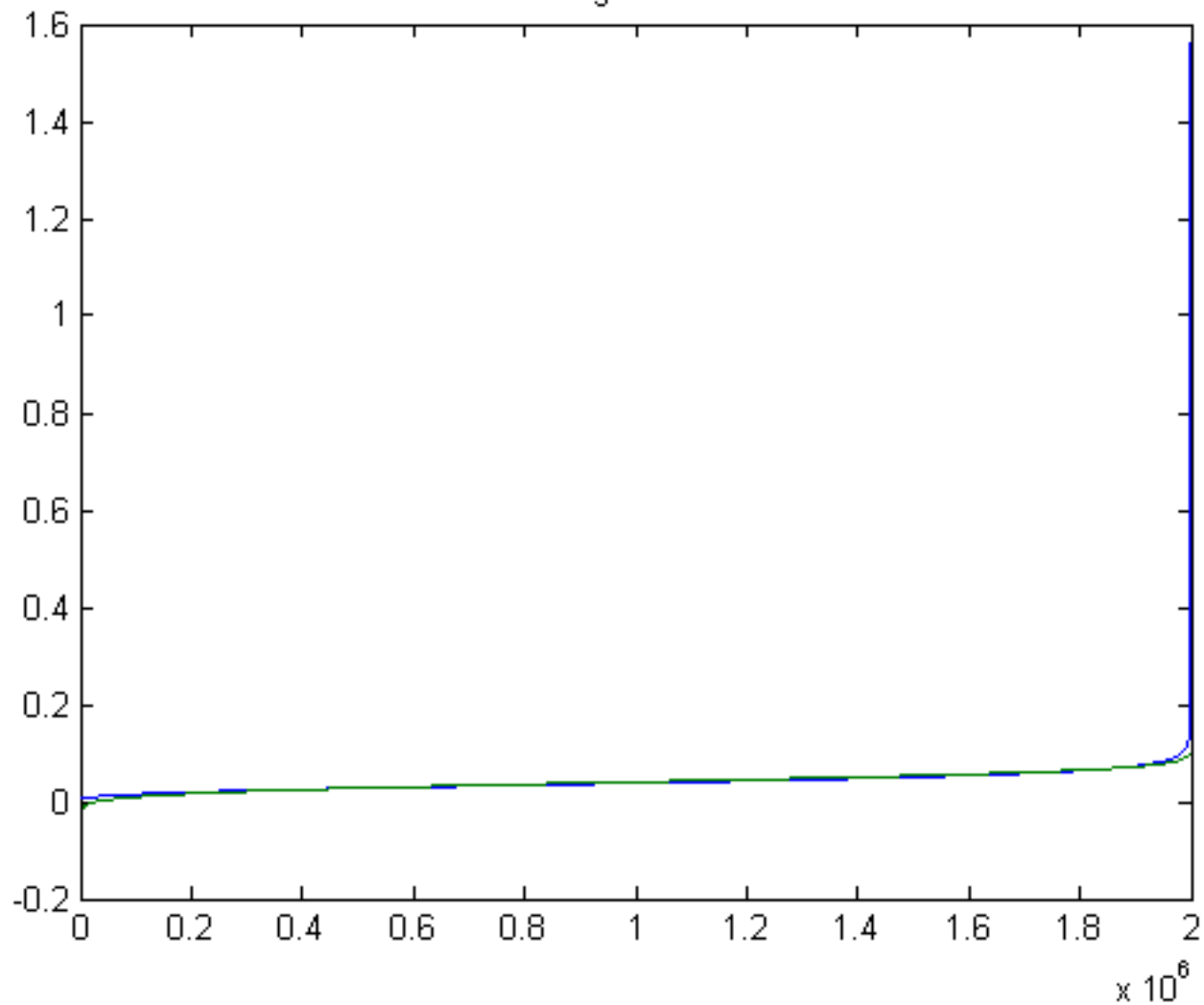


Figure 61

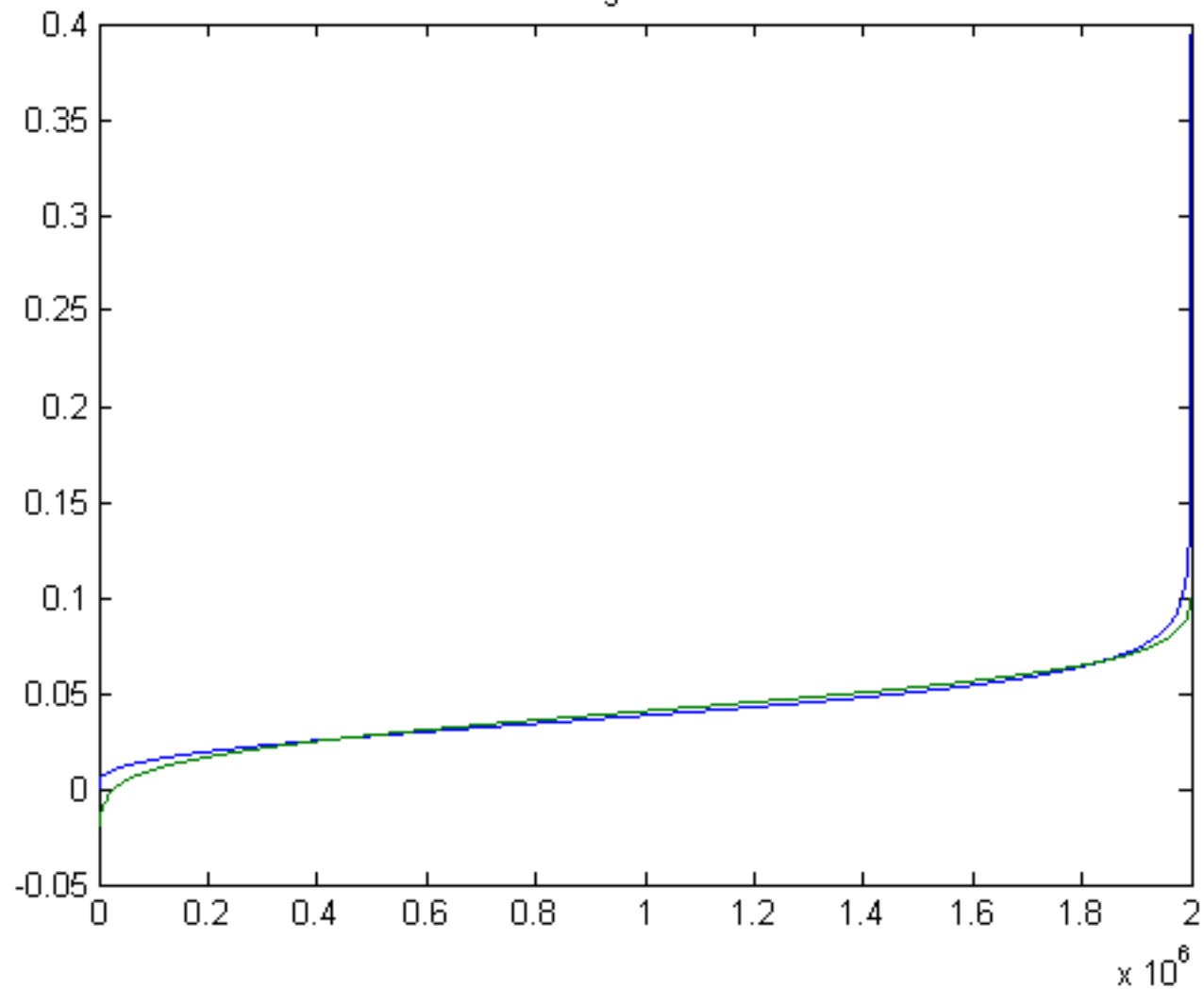


Figure 62

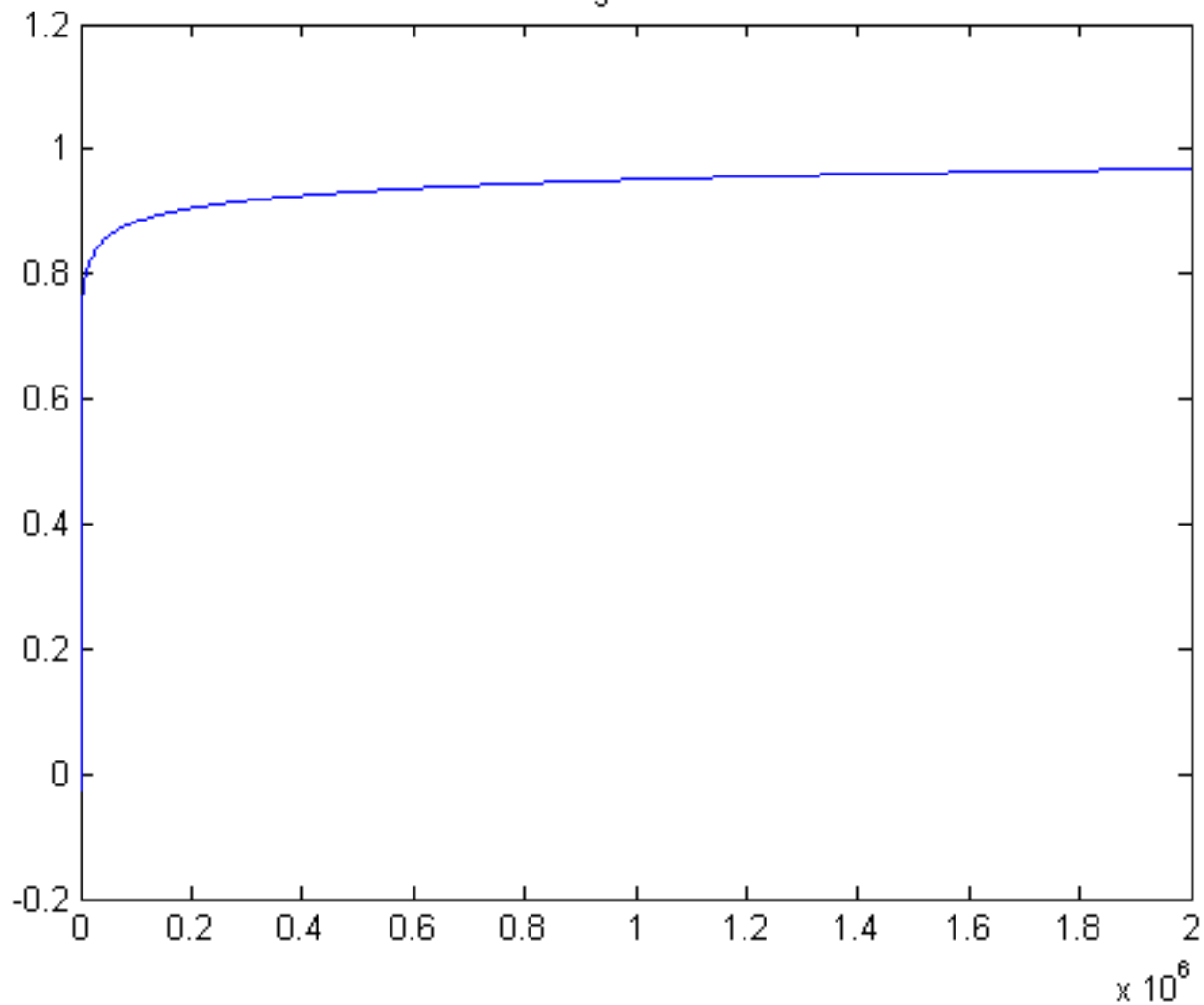


Figure 63

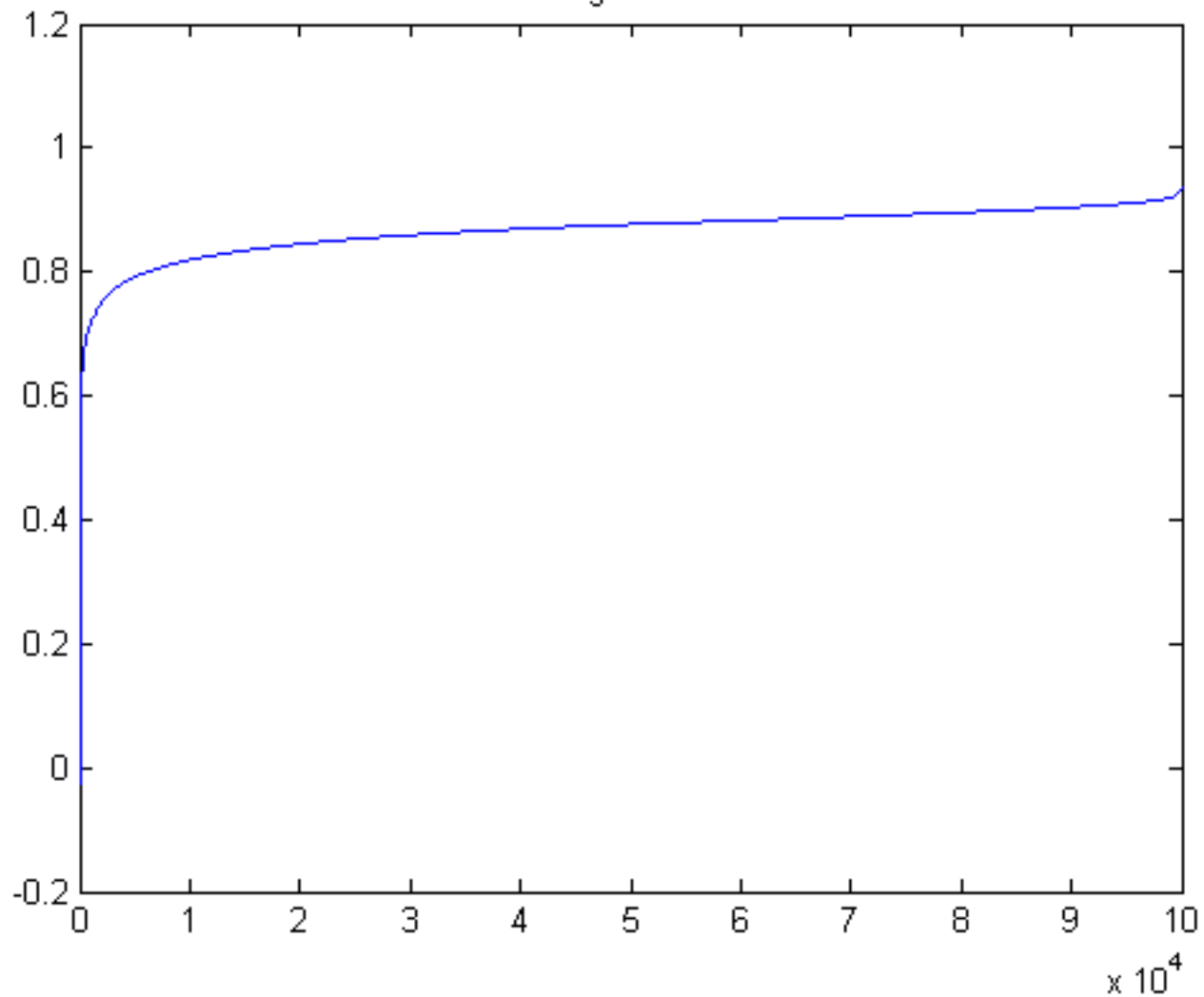


Figure 64

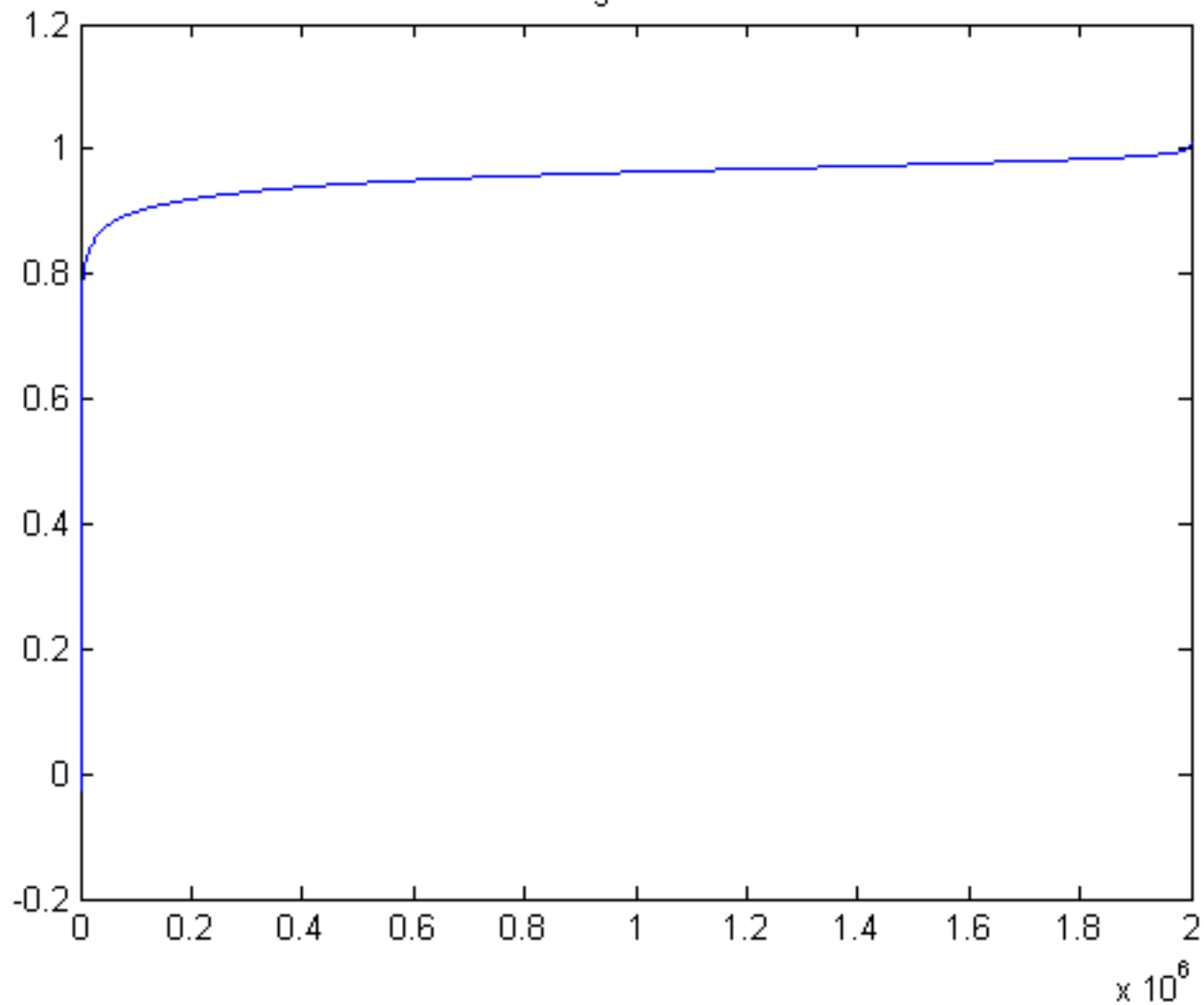


Figure 65

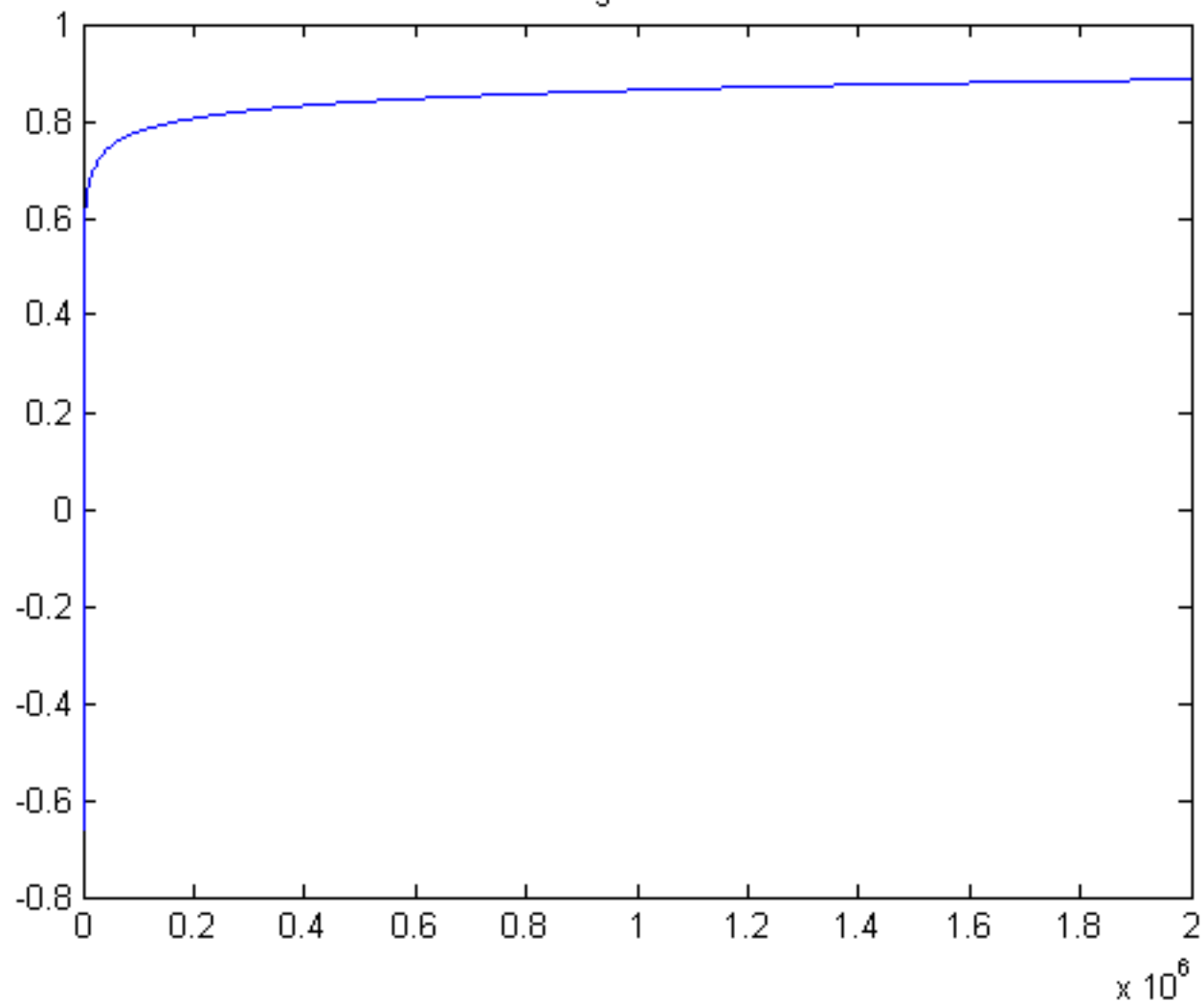


Figure 66

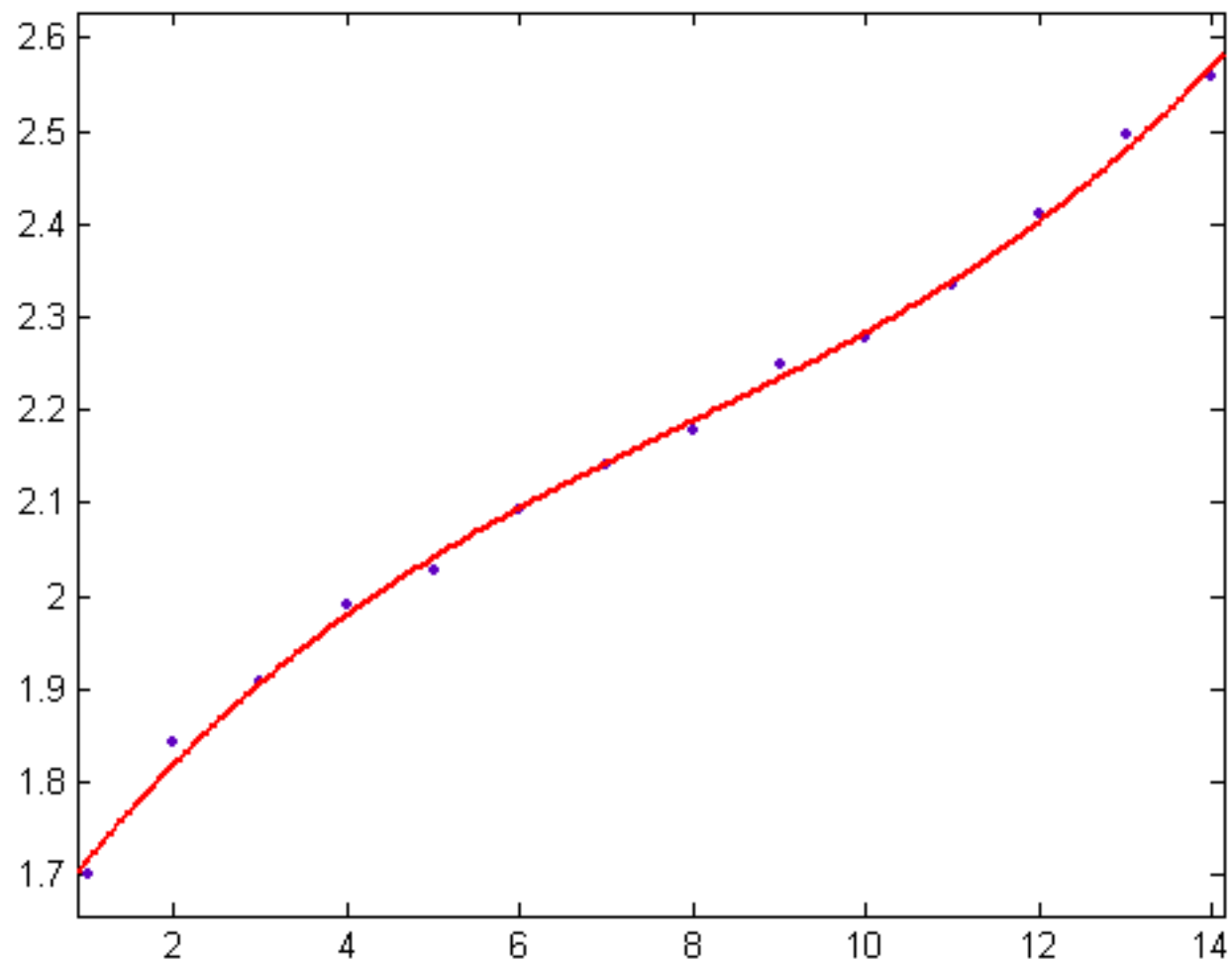


Figure 67

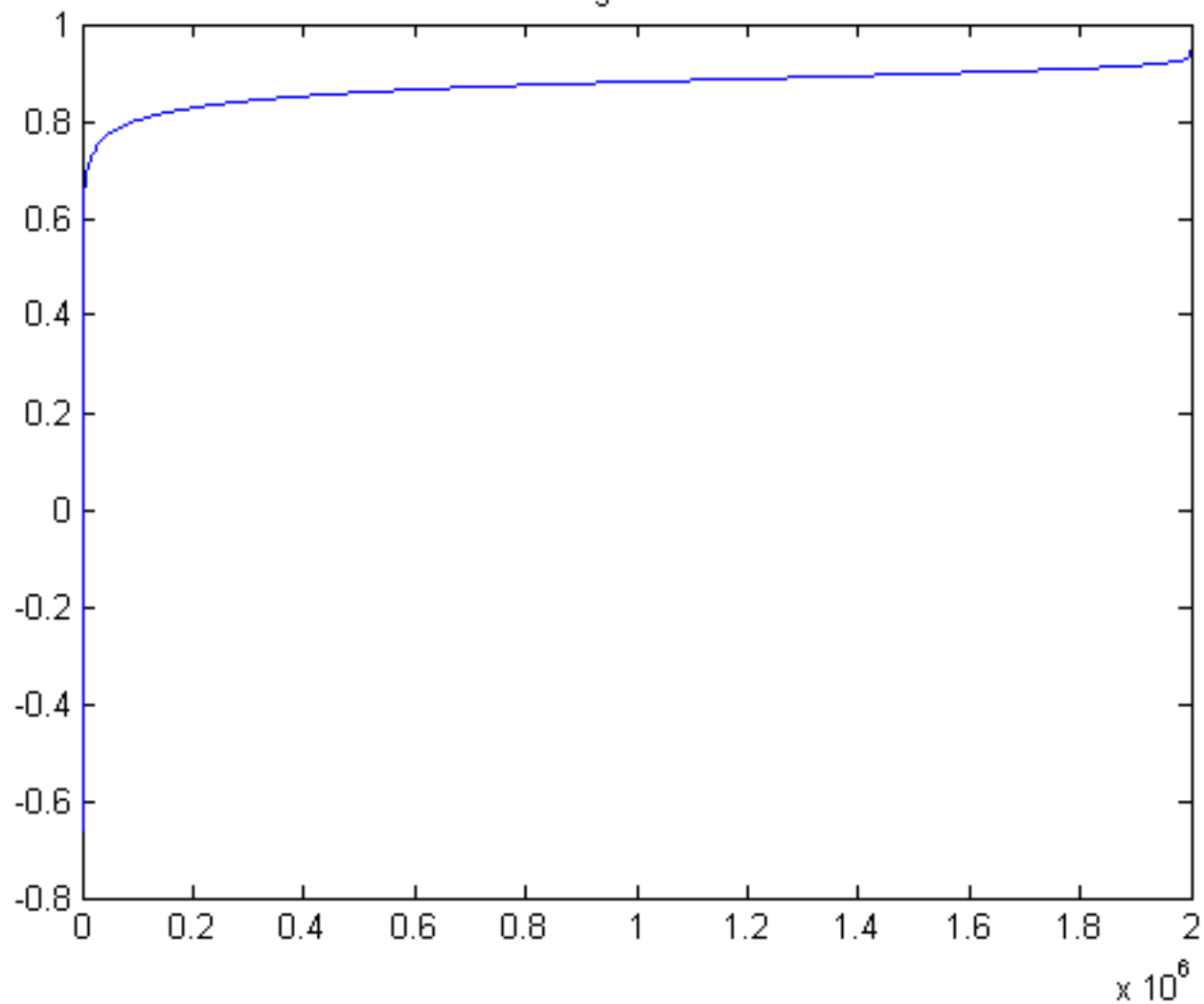


Figure 68

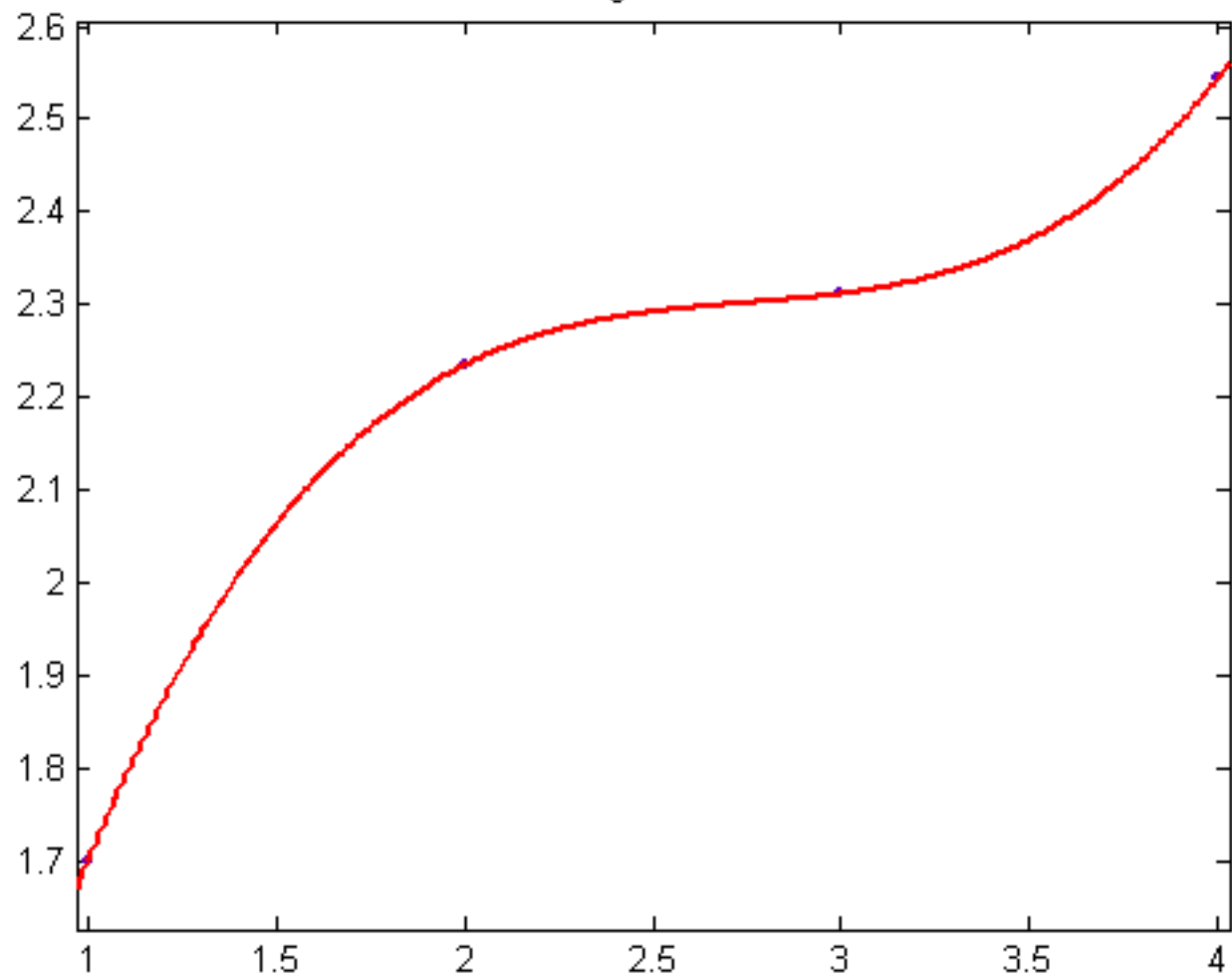


Figure 69

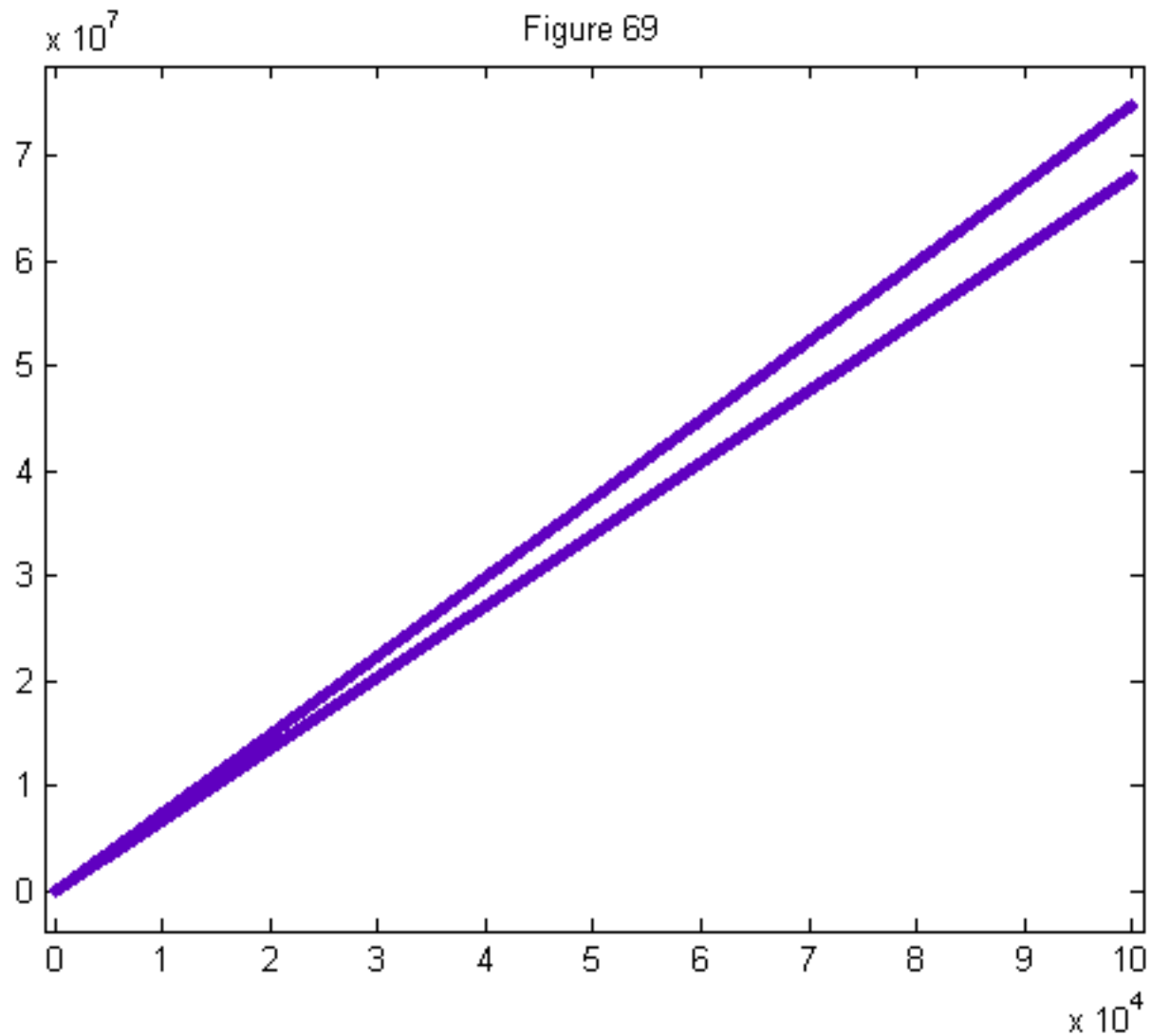


Figure 70

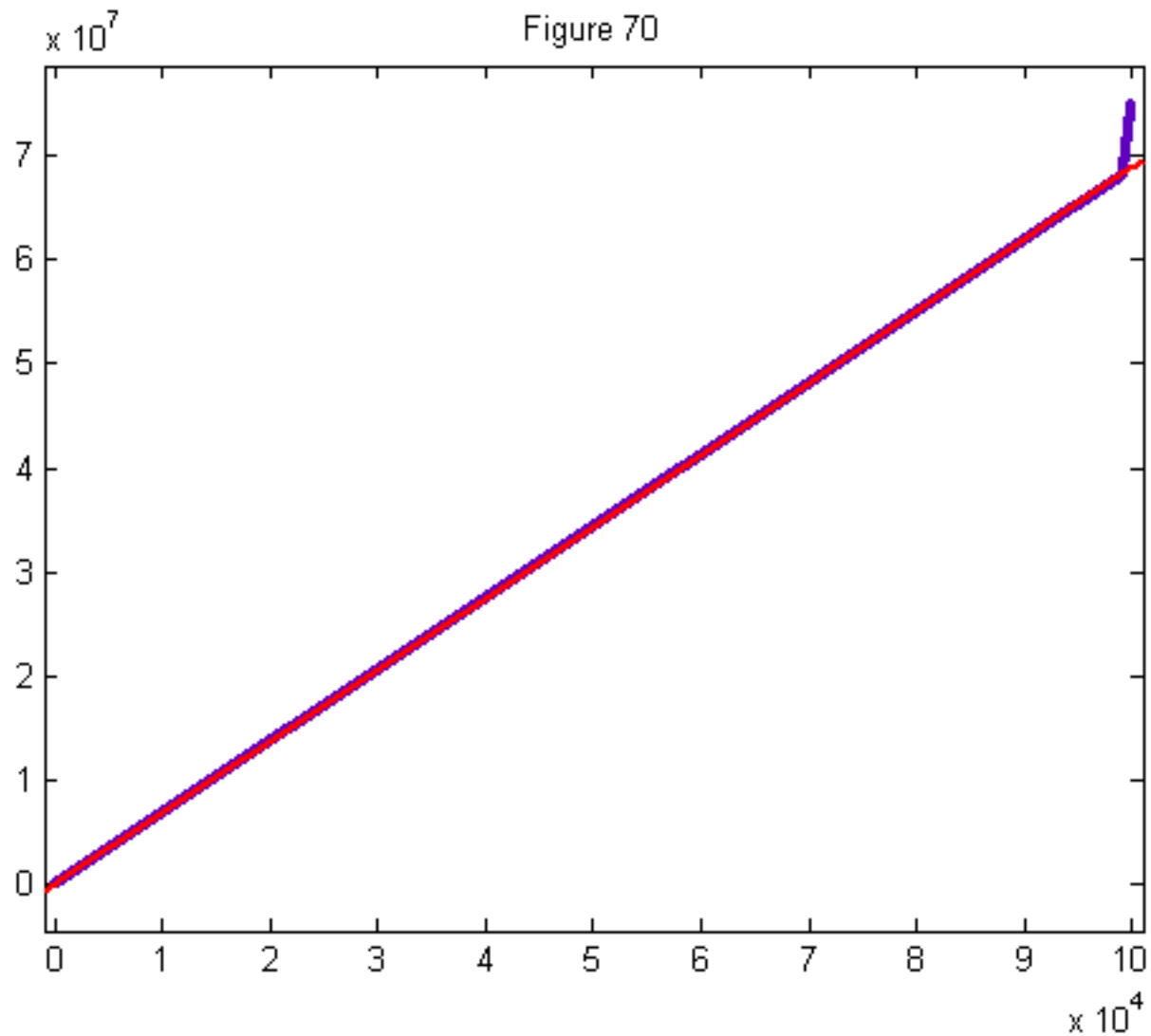


Figure 71

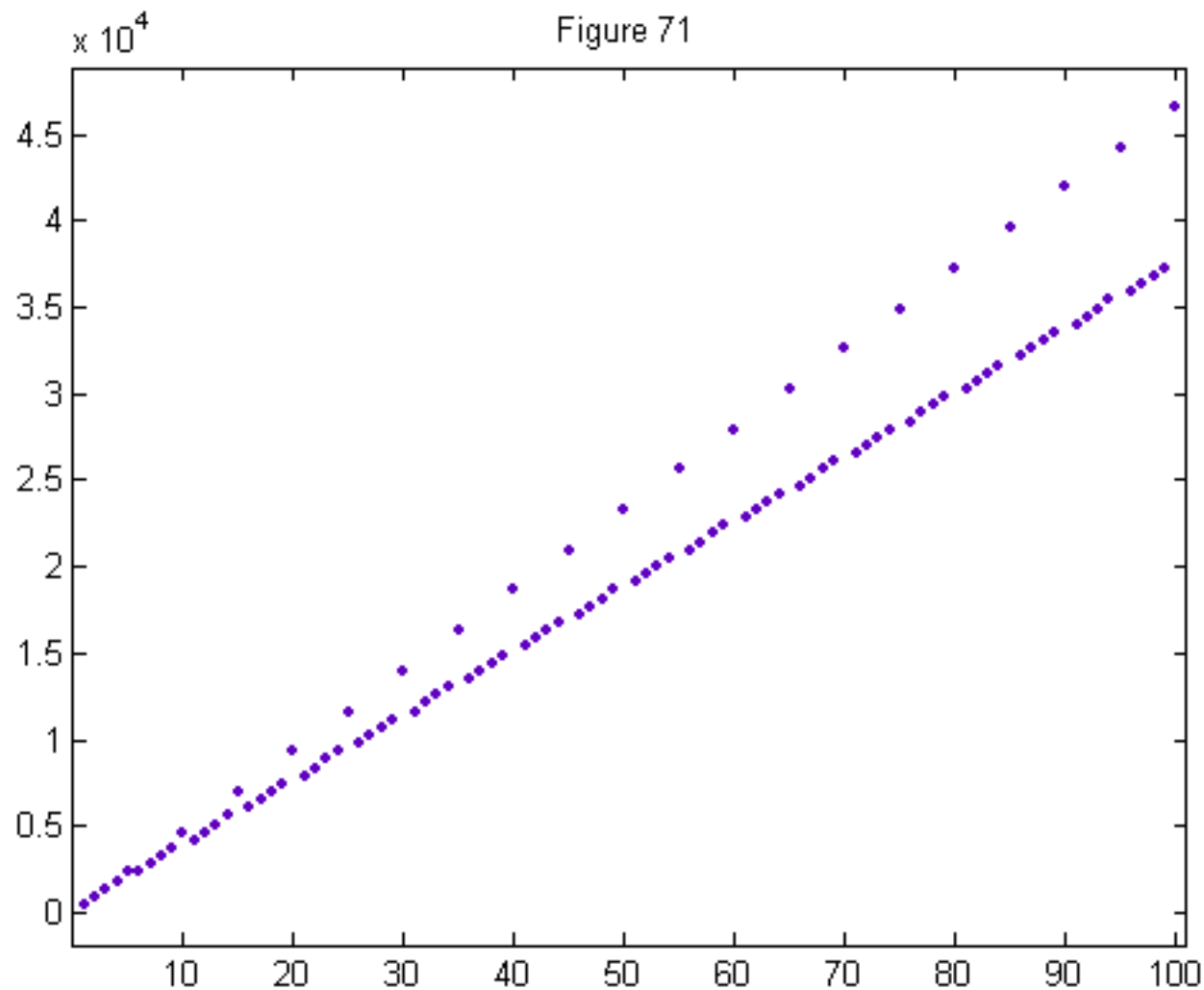


Figure 72

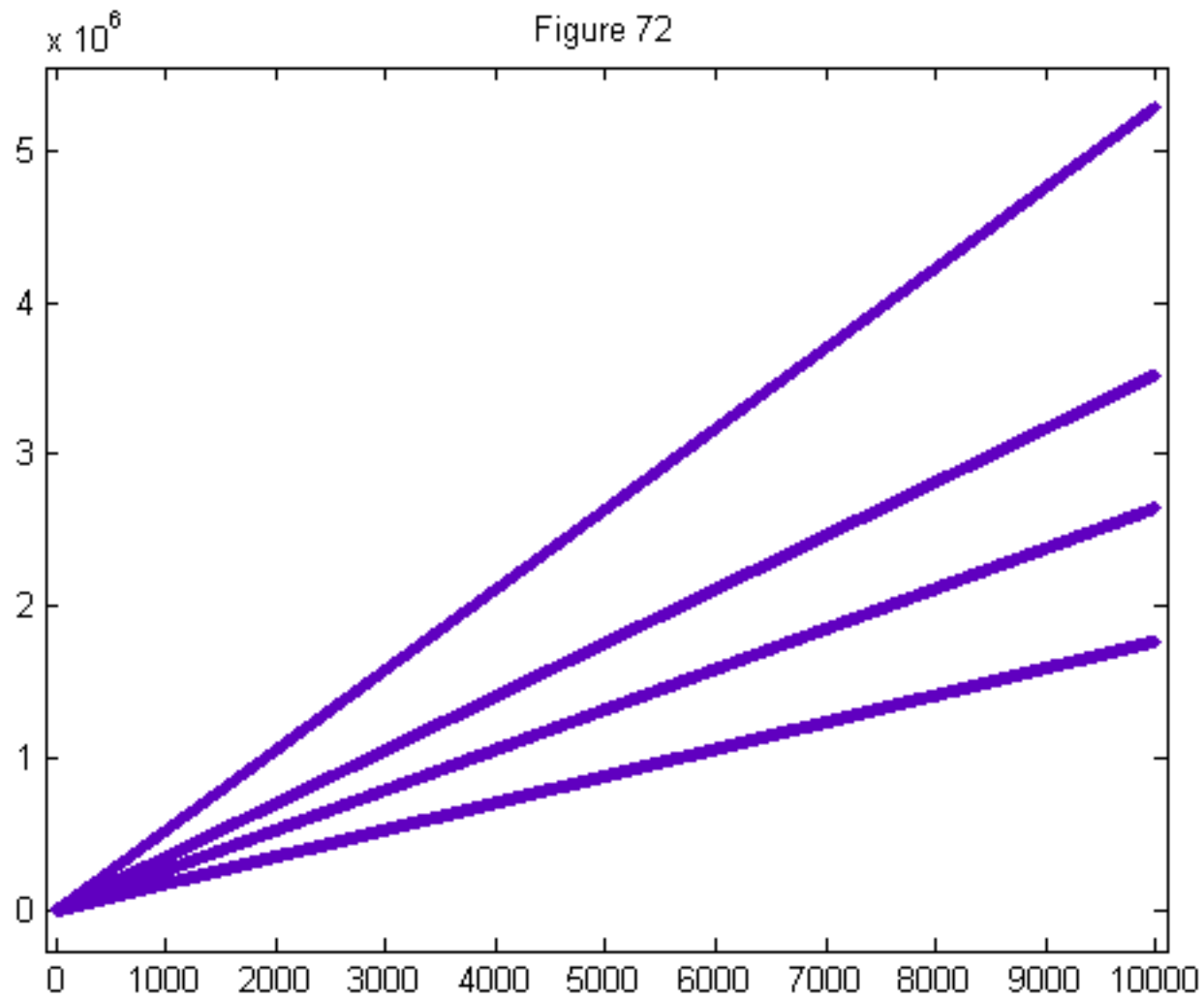


Figure 73

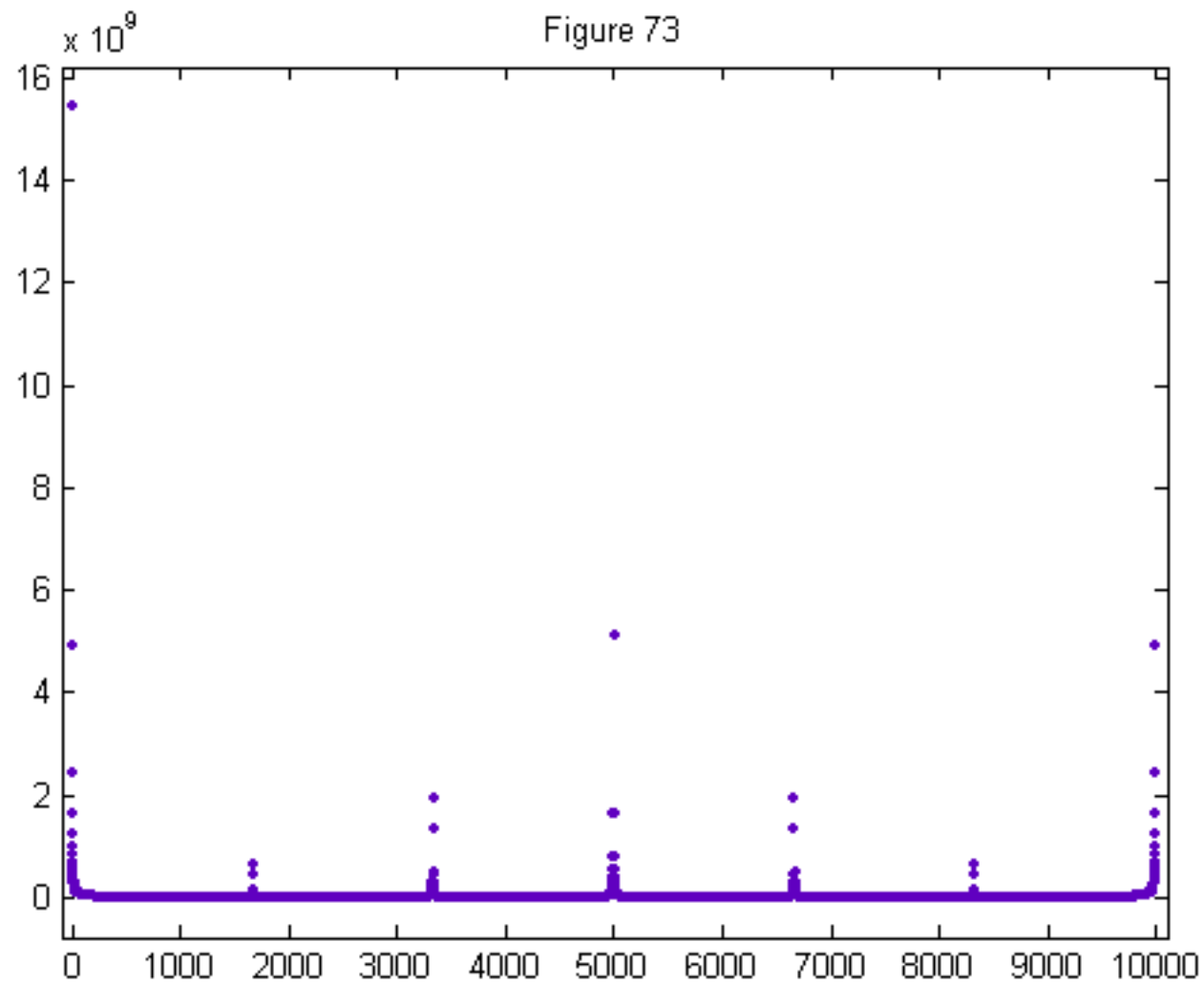


Figure 74

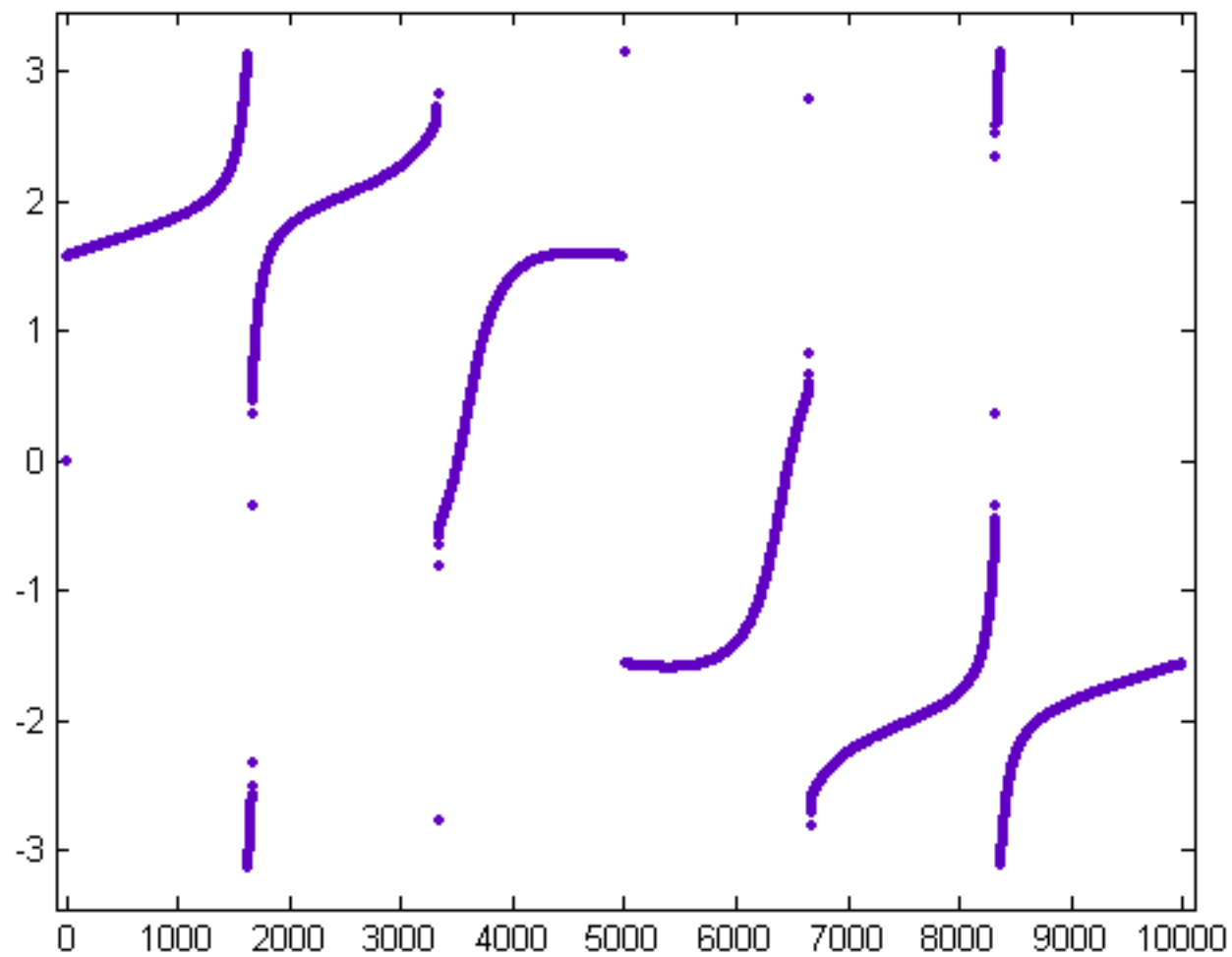


Figure 75

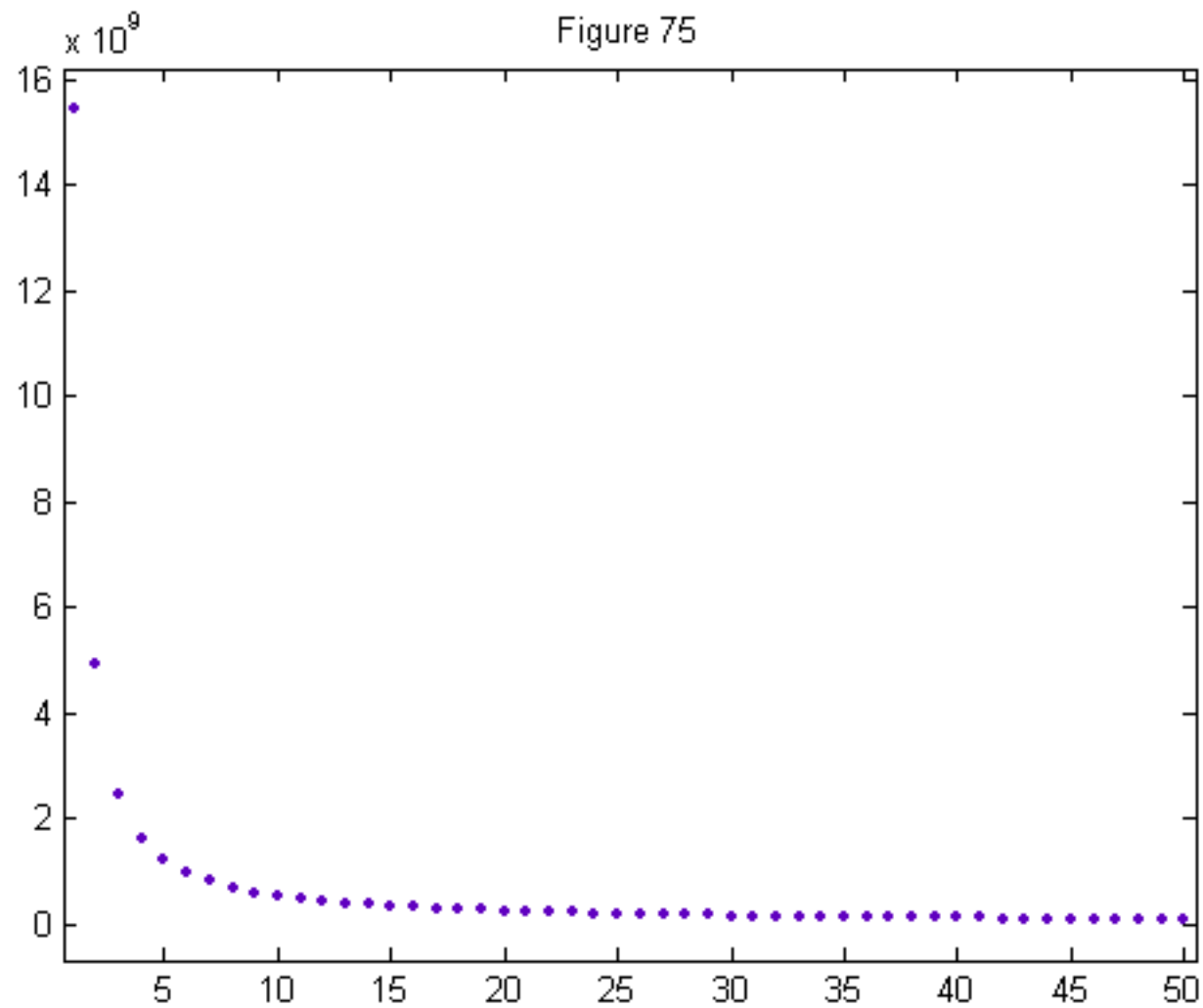


Figure 76

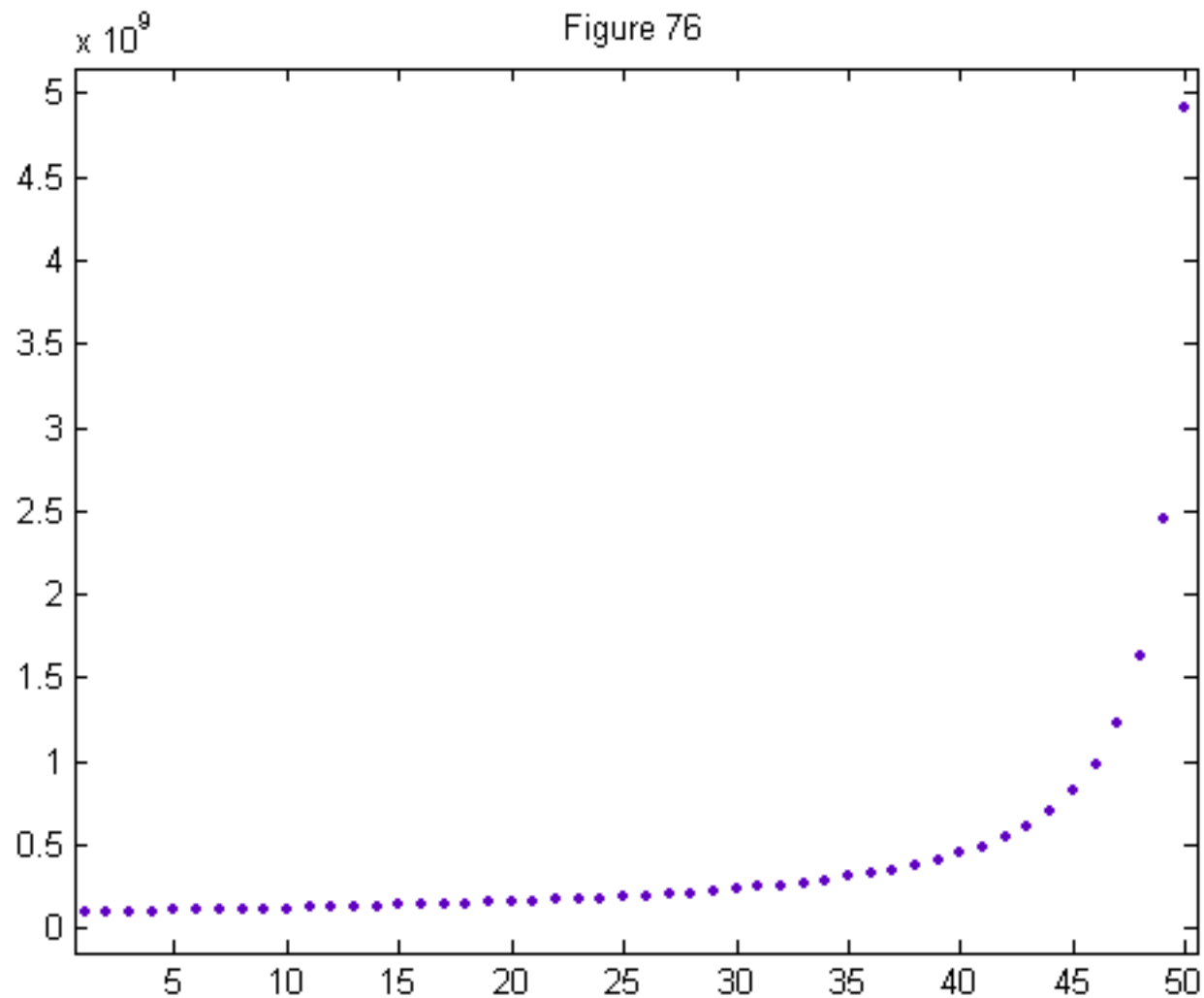


Figure 77

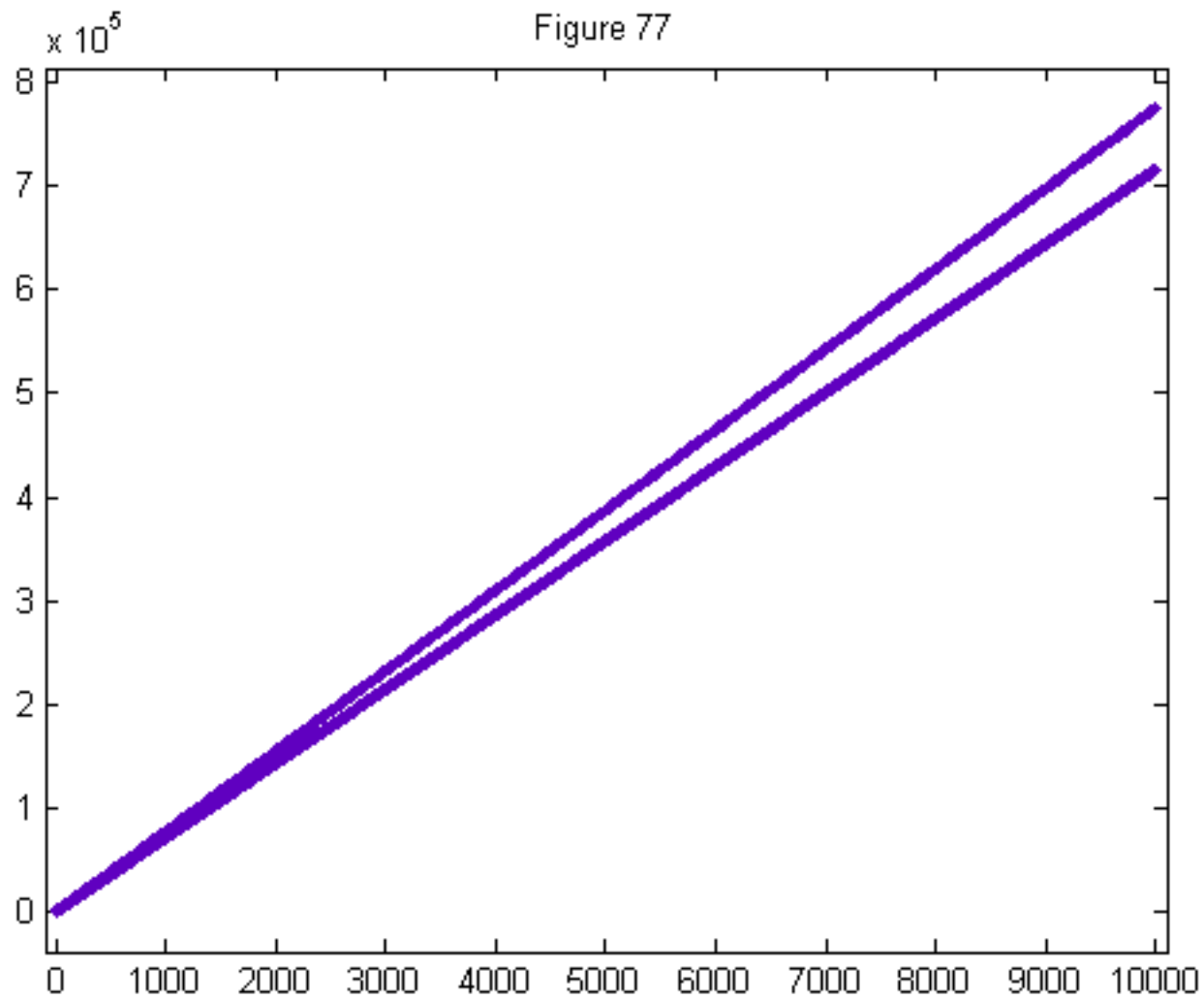


Figure 78

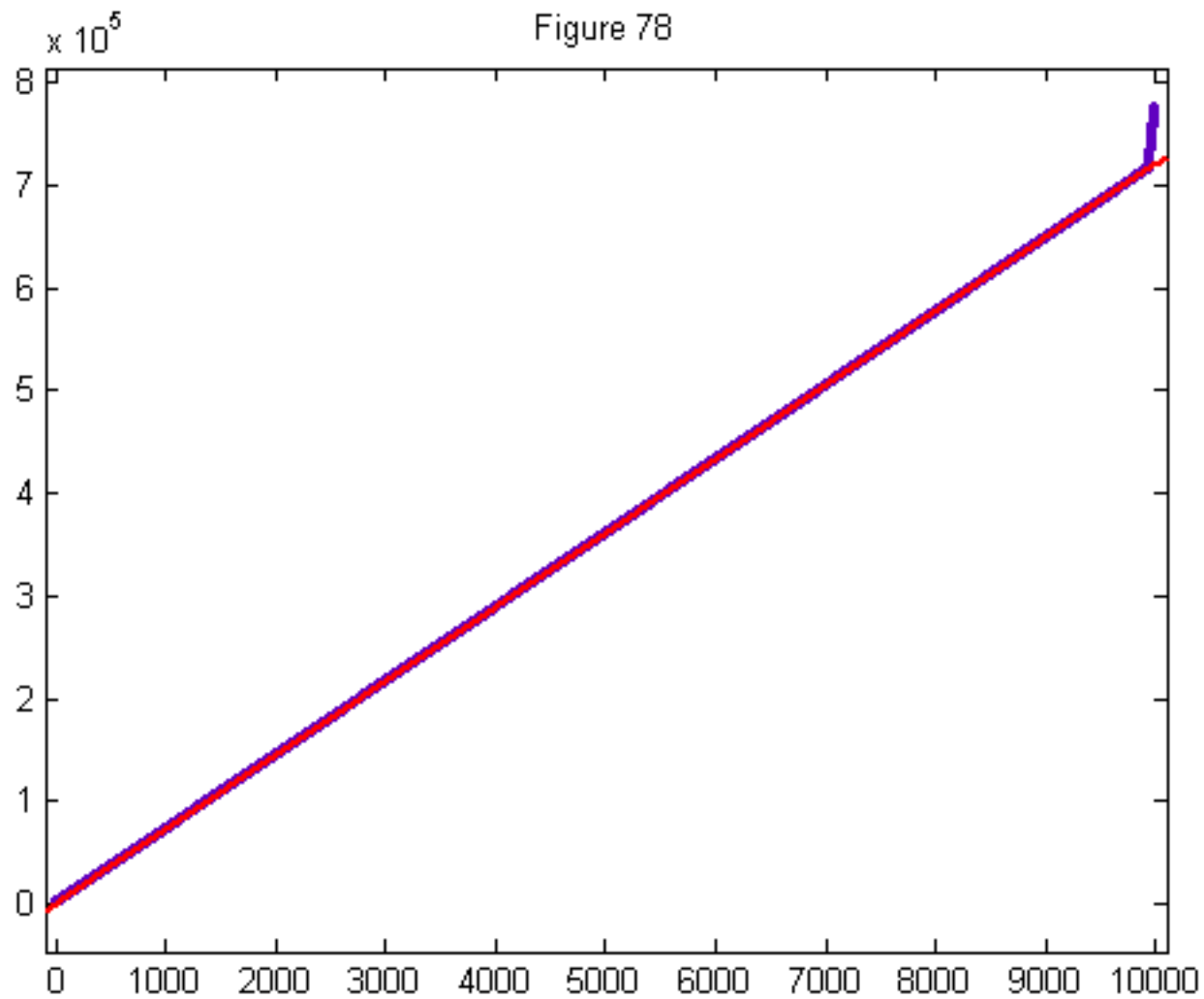


Figure 79

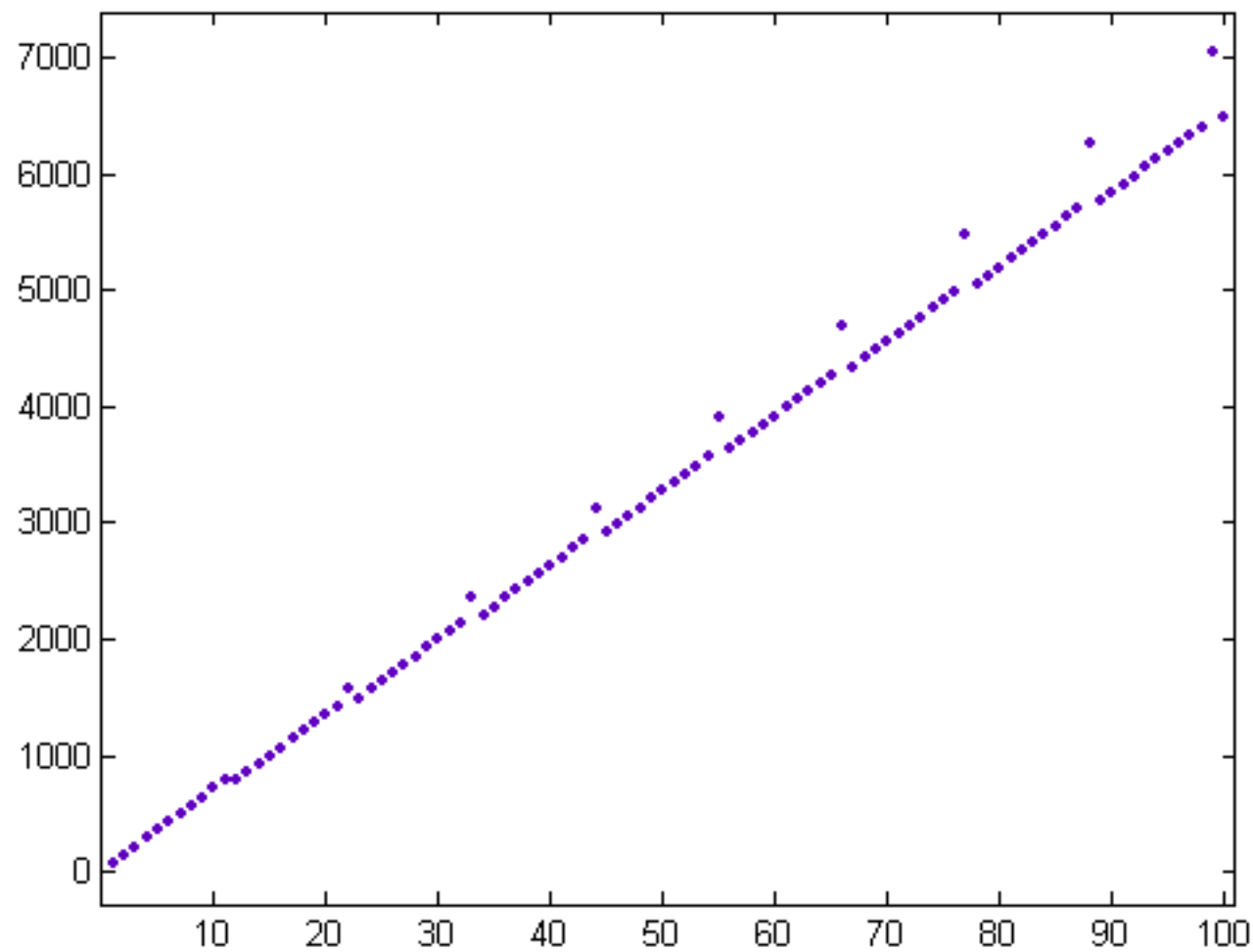


Figure 80

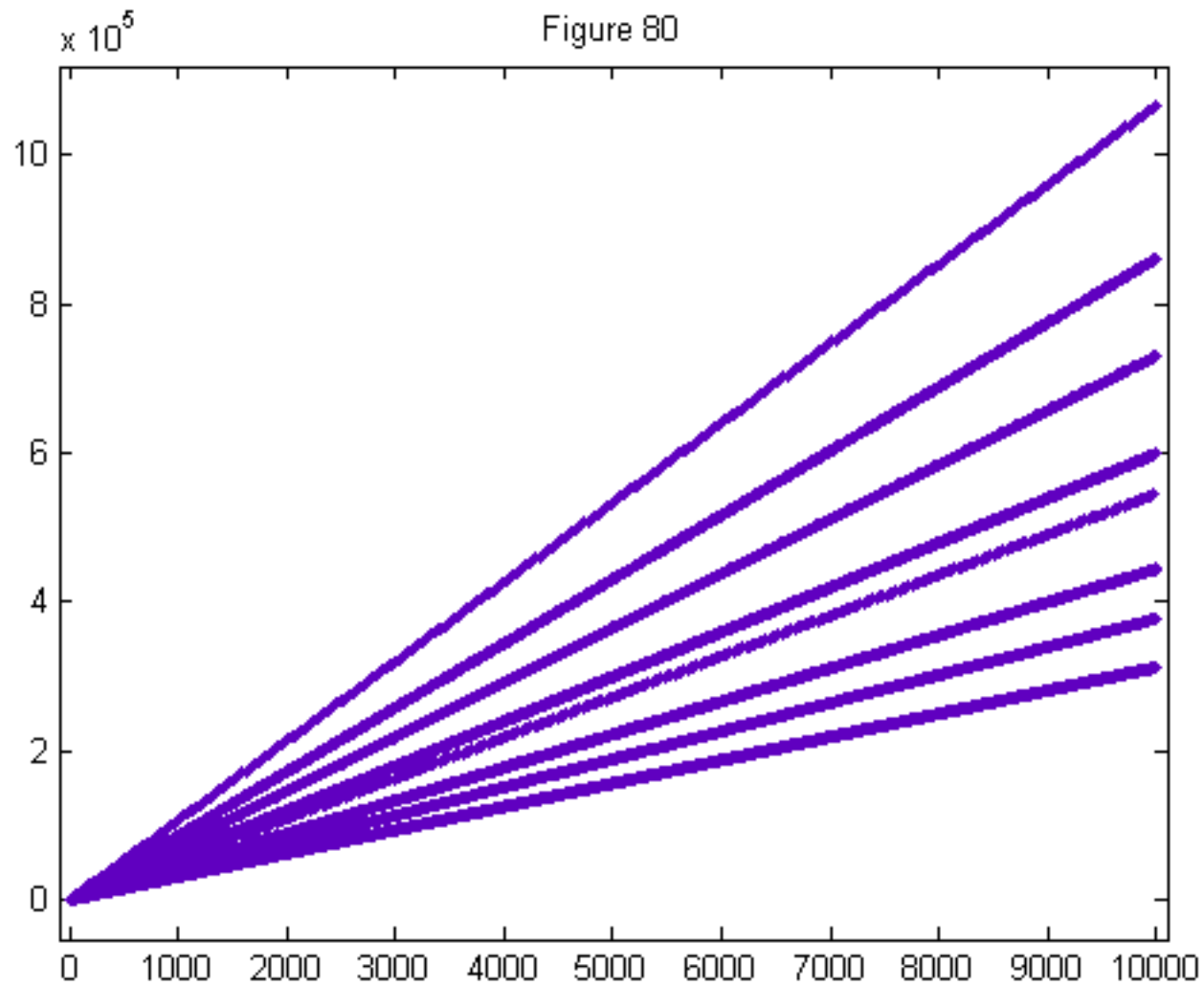


Figure 81

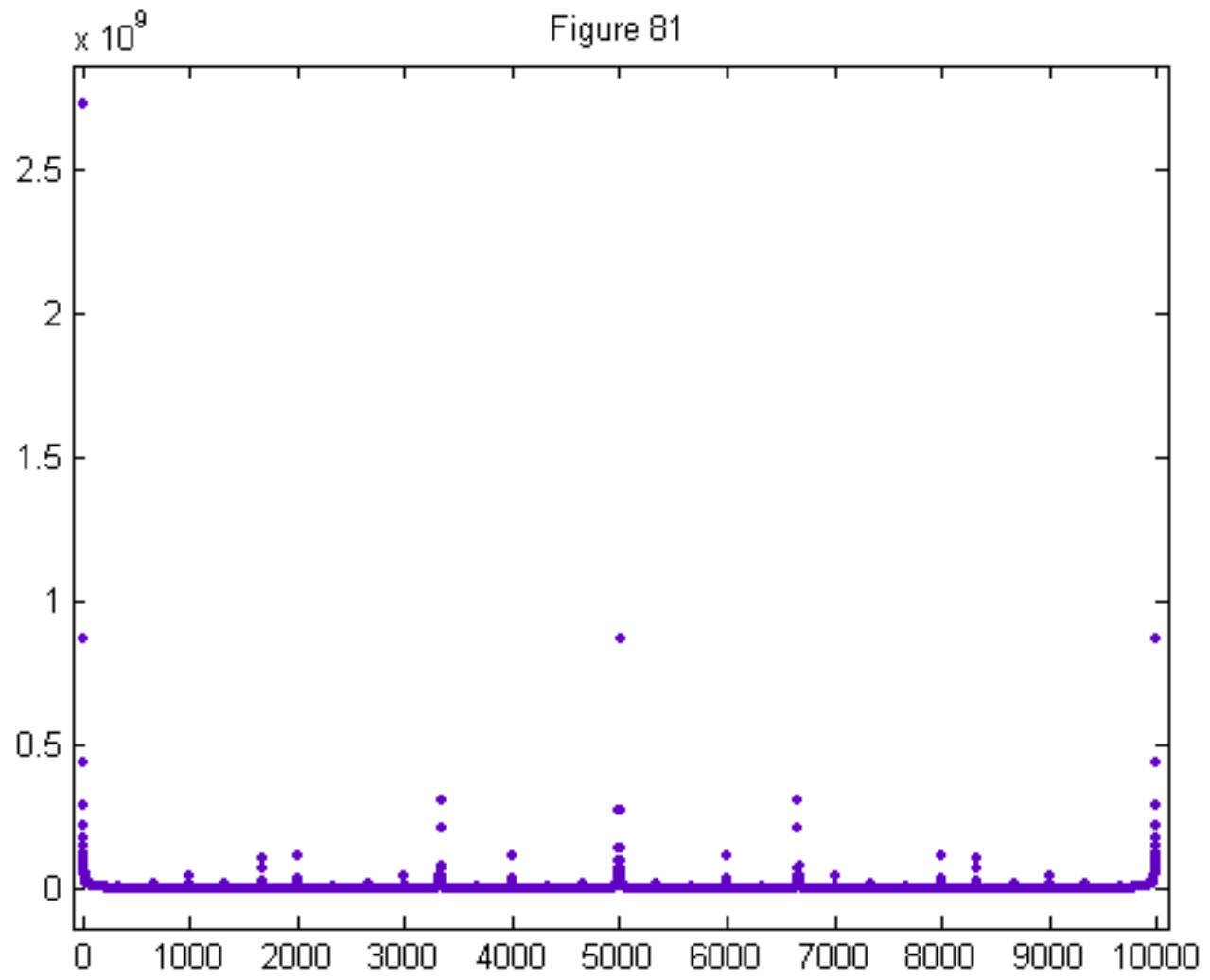


Figure 82

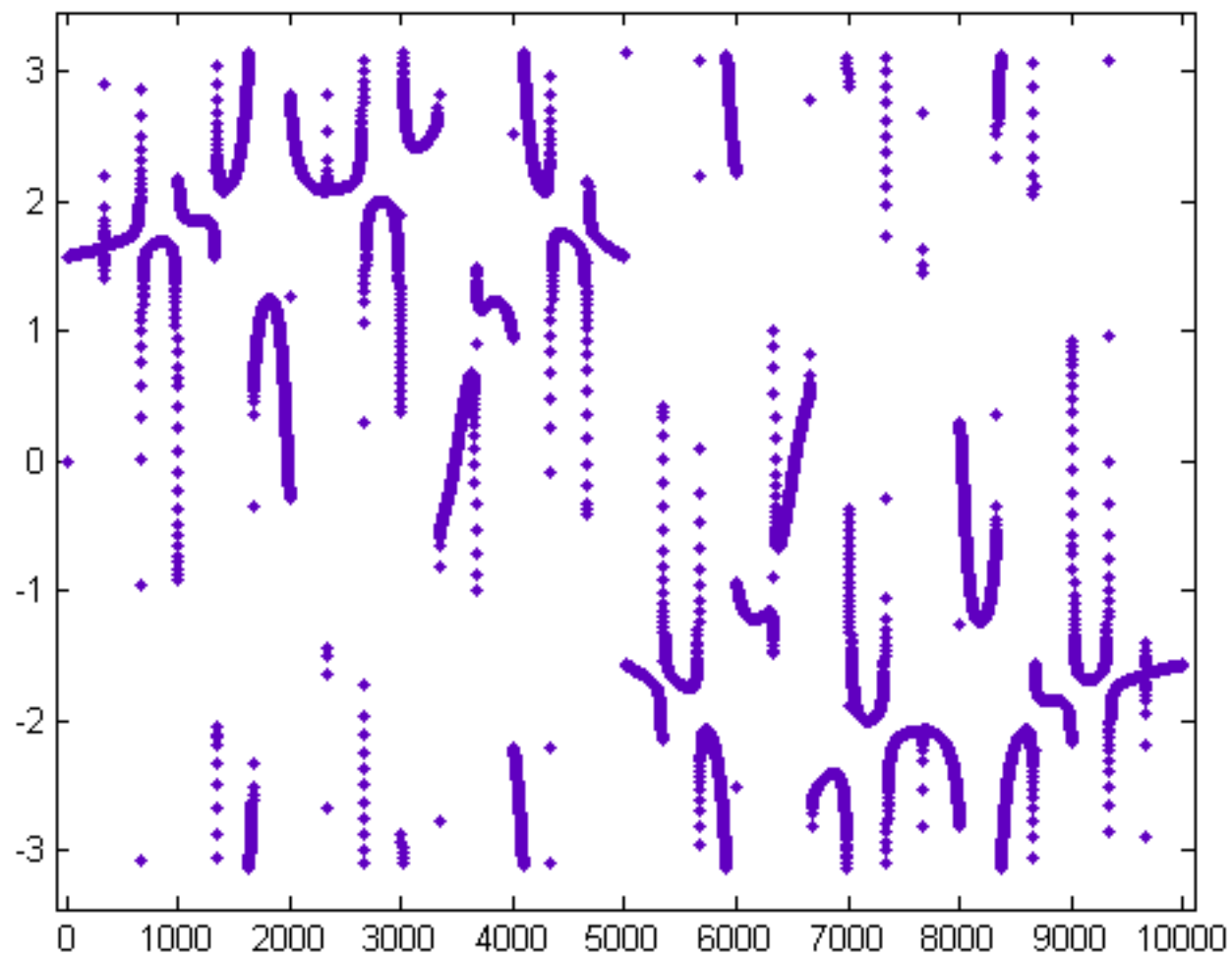


Figure 83

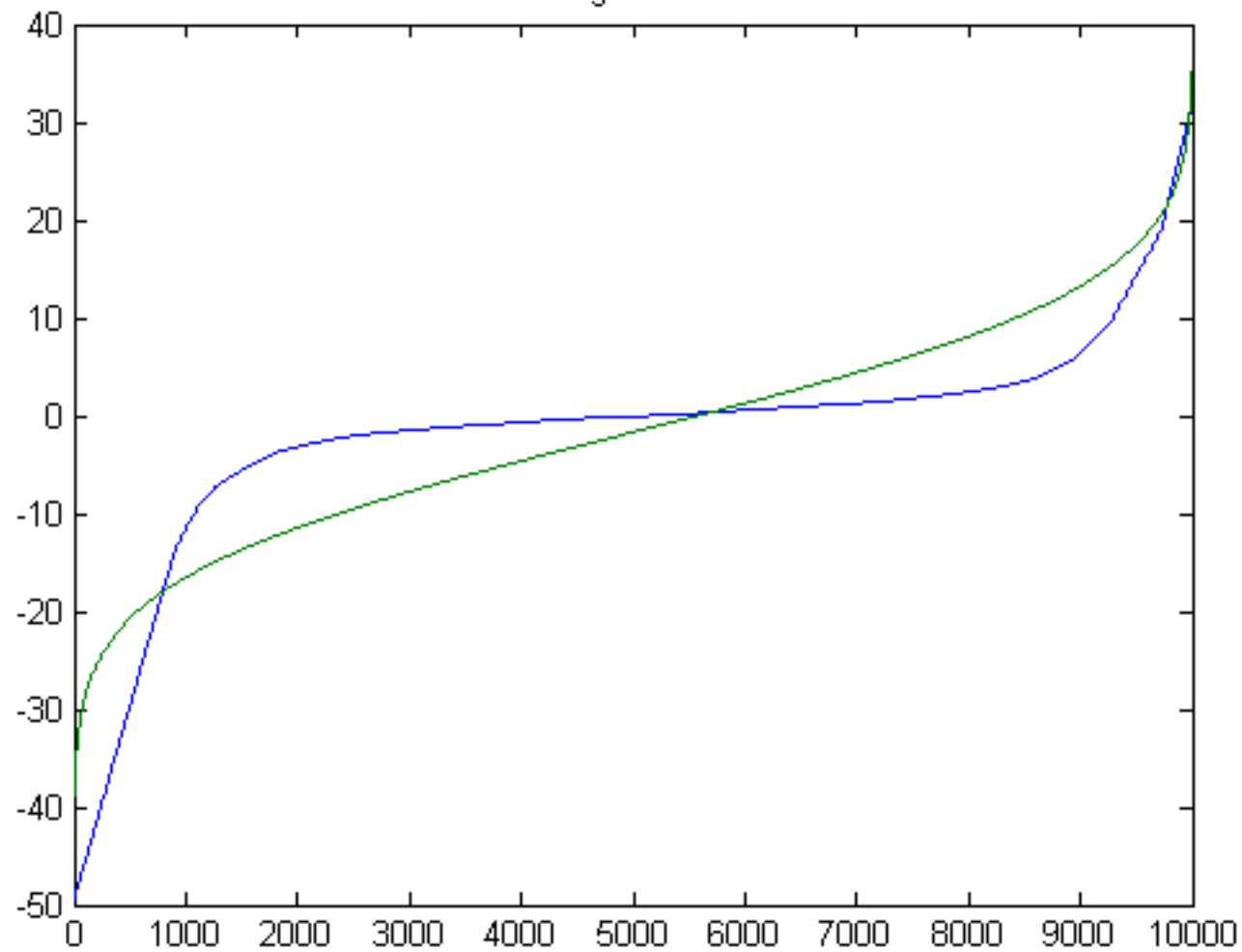


Figure 84

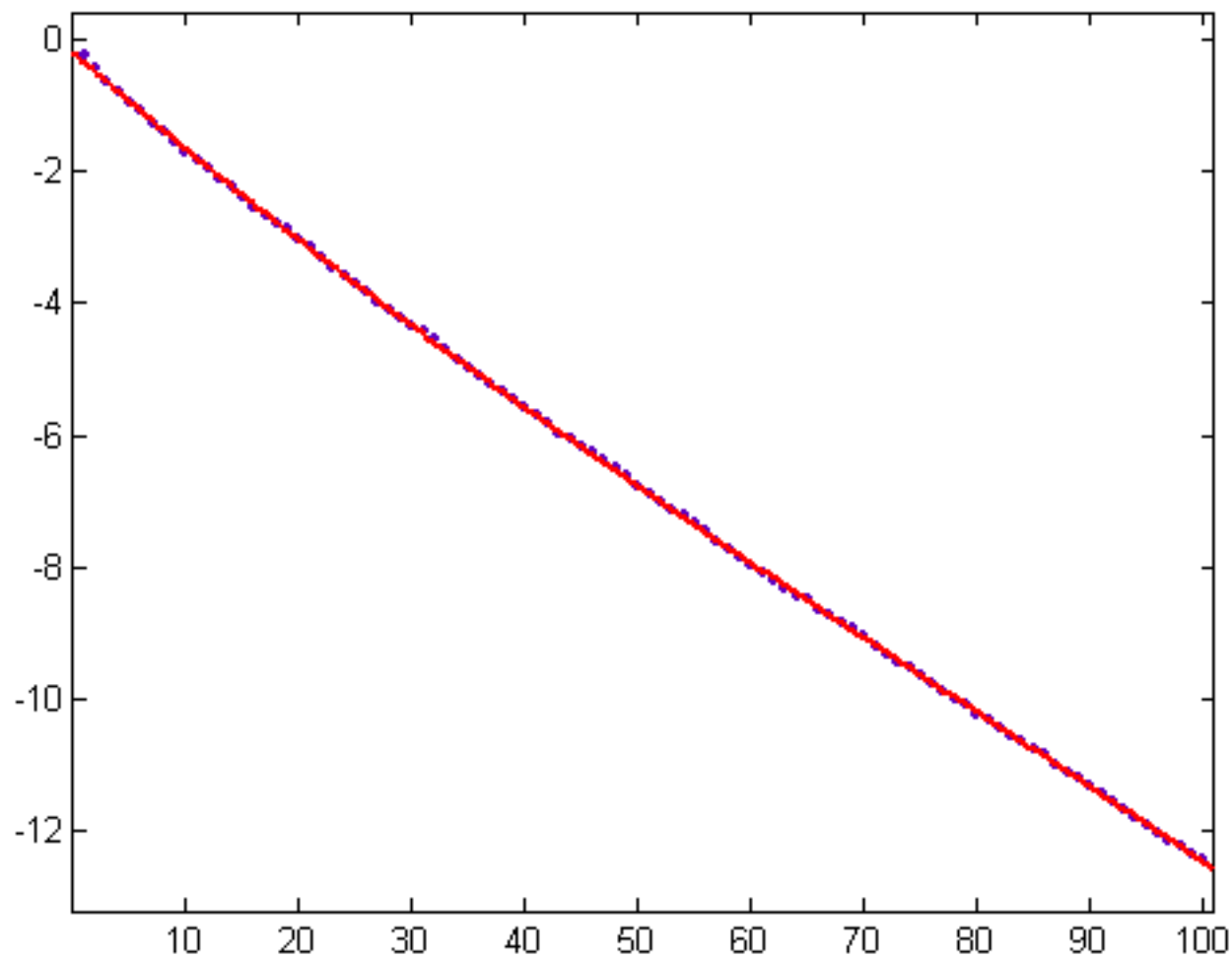


Figure 85

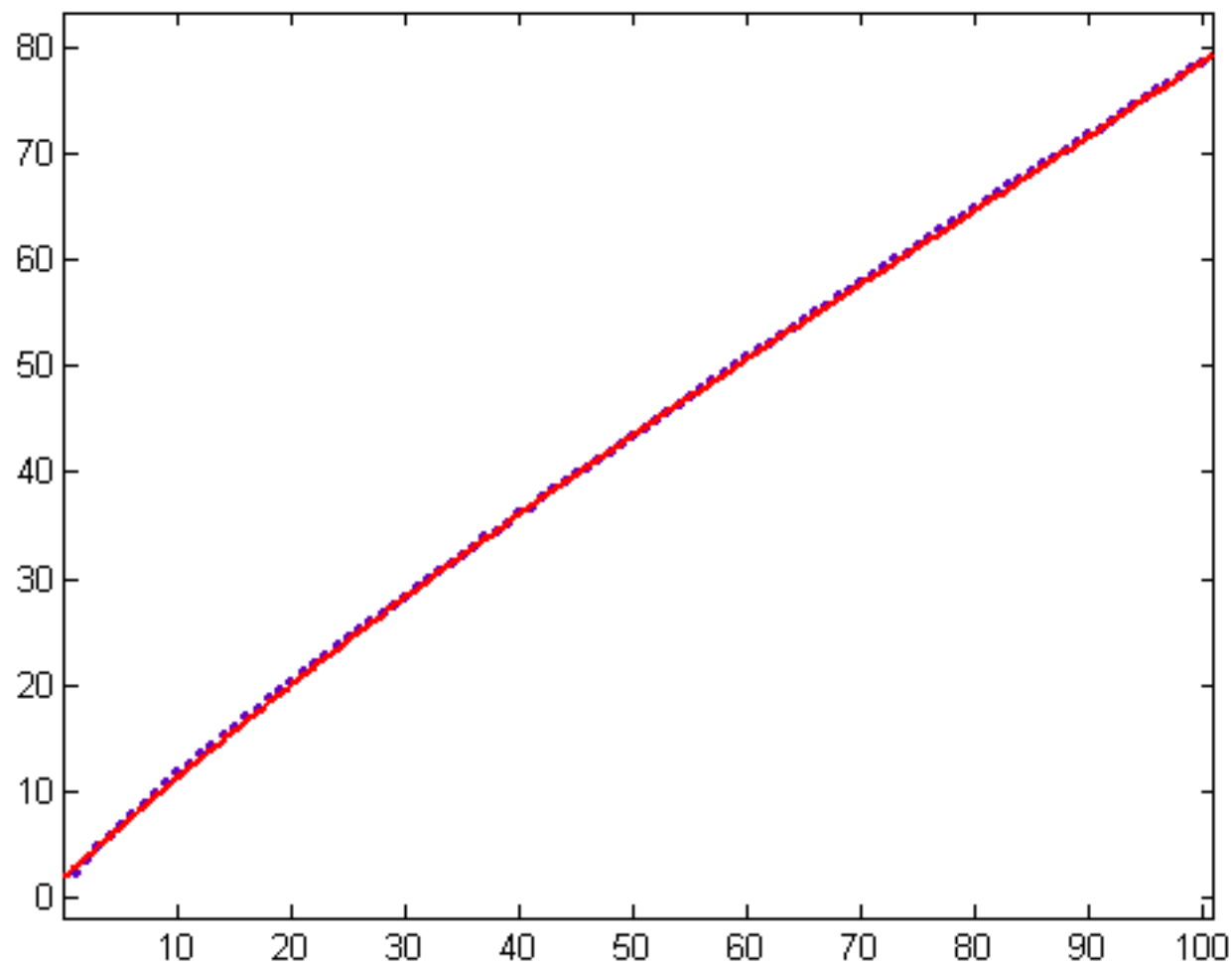


Figure 86

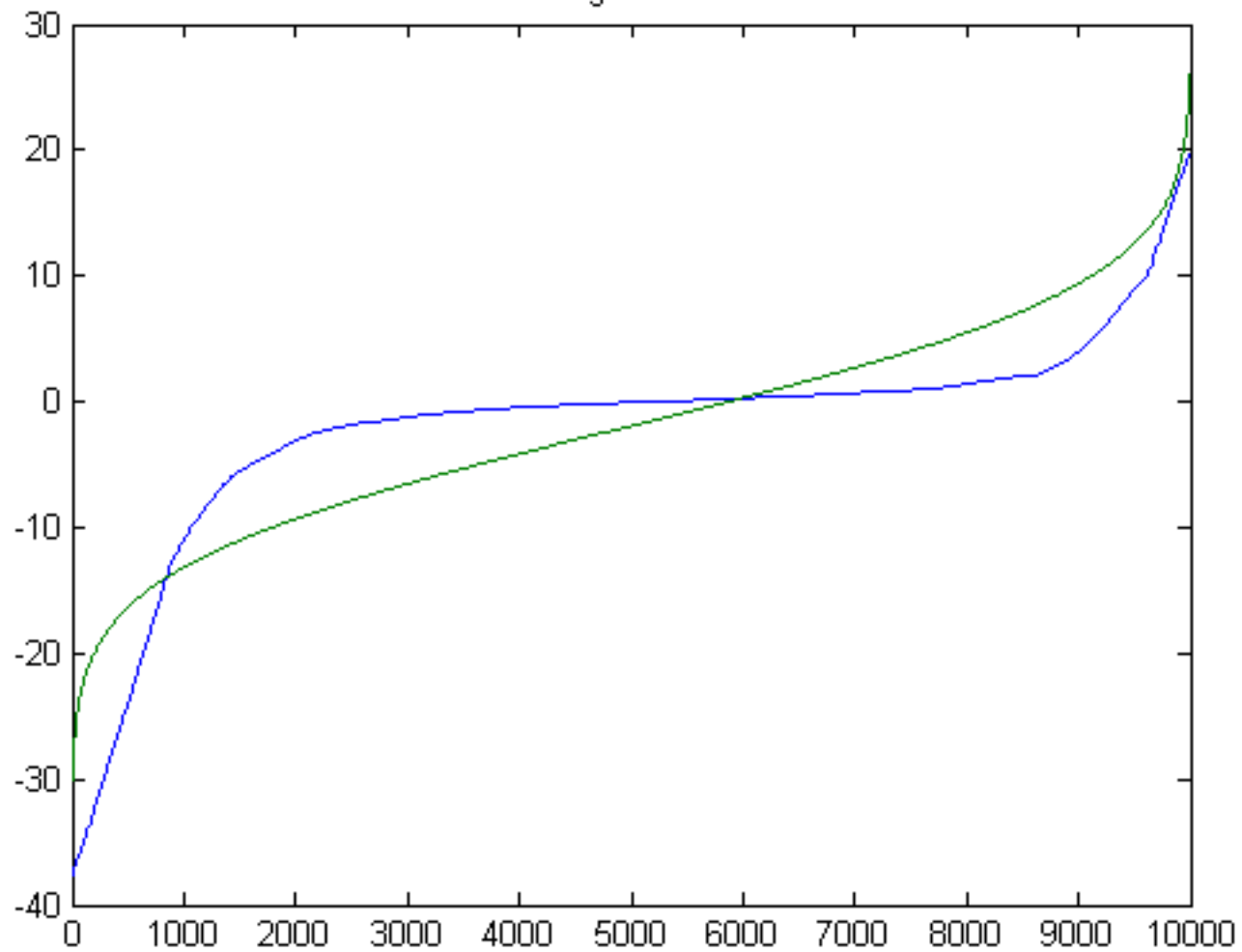


Figure 87

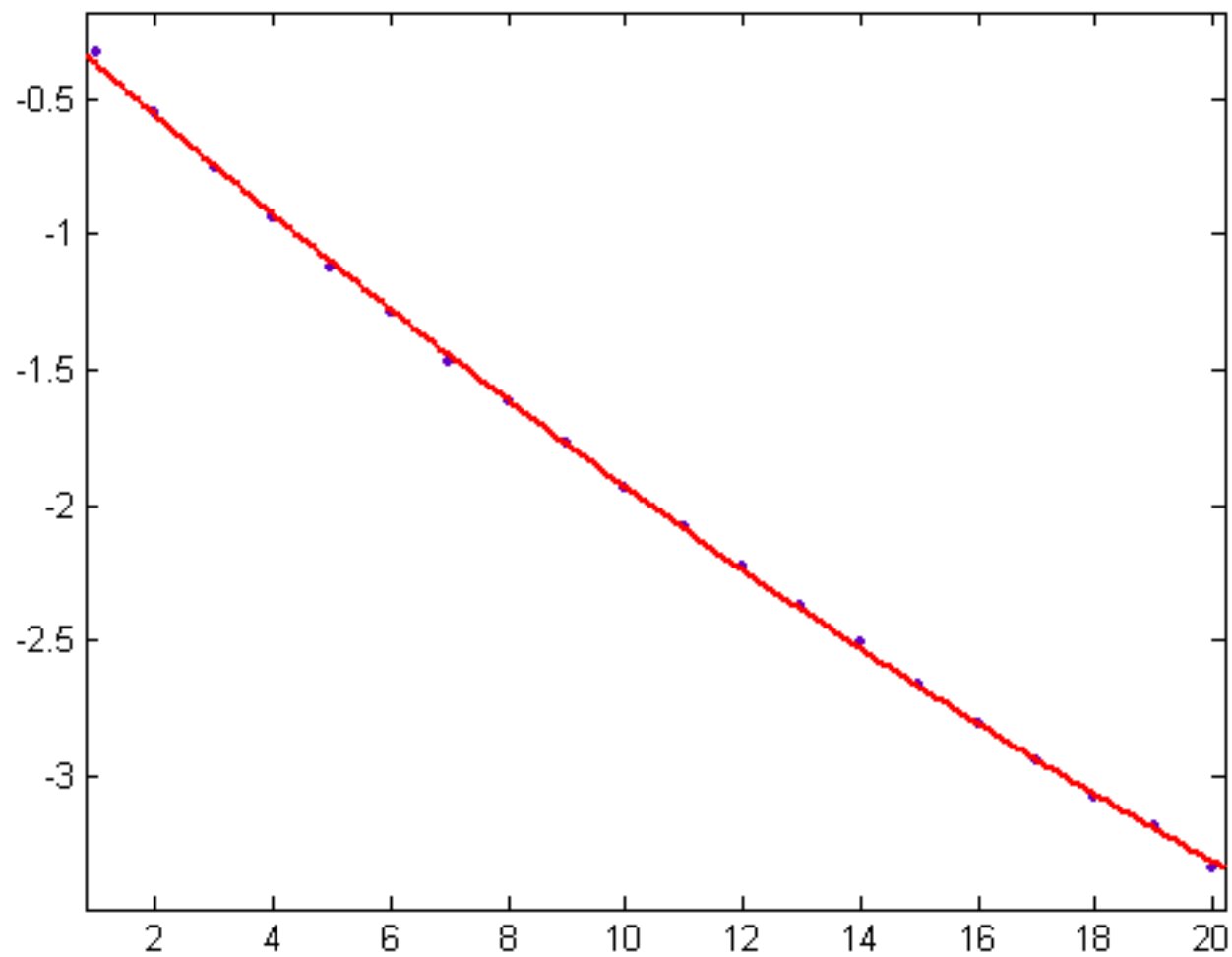


Figure 88

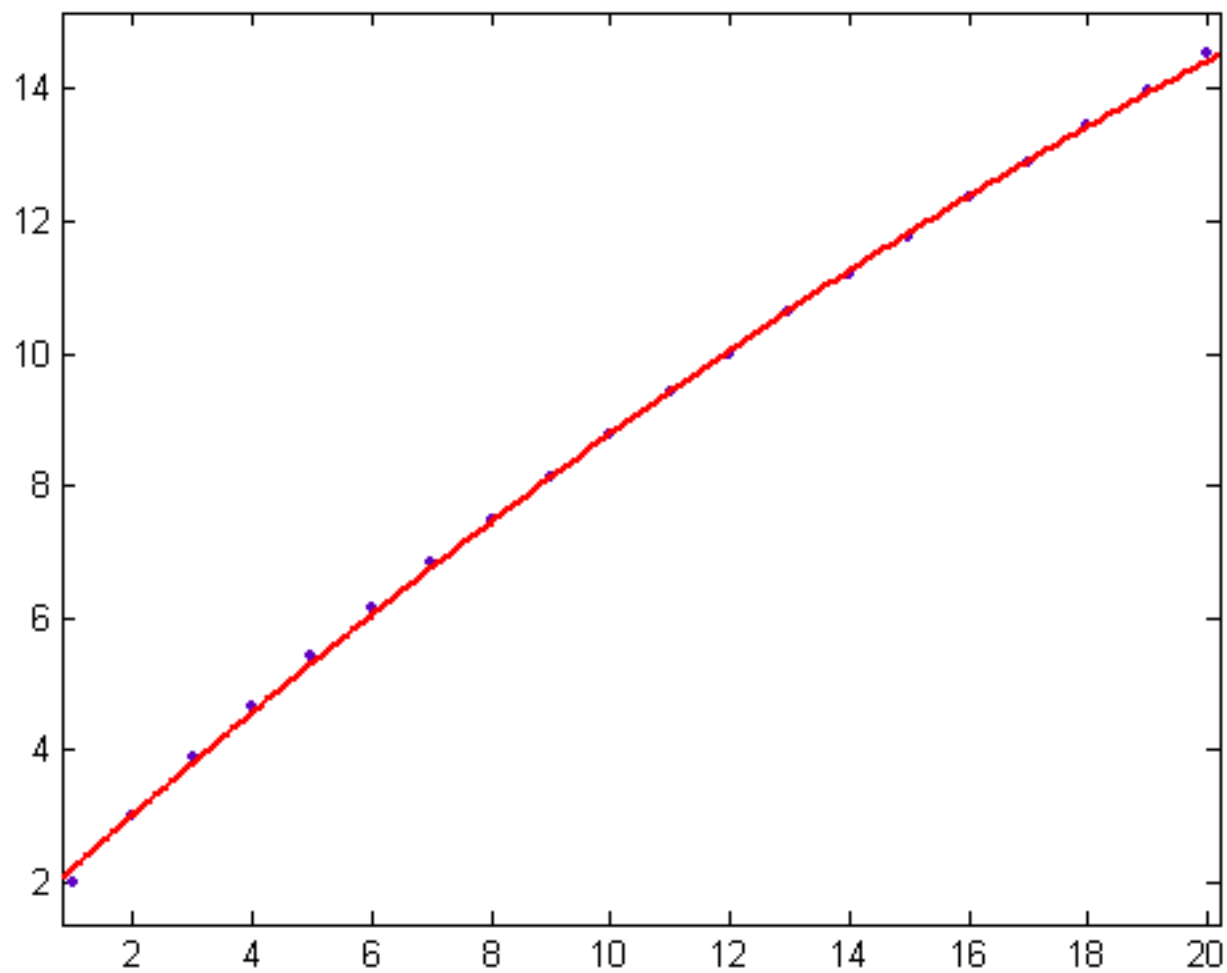


Figure 89

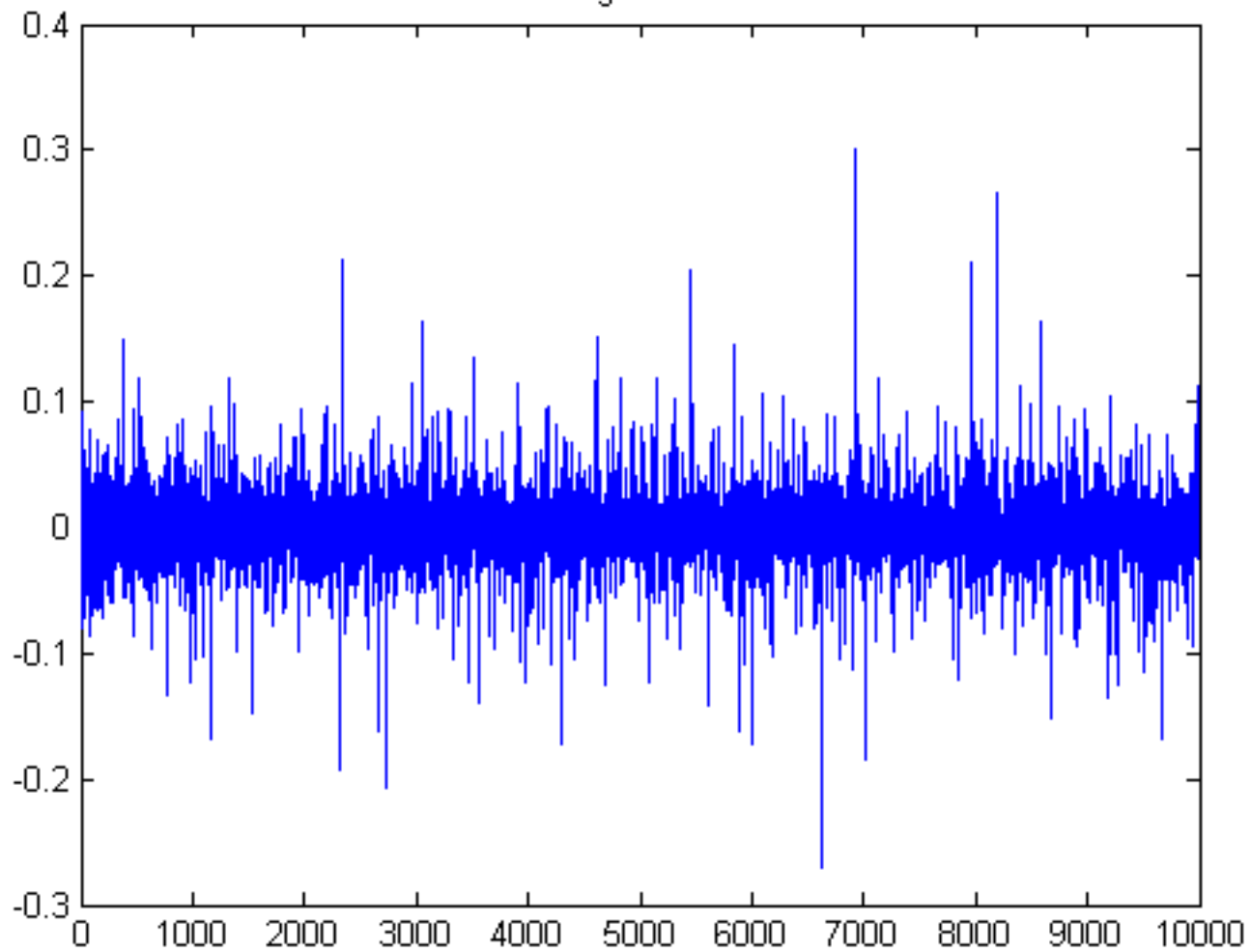


Figure 90

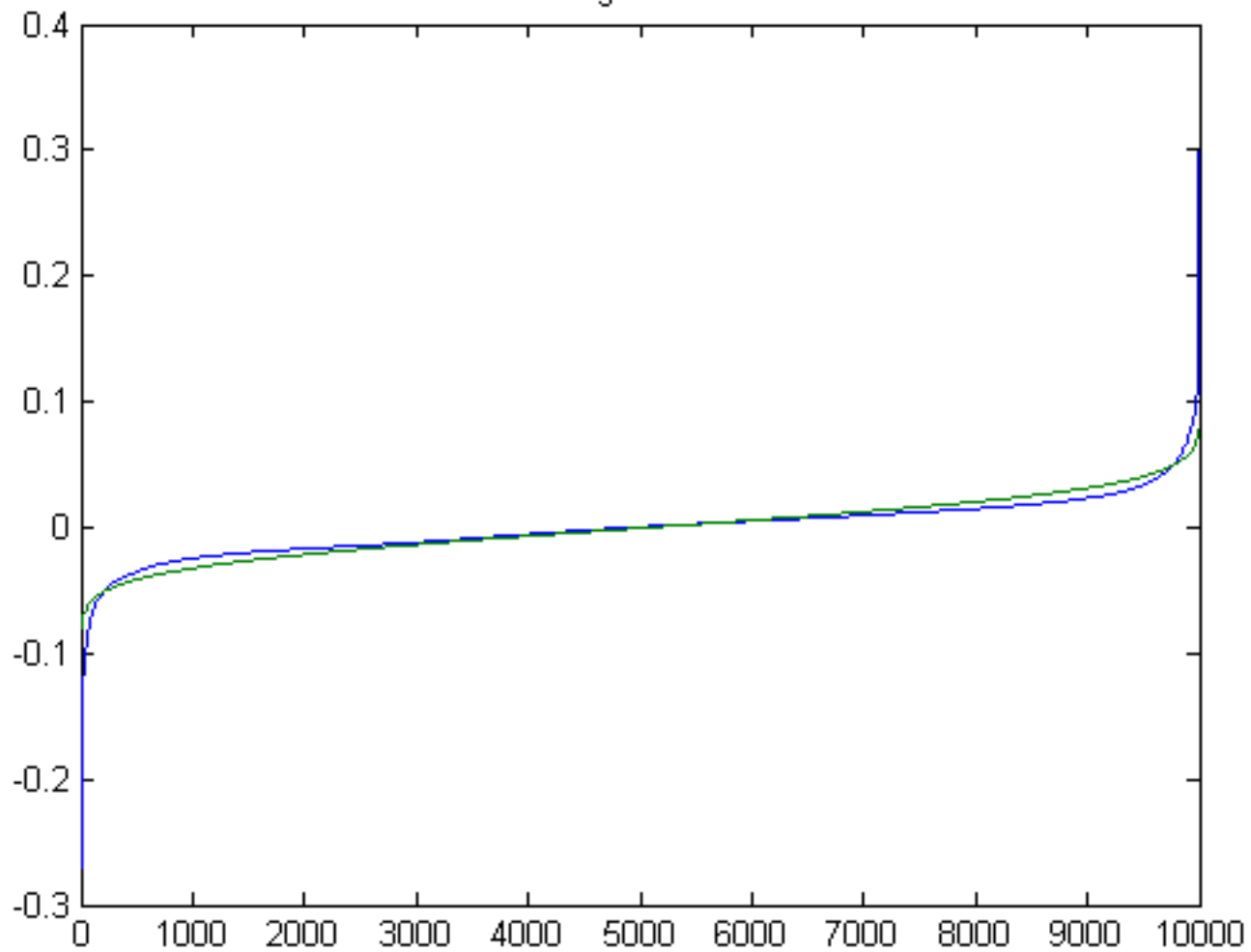


Figure 91

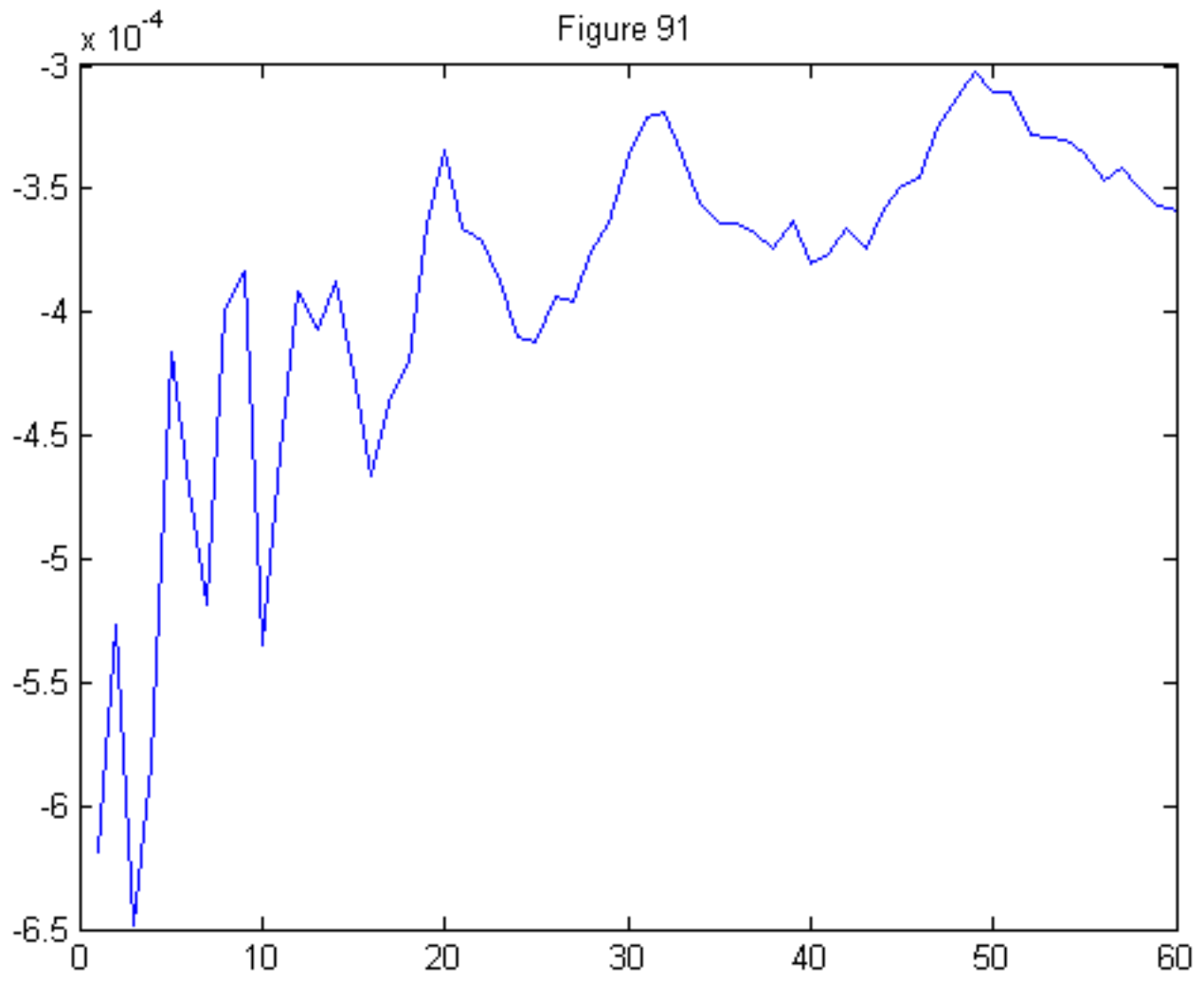


Figure 92

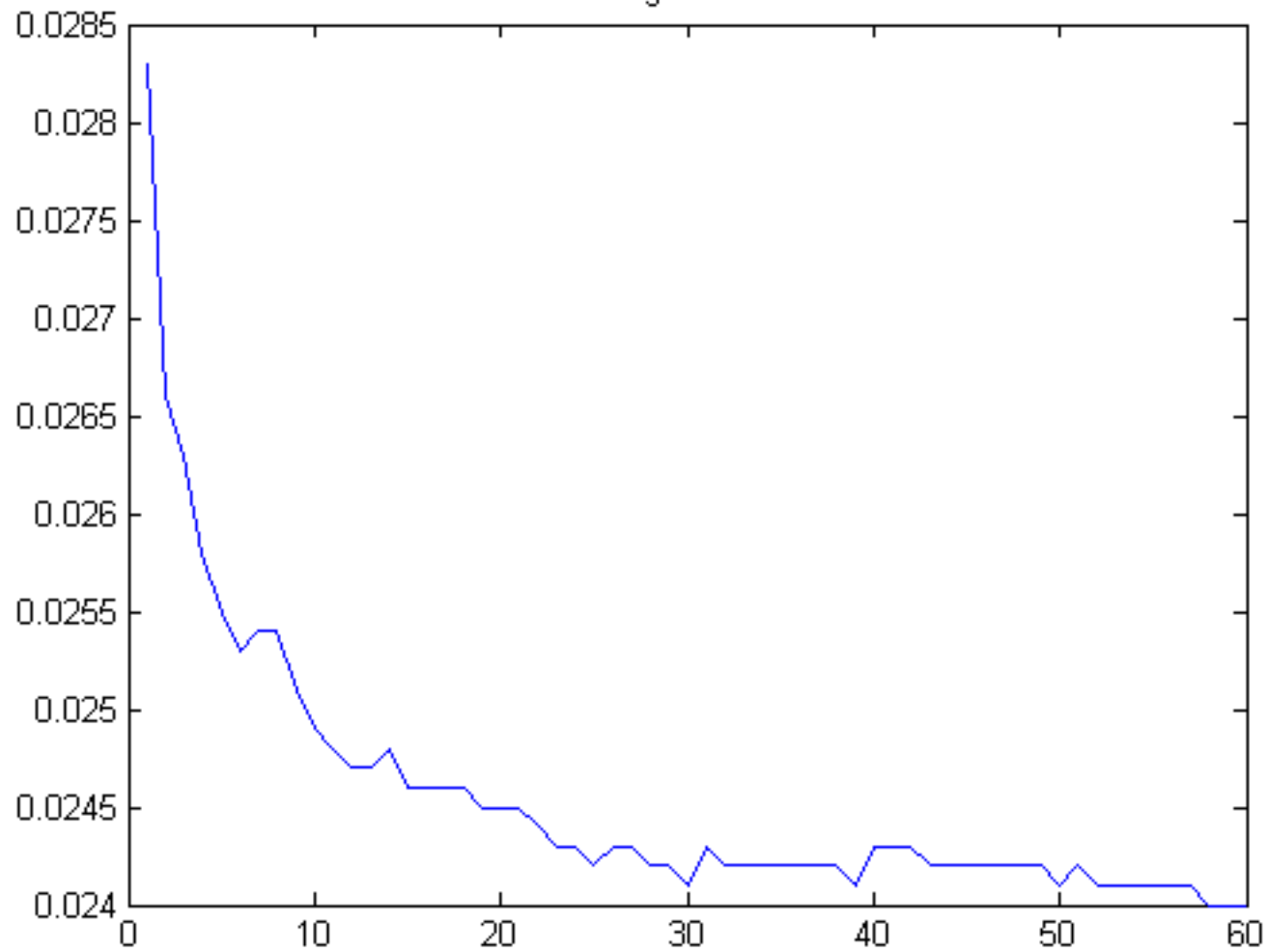


Figure 93

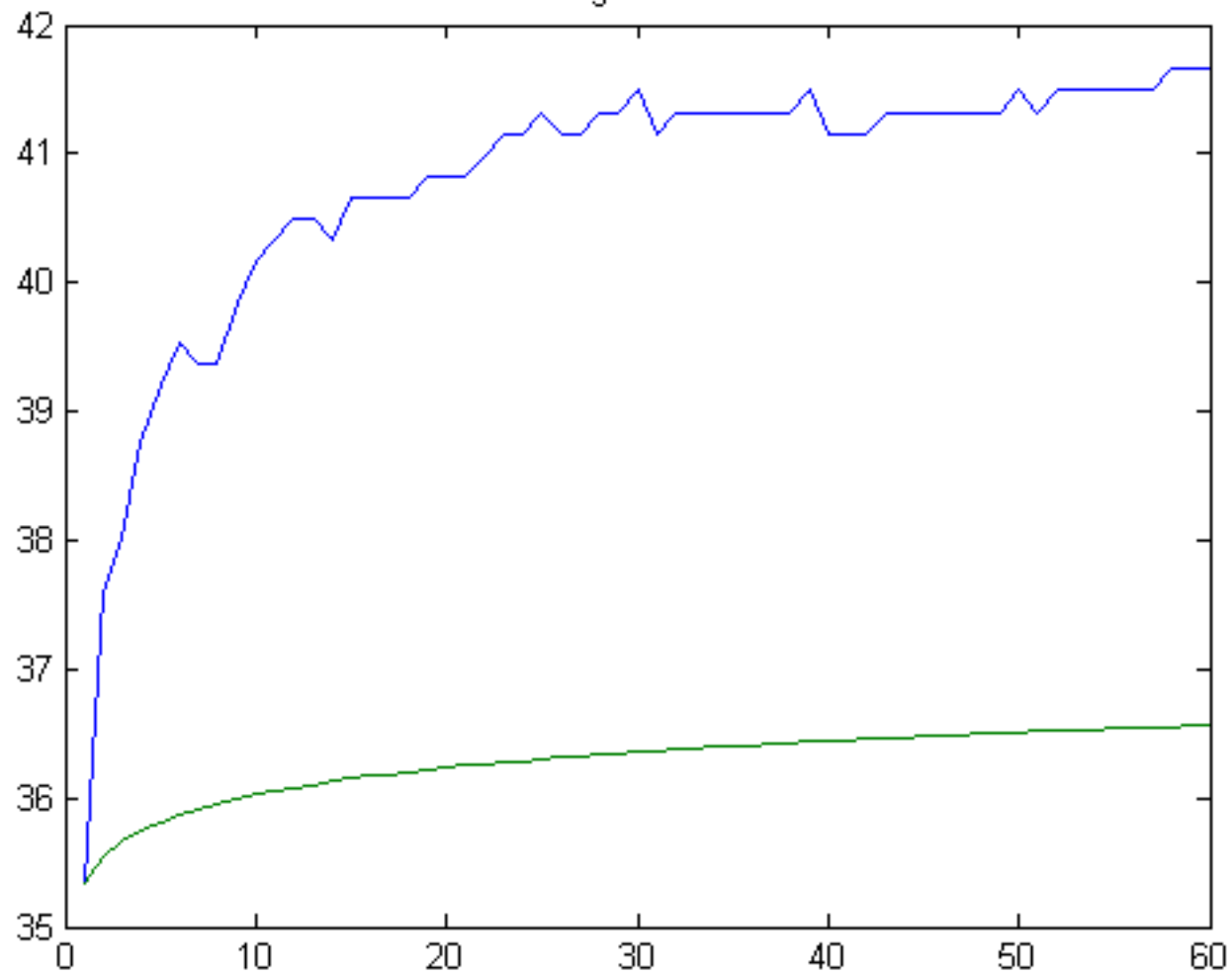


Figure 94

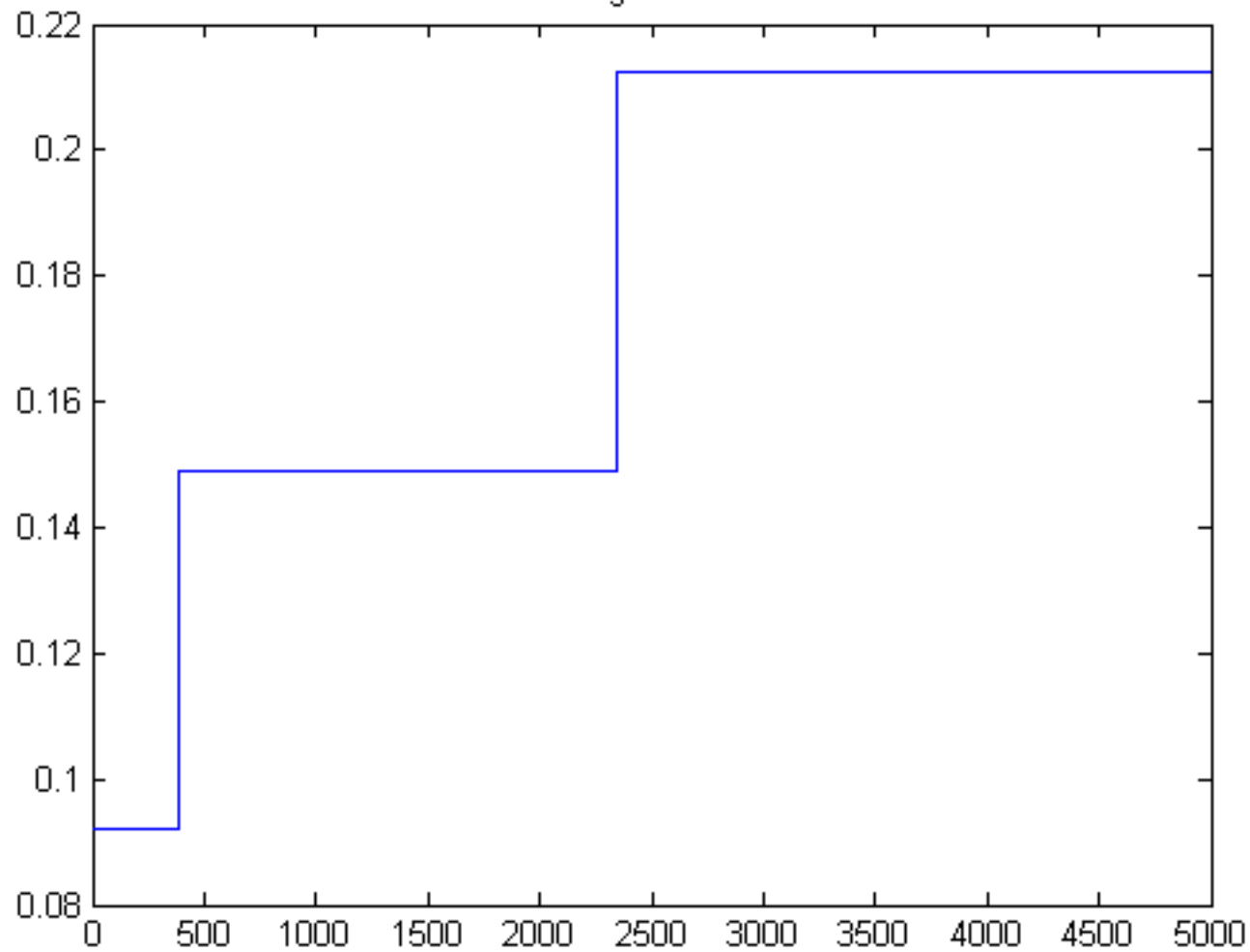


Figure 95

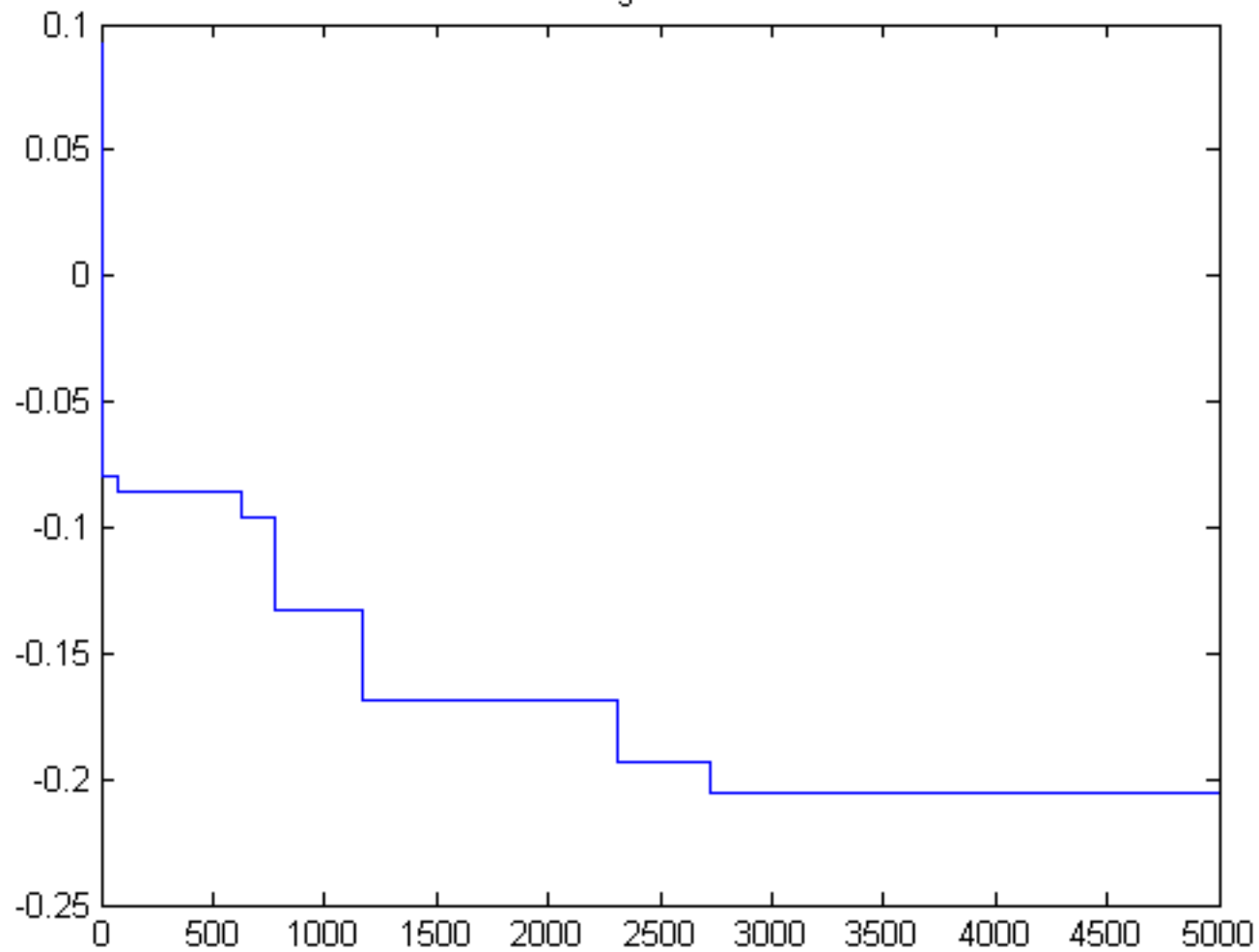


Figure 96

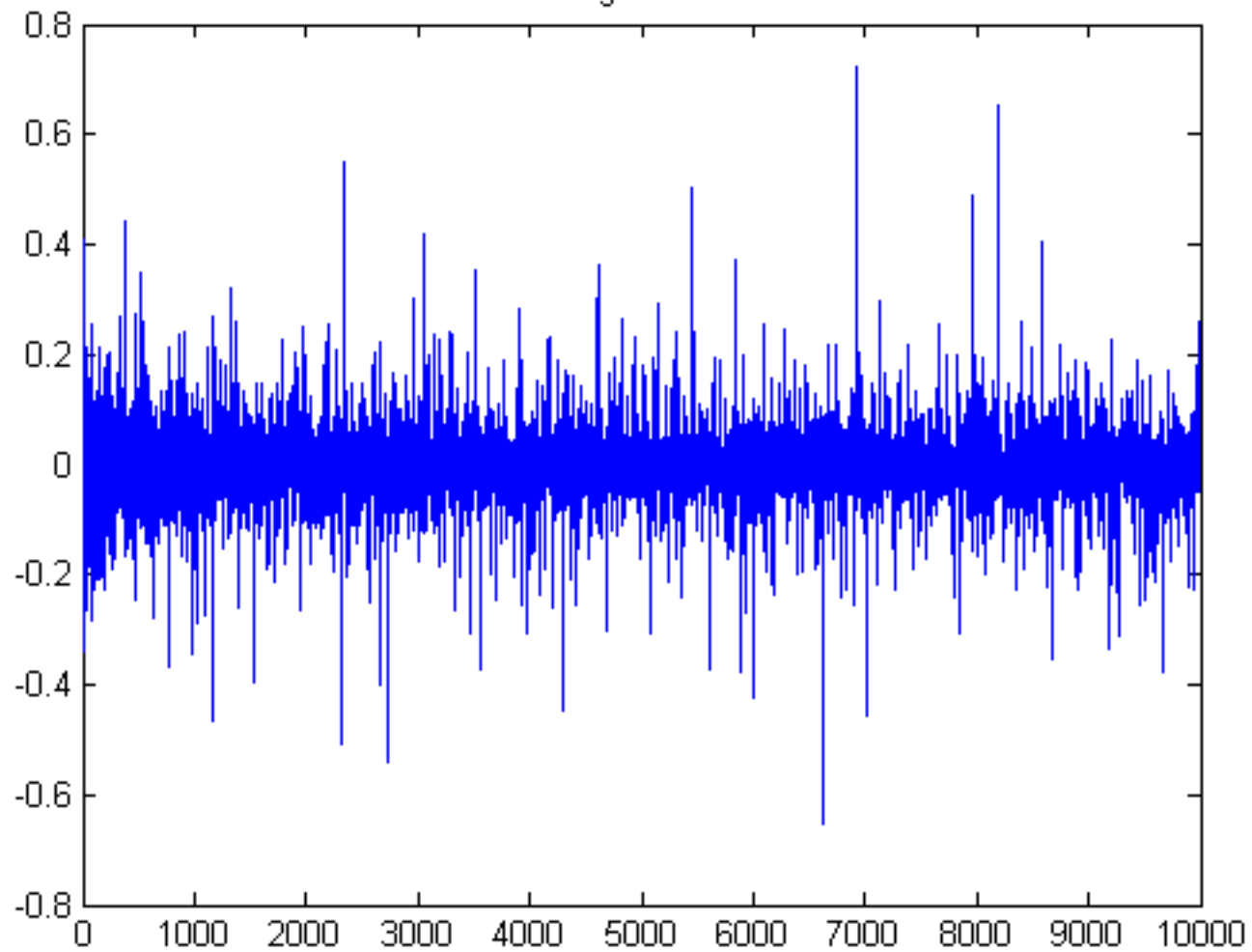


Figure 97

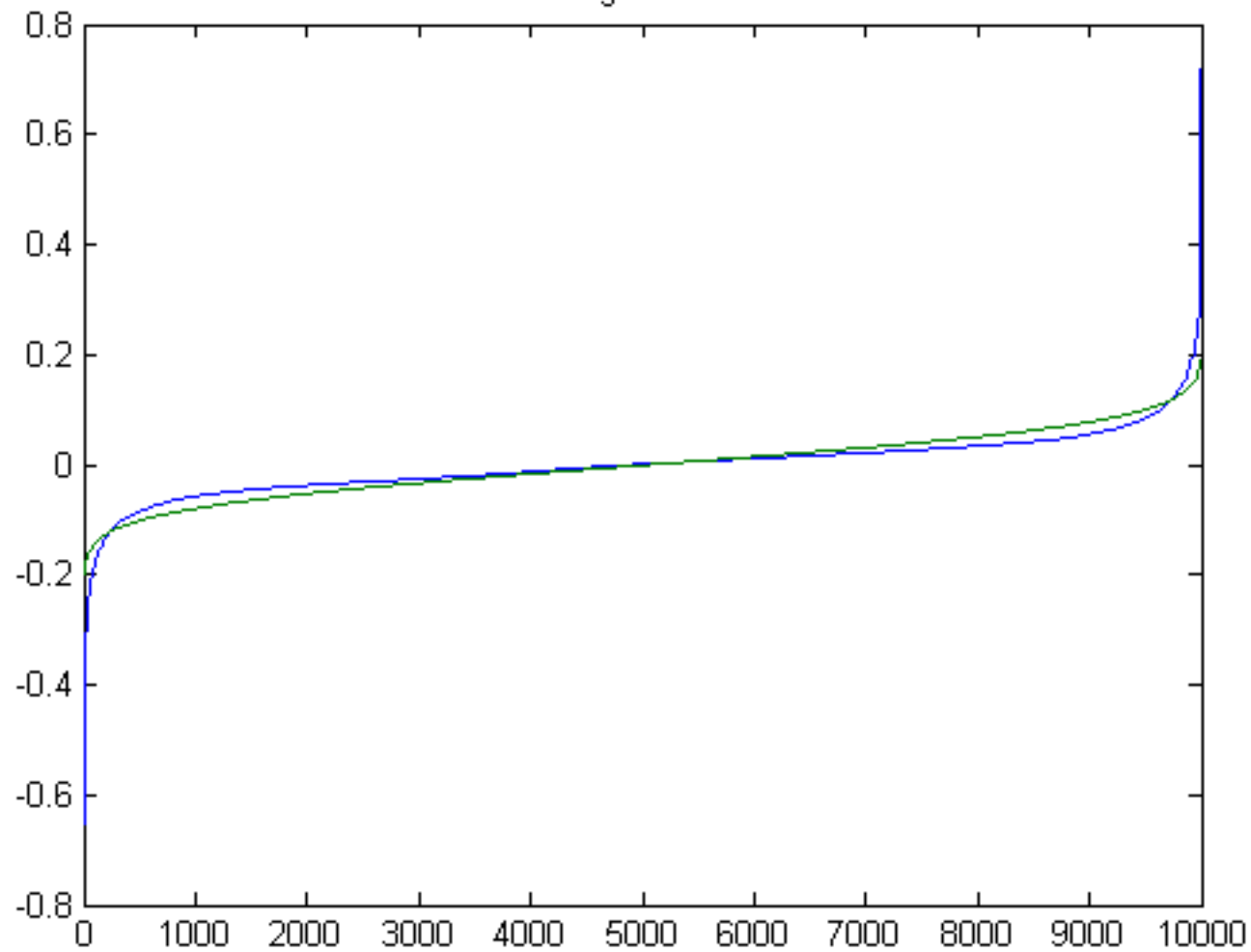


Figure 98

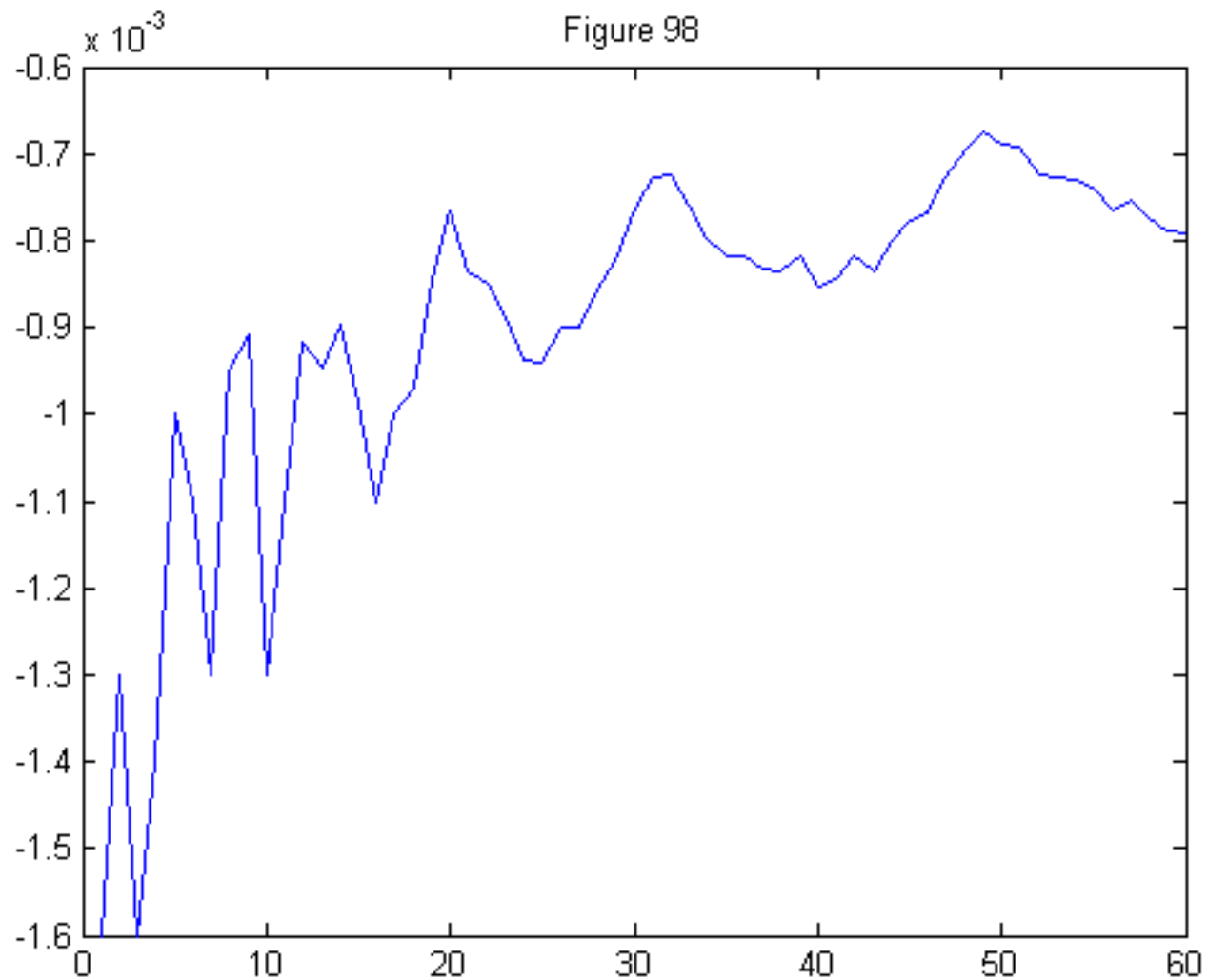


Figure 99

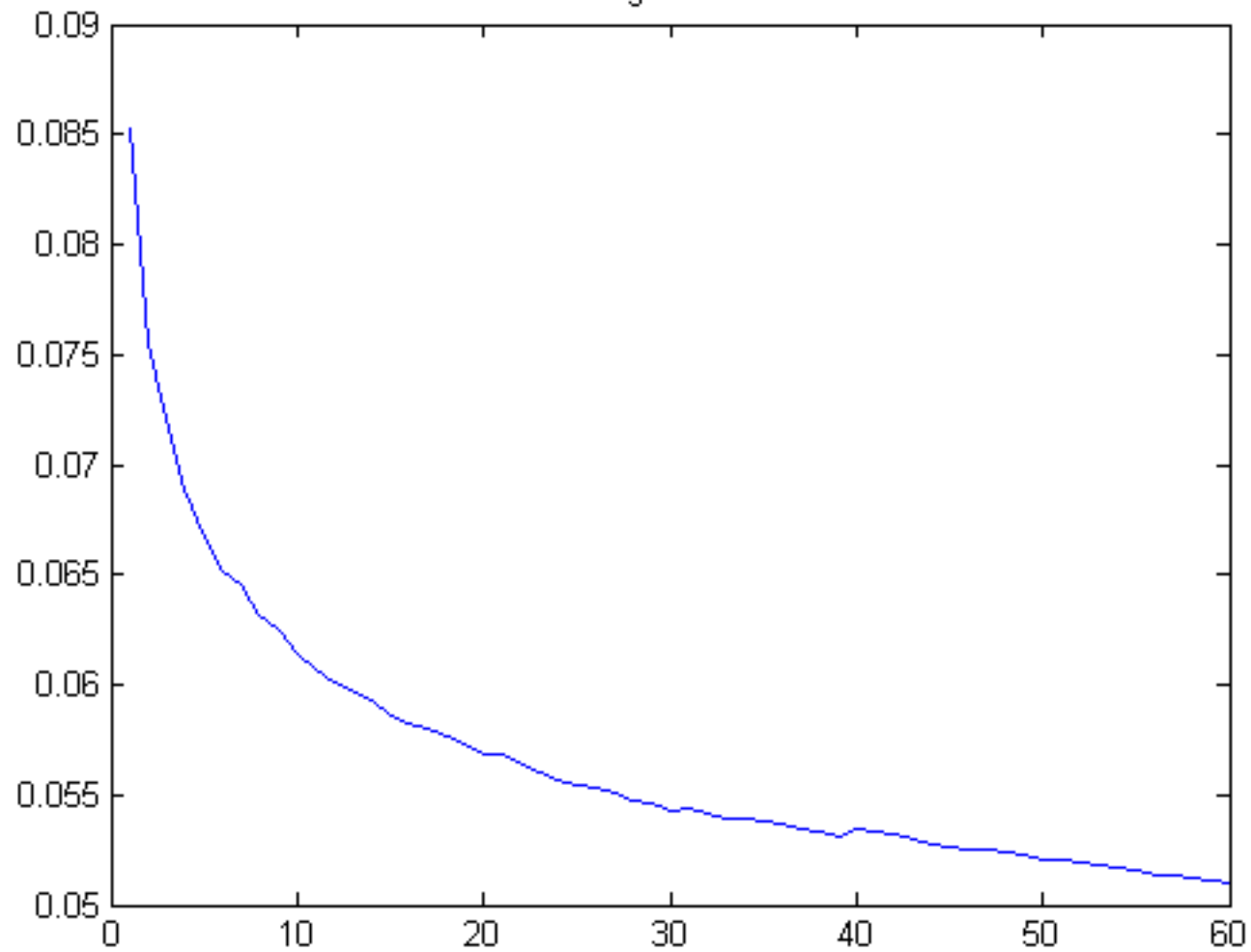


Figure 100

